

1 A synthesis of ~~SNAPO-CO2~~ ocean total alkalinity and ~~total~~ dissolved  
2 inorganic carbon measurements from 1993 to 2022: the SNAPO-  
3 CO2-v1 dataset

4  
5 Nicolas Metzl<sup>1</sup>, Jonathan Fin<sup>1,2</sup>, Claire Lo Monaco<sup>1</sup>, Claude Mignon<sup>1</sup>, Samir Alliouane<sup>3</sup>,  
6 David Antoine<sup>3,4</sup>, Guillaume Bourdin<sup>5</sup>, Jacqueline Boutin<sup>1</sup>, Yann Bozec<sup>6</sup>, Pascal Conan<sup>7,8</sup>,  
7 Laurent Coppola<sup>3,8</sup>, Frédéric Diaz<sup>\*</sup>, Eric Douville<sup>9</sup>, Xavier Durrieu de Madron<sup>10</sup>, Jean-Pierre  
8 Gattuso<sup>3,11</sup>, Frédéric Gazeau<sup>3</sup>, Melek Golbol<sup>8,12</sup>, Bruno Lansard<sup>9</sup>, Dominique Lefèvre<sup>13</sup>,  
9 Nathalie Lefèvre<sup>1</sup>, Fabien Lombard<sup>3,14</sup>, Ferial Louanchi<sup>15</sup>, Liliane Merlivat<sup>1</sup>, Léa Olivier<sup>1,16</sup>,  
10 Anne Petrenko<sup>13</sup>, Sébastien ~~Petton~~<sup>16</sup> Petton<sup>17</sup>, Mireille Pujon-Pay<sup>7</sup>, Christophe Rabouille<sup>9</sup>,  
11 Gilles Reverdin<sup>1</sup>, Céline Ridame<sup>1</sup>, Aline Tribollet<sup>1</sup>, Vincenzo Vellucci<sup>8,12</sup>, Thibaut Wagener<sup>13</sup>,  
12 Cathy Wimart-Rousseau<sup>13,17,18</sup>

Mis en forme : Exposit

13  
14 <sup>1</sup> Laboratoire LOCEAN/IPSL, Sorbonne Université-CNRS-IRD-MNHN, Paris, 75005, France

15 <sup>2</sup> OSU Ecce Terra, Sorbonne Université-CNRS, Paris, 75005, France

16 <sup>3</sup> Sorbonne Université, CNRS, Laboratoire d'Océanographie de Villefranche, LOV, F-06230 Villefranche-sur-  
17 Mer, France

18 <sup>4</sup> Remote Sensing and Satellite Research Group, School of Earth and Planetary Sciences, Curtin University,  
19 Perth WA 6845, Australia

20 <sup>5</sup> School of Marine Sciences, University of Maine, Orono, USA

21 <sup>6</sup> Station Biologique de Roscoff, UMR 7144 – EDYCO-CHIMAR, Roscoff, France

22 <sup>7</sup> Sorbonne Université, CNRS, Laboratoire d'Océanographie Microbienne, LOMIC, F-66650 Banyuls-sur-Mer,  
23 France

24 <sup>8</sup> Sorbonne Université, CNRS, OSU Station Marines, STAMAR, Paris, F-75006, France

25 <sup>9</sup> Laboratoire des Sciences du Climat et de l'Environnement, LSCE/IPSL, UMR 8212 CEA- CNRS-UVSQ,  
26 Université Paris-Saclay, 91191 Gif-sur-Yvette, France

27 <sup>10</sup> CEFREM, CNRS-Université de Perpignan Via Domitia, 52 Avenue Paul Alduy, 66860 Perpignan, France

28 <sup>11</sup> Institute for Sustainable Development and International Relations, Sciences Po, 27 rue Saint Guillaume, F-  
29 75007 Paris, France

30 <sup>12</sup> Sorbonne Université, CNRS, Institut de la Mer de Villefranche, IMEV, Villefranche-sur-Mer, F-06230, France

31 <sup>13</sup> Aix Marseille Univ, Université de Toulon, CNRS, IRD, MIO, Marseille, France

32 <sup>14</sup> Research Federation for the study of Global Ocean Systems Ecology and Evolution, FR2022/Tara GOSEE,  
33 75000, Paris, France.

34 <sup>15</sup> CVRM: Laboratoire de Conservation et de Valorisation des Ressources Marines, Ecole Nationale Supérieure  
35 des Sciences de la Mer et de l'Aménagement du Littoral (ENSSMAL), Station de recherche de Sidi Fredj,  
36 Algeria

37 <sup>16,16</sup> Alfred Wegener Institute, Helmholtz Centre for Polar and Marine Research, Bremerhaven, Germany

38 <sup>17</sup> Ifremer, Univ Brest, CNRS, IRD, LEMAR, F-29840 Argenton, France

39 <sup>17</sup> ~~Marine Biogeochemistry~~,<sup>18</sup> GEOMAR Helmholtz Centre for Ocean Research Kiel, 24105 Kiel, Germany

40 \* Passed away 14/3/2021

41 *Correspondence to:* Nicolas Metzl (nicolas.metzl@locean.ipsl.fr)

42 **Abstract.** Total alkalinity ( $A_T$ ) and ~~total~~ dissolved inorganic carbon ( $C_T$ ) in the oceans are important properties  
43 to understand the ocean carbon cycle and its link with climate global change (ocean carbon sinks and sources) ~~or~~  
44 ~~global change~~ (-, ocean acidification-) and ultimately find carbon based solutions or mitigation procedures  
45 (marine carbon removal). We present a data-based database of more than 44 400  $A_T$  and  $C_T$  observations along  
46 with basic ancillary data (time and space location, depth, temperature and salinity) in various ocean regions  
47 obtained since 1993 mainly in the frame of French projects. This includes both surface and water column data

Mis en forme : Barré

48 | acquired in open oceans, coastal zones and in the Mediterranean Sea and either from time-series or punctual  
49 | cruises. Most  $A_T$  and  $C_T$  data in this synthesis were measured from discrete samples using the same closed-cell  
50 | potentiometric titration calibrated with Certified Reference Material, with an overall accuracy of  $\pm 4 \mu\text{mol kg}^{-1}$   
51 | for both  $A_T$  and  $C_T$ . ~~Given the lack of observations in the Indian and Southern Oceans, we added sea surface~~  
52 | ~~underway  $A_T$  and  $C_T$ . The data obtained in 1998–2018 in the frame of OISO cruises and in 2019 during the CLIM-~~  
53 | ~~EPARSES cruise measured onboard using the same technique. Separate are provided in two separate~~ datasets for  
54 | the global ocean, and for the Mediterranean Sea ~~are provided in a single format~~ (<https://doi.org/10.17882/95414>,  
55 | Metzl et al., 2023) that offers a direct use for regional or global purposes, e.g.  $A_T$ /Salinity relationships, long-  
56 | term  $C_T$  estimates, constraint and validation of diagnostics  $C_T$  ~~and~~  $A_T$  reconstructed fields or ocean carbon and  
57 | coupled climate/carbon models simulations, as well as data derived from ~~BG-ARGO~~ Biogeochemical-Argo  
58 | (~~BGC-Argo~~) floats. When associated with other properties, these data can also be used to calculate pH, fugacity  
59 | of  $\text{CO}_2$  ( $f\text{CO}_2$ ) and other carbon ~~systemssystem~~ properties to derive ocean acidification rates or air-sea  $\text{CO}_2$   
60 | fluxes.

Mis en forme : Barré

Mis en forme : Couleur de police :  
Automatique

Mis en forme : Couleur de police :  
Automatique

Mis en forme : Police :Italique

61

## 62 | 1 Introduction

63

64 | Since 1750, humans activities have added 700 ( $\pm 75$ ) PgC anthropogenic carbon dioxide to the  
65 | atmosphere by burning fossil fuels, producing cement and changing land use (Friedlingstein et al., 2022) driving  
66 | up the atmospheric carbon dioxide ( $\text{CO}_2$ ) concentration level and leading to unequivocal global warming change.  
67 | The ocean plays a major role in reducing the impact of climate change by absorbing more than 90% of the  
68 | excess heat in the climate system (Cheng et al., 2020; von Schuckmann et al., 2020, 2023; IPCC, 2022) and about  
69 | 25% of human released  $\text{CO}_2$  (Friedlingstein et al., 2022). However, the oceanic  $\text{CO}_2$  uptake changes the  
70 | chemistry of seawater reducing its buffering capacity (Revelle and Suess, 1957; Jiang et al., 2023a) and leading  
71 | to a process known as ocean acidification with potential impacts on marine organisms (Fabry et al., 2008; Doney  
72 | et al., 2009, 2020; Gattuso et al., 2015). With atmospheric  $\text{CO}_2$  concentrations, surface ocean temperature and  
73 | ocean heat content, sea-level, sea-ice and glaciers, the ocean acidification (decrease of pH) is now recognized by  
74 | the World Meteorological Organization as one of the 7 key properties for global climate indicators (WMO,  
75 | 2018). In the frame of the 2030 Agenda, the United Nations established a set of Sustainable Development Goals  
76 | (SDG; United Nations, 2020), including a goal dedicated to the ocean (SDG 14, “Life below water”) which calls  
77 | to “conserve and sustainably use the oceans, seas and marine resources for sustainable development”. Ocean  
78 | acidification is specifically referred in the SDG indicator 14.3.1 coordinated at the Intergovernmental  
79 | Oceanographic Commission (IOC) of UNESCO. Observing the carbonate system in the oceans and marginal  
80 | seas and understanding how this system changes over time is thus highly relevant not only to quantify the global  
81 | ocean carbon budget, the anthropogenic  $\text{CO}_2$  inventories or ocean acidification rates, but also to understand and  
82 | simulate the processes that govern the complex  $\text{CO}_2$  cycle in the ocean and to better predict the future evolution  
83 | of climate and global changes (Eyring et al., 2016; Kwiatkowski et al., 2020; Jiang et al., 2023a).

84 | The number and quality of ocean  $f\text{CO}_2$ ,  $A_T$ ,  $C_T$  and pH measurements hashave increased substantially  
85 | over the past few decades. Quality-controlled observations are now regularly assembled in global data syntheses  
86 | such as SOCAT (Surface Ocean  $\text{CO}_2$  Atlas, Pfeil et al., 2013; Bakker et al., 2014, 2016) and GLODAP (Global  
87 | Ocean Data Analysis Project, Key et al., 2004; Olsen et al., 2016, 2019, 2020; Lauvset et al., 2021, 2022). These  
88 | datasets allow evaluation of properties trends in the global ocean, including the change of the ocean  $\text{CO}_2$  sink  
89 | (e.g. Wanninkhof et al., 2013; Friedlingstein et al., 2022; Watson et al., 2020), anthropogenic  $\text{CO}_2$  inventories

90 (e.g. Sabine et al., 2004; Khatiwala et al., 2013; Gruber et al., 2019) and ocean acidification (Lauvset et al.,  
91 2015, 2020; Jiang et al., 2019); [Feely et al., 2023](#); [Ma et al., 2023](#)). Thanks to ~~the GLODAP data base, publicly~~  
92 [available consistent and quality controlled databases](#) new methods were recently developed ([Carter et al., 2016](#);  
93 [Sauzède et al., 2017](#); [Bittig et al., 2018](#)) to reproduce  $A_T$  and  $C_T$  distributions from other properties like  
94 temperature, salinity and oxygen more often observed in the water column especially from autonomous floats  
95 ([Claustre et al., 2020](#); [Mignot et al., 2023](#)). These methods (named CANYON-B and CONTENT, [Bittig et al.,](#)  
96 [2018](#)) are now also used to help decisions on GLODAP data quality control or to fill in observational gaps  
97 ([Olsen et al., 2019, 2020](#); [Tanhua et al., 2019, 2021](#)). The GLODAP data-products were also successfully used  
98 to construct new global ocean  $A_T$  and  $C_T$  climatological monthly fields in surface and water column using neural  
99 network method (e.g. [Broullón et al., 2019, 2020](#)).

Mis en forme : Police :+Corps  
(Calibri), 11 pt

100 Following pioneer works that produced various global-ocean climatologies of the sea-surface carbonate  
101 system ([Millero et al., 1998](#); [Lee et al., 2000, 2006](#); [Takahashi et al., 2002, 2009, 2014](#); [Sasse et al., 2013](#); [Jiang](#)  
102 [et al., 2019](#)), the coupling of  $fCO_2$  data (from SOCAT) and  $A_T$  data (from GLODAP) now enables reconstruction  
103 of the full carbonate system in the surface ocean at monthly scale to investigate temporal trends at decadal scale  
104 (e.g. [Gregor and Gruber, 2021](#); [Keppler et al., 2023](#)).

105 International projects such as SOCAT and GLODAP offer important way to synthesize ocean carbon  
106 data. In these projects, each observation is quality controlled offering to users high quality observations for  
107 regional or global analysis, either for processes analysis or to constraint or validate of ocean and coupled  
108 climate/carbon models (CMIP6, e.g. [Lerner et al., 2021](#)). SOCAT is a publicly available synthesis product  
109 initiated in 2007 ([Metzl et al., 2007](#)) for quality-controlled, surface ocean  $fCO_2$  (fugacity of carbon dioxide)  
110 observations made by the international marine carbon research community ([Bakker et al., 2016](#)). The first  
111 SOCAT version was released in 2011 ([Pfeil et al., 2013](#); [Sabine et al., 2013](#)), followed by 6 SOCAT versions  
112 ([Bakker et al., 2014, 2016](#)). The last version in 2023 includes more than 40 million  $fCO_2$  data with accuracy  
113 better than 5  $\mu atm$  ([Bakker et al., 2023](#)). One important product from SOCAT is the use of data to estimate  
114 global air-sea  $CO_2$  fluxes based on reconstructed  $pCO_2$  fields (e.g. ~~SOCOM project~~, Surface Ocean  $pCO_2$   
115 Mapping Intercomparison, [SOCOM](#), [Rödenbeck et al., 2015](#)). Since 2015, these results are included each year  
116 for the global carbon budget ([Le Quere et al., 2015](#); [Friedlingstein et al., 2022](#)).

Mis en forme : Police :Italique

Mis en forme : Police :Italique

Mis en forme : Police :Italique

Mis en forme : Police :Italique

Mis en forme : Couleur de police :  
Automatique

117 On the other hand, following WOCE/JGOFS era in the 90s when almost all observations were started to  
118 be synthesized in a specific recommended format ([Joyce and Corry, 1994](#)), GLODAP focusses on water-column  
119 carbon observations (and other properties). Following the original GLODAP data-product ([Key et al., 2004](#)), the  
120 project accumulated many new quality controlled observations. One important achievement from GLODAP is  
121 the use of data to estimate the anthropogenic  $CO_2$  inventory or its change over decades ([Sabine et al., 2004](#);  
122 [Gruber et al., 2019](#)). Both products, SOCAT and GLODAP, are relevant tools to detect oceanic acidification  
123 rates ([Lauvset et al., 2015](#); [Jiang et al., 2019](#); [Feely et al., 2023](#); [Ma et al., 2023](#)).

124 Although these projects include many international ocean observations there are ocean  $CO_2$  related  
125 observations all around the world (published or not published), such as total alkalinity and dissolved inorganic  
126 carbon, ~~that are~~ not included in SOCAT or GLODAP. This is because SOCAT accepts and controls only  $fCO_2$   
127 data, whereas GLODAP includes and controls water-columns data mainly from WOCE/GO-SHIP/CLIVAR  
128 cruises. It should be noticed that many ocean carbon observations in various formats can be also found in  
129 dedicated [data-basedatabase](#) such as NCEI/OCADS (former CDIAC-Ocean, [Jiang et al., 2013b, 2023b](#),  
130 <https://www.ncei.noaa.gov/products/ocean-carbon-acidification-data-system>), PANGAEA  
131 (<https://www.pangaea.de/>) or [SeaNoeSeano](#) (<https://www.seano.org/>). In this context it is recommended to

Mis en forme : Couleur de police :  
Automatique

Mis en forme : Couleur de police :  
Automatique

132 progress in data synthesis of the ocean carbon observations that would offer new high quality products for the  
133 community (e.g. for GOA-ON, [www.goa-on.org](http://www.goa-on.org), IOC/SDG 14.1.3, <https://oa.iode.org/>, Tilbrook et al., 2019).

134 In this work, we present a synthesis of more than 44 400  $A_T$  and  $C_T$  observations obtained over the  
135 1993-2022 period during various cruises or at time-series stations mainly supported by French projects. This  
136 dataset merges observations measured with the same instruments thus being analytically coherent. Most of the  
137 data have accuracy better than  $\pm 4 \mu\text{mol kg}^{-1}$ , i.e. between the climate ( $\pm 2 \mu\text{mol kg}^{-1}$ ) and weather ( $\pm 10 \mu\text{mol kg}^{-1}$ )  
138 goals (Newton et al., 2015; Bockmon and Dickson, 2015). Hereafter this dataset will be cited as **SNAPO-CO2-**  
139 **VI**. We describe the data assemblage and associated quality control and discuss some potential uses of this  
140 dataset.

141

## 142 2 Data collections

143

144 The time series projects and research cruises from which data were collated are listed in Table 1 with  
145 references in the Supplementary file ([SNAPO-CO2-cruisesTable S1](#)) and the sampling locations displayed in  
146 Figure 1. Sampling was performed either from CTD-Rosette casts (Niskin bottles) or from the ship's seawater  
147 supply (intake at about 5m depth depending the ship and swell). Samples collected in 500 mL borosilicate glass  
148 bottles were poisoned with 100 to 300  $\mu\text{L}$  of  $\text{HgCl}_2$  depending on the cruises, closed with greased stoppers  
149 (Apiezon®) and held tight using elastic band following the SOP protocol (Dickson et al., 2007). Some samples  
150 were also collected in 500 mL bottles closed with screw caps. After completion of each cruise, discrete samples  
151 were returned back to the LOCEAN laboratory (Paris, France) and stored in a dark room at 4 °C before analysis  
152 generally within 2-3 months after sampling (sometimes within a week). Some samples were also measured for  
153 specific processes studies on benthic corals (e.g. Maier et al., 2012; McCulloch et al., 2012) or for mesocosm  
154 and culture experiments but the data are not included in this synthesis as they do not represent natural ocean state  
155 (e.g. addition of Sahara dust during the DUNE project, Ridame et al., 2014).

156 As opposed to  $p\text{CO}_2$ , surface  $A_T$  or  $C_T$  observations are generally obtained from discrete sampling  
157 (measured onboard or onshore). Few cruises offer sea-surface semi-continuous  $A_T$  or  $C_T$  observations (e.g. Metzl  
158 et al., 2006) but new instrumental developments (Seilmann et al., 2020) now enable  $A_T$  measurements on **SOOP**  
159 **lines**, Ship of Opportunity Program (Seilmann et al., 2020) **lines** (SOOP). In addition to discrete samples analyzed  
160 for various projects conducted mainly in the North Atlantic, Tropical Atlantic, Tropical Pacific, Mediterranean  
161 sea and coastal regions (Table 1), we complemented this synthesis with  $A_T$  and  $C_T$  surface observations obtained  
162 in the Indian and Southern oceans during the OISO cruises in 1998-2018 (Metzl et al., 2006; Leseurre et al.,  
163 2022; data also available at NCEI/OCADS: [www.nodc.noaa.gov/ocads/oceans/VOS\\_Program/OISO.html](http://www.nodc.noaa.gov/ocads/oceans/VOS_Program/OISO.html)) and  
164 the recent CLIM-EPARSEES cruise conducted in the Mozambique Channel in April 2019 (Lo Monaco et al.,  
165 2020, 2021). For OISO cruises the water-column observations are part of the CARINA (CARbon IN the  
166 Atlantic) and GLODAP synthesis products (Lo Monaco et al., 2010; Olsen et al., 2016, 2019, 2020) and not  
167 included here. Excepted when specified, all data in this synthesis were obtained using the same technique used  
168 either in laboratory or at sea (for OISO 1998-2018 and CLIM-EPARSEES 2019 cruises).

169

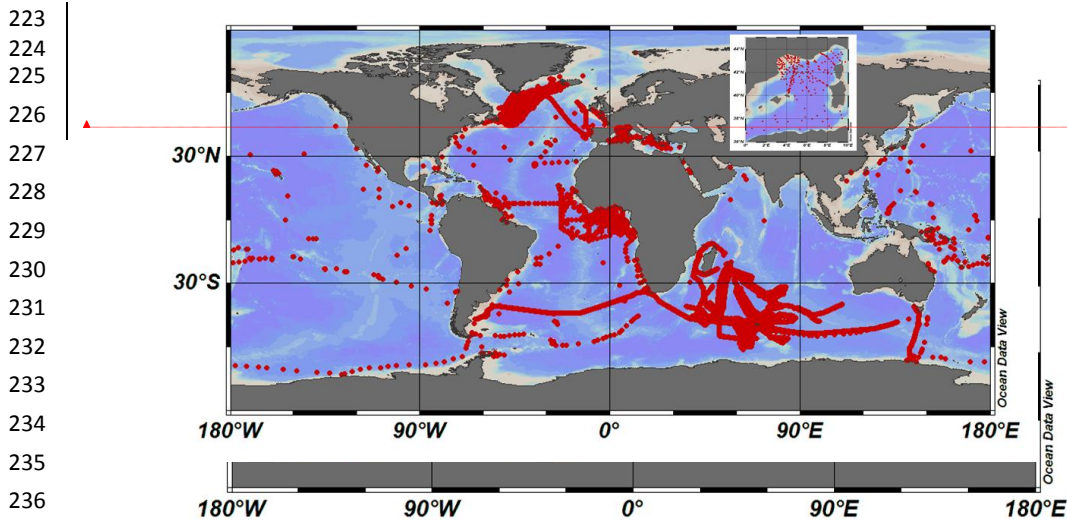
Mis en forme : Police :Italique

170 | **Table 1:** List of cruises in the SNAPO-CO2-v1 dataset. This is organized by region: Global Ocean and coastal  
 171 | zones, and Mediterranean Sea (MedSea). See Tables S1, S2, S4 and S4 in the Supplementary Material for a list  
 172 | of laboratories, of CRMs used, for references and for DOI of cruises. Nb = the number of data for each cruise or  
 173 | time-series. \* indicates the measurements at sea (surface underway)

Mis en forme : Couleur de police : Violet

Cruise/Project	Start	End	Region	Sampling	Nb	
179	AWIPEV	2015	2021	Arctic	Surface and sub-surface	195
180	SURATLANT+RREX	1993	2017	North Atlantic	Surface	2832
181	OVIDE	2006	2018	North Atlantic	Surface, Water Column	397
182	STRASSE	2012		North Atlantic	Water Column	205
183	EUREC4A-OA	2020		North Atlantic	Surface, Water Column	135
184	PROTEUS	2010		North Atlantic	Water Column	27
185	CHANNEL	2012	2015	English Channel	Surface	696
186	SOMLIT-Brest	2008	2019	Coastal North Atl	Surface	1174
187	SOMLIT-Roscoff	2009	2019	Coastal North Atl	Surface and 60m	801
188	ECOSCOPIA	2017	2019	Coastal North Atl	Surface	67
189	PENZE	2011	2020	River Brittany	Surface and sub-surface	148
190	AULNE	2009	2010	River Brittany	Surface	27
191	ELORN	2009	2009	River Brittany	Surface	28
192	BIOZAIRE	2003	2004	Trop Atlantic	Water Column	87
193	EGEE	2005	2007	Trop Atlantic	Surface	199
194	PIRATA-FR	2009	2017	Trop Atlantic	Surface, Water Column	513
195	PLUMAND	2007		Trop Atlantic	Surface	38
196	OUTPACE	2015		Trop Pacific	Water Column	240
197	PANDORA	2012		Solomon Sea	Water Column	178
198	TARA-Pacific	2016	2018	Trop Pac, <del>NATL</del> North Atl	Surface and sub-surface	325
199	TARA-Ocean	2009	2012	Global Ocean	Surface + 400m	123
200	TARA-Microbiome	2021	2022	Atlantic	Surface, Water Column	216
201	ACE	2016	2017	Southern Ocean	Surface, Water Column	135
202	MOBYDICK	2019		Southern Ocean	Water Column	64
203	CLIM-EPARSES *	2019		Indian	Surface	790
204	OISO *	1998	2018	South Indian	Surface	24950
205						
206	DYFAMED	1998	2017	MedSea	Water Column	2118
207	BOUSSOLE	2014	2019	MedSea	Surface + 10m	172
208	SOMLIT-PointB	2007	2015	MedSea Coastal	Surface + 50m	2397
209	ANTARES	2010	2016	MedSea	Water Column	502
210	MOLA	2010	2013	MedSea Coastal	Water Column	66
211	SOLEMIO	2016	2018	MedSea Coastal	Water Column	212
212	MOOSE-GE	2010	2019	MedSea	Water Column	1847
213	LATEX	2010		MedSea	Water Column	51
214	CARBORHONE	2011	2012	MedSea	Water Column	706
215	CASCADE	2011		MedSea	Water Column	218
216	DEWEX	2013		MedSea	Water Column	367
217	SOMBA	2014	2014	MedSea	Water Column	203
218	AMOR-BFLUX	2015		MedSea Coastal	Water Column	6
219	PEACETIME	2017	2017	MedSea	Water Column	233
220	PERLE	2018	2021	MedSea	Water Column	805

221  
222



Mis en forme : Police :Gras, Couleur de police : Automatique  
 Mis en forme : Gauche

Figure 1: Locations of  $A_T$  and  $C_T$  data (1993-2022) in the Global Ocean and the Western Mediterranean Sea (white box, insert-) in the SNAPO-CO2-v1 dataset. Figure produced with ODV (Schlitzer, 2018).

### 3 Method, accuracy, reproducibility, inter-comparison, repeatability, inter-comparison and quality control

#### 3.1 Method and accuracy

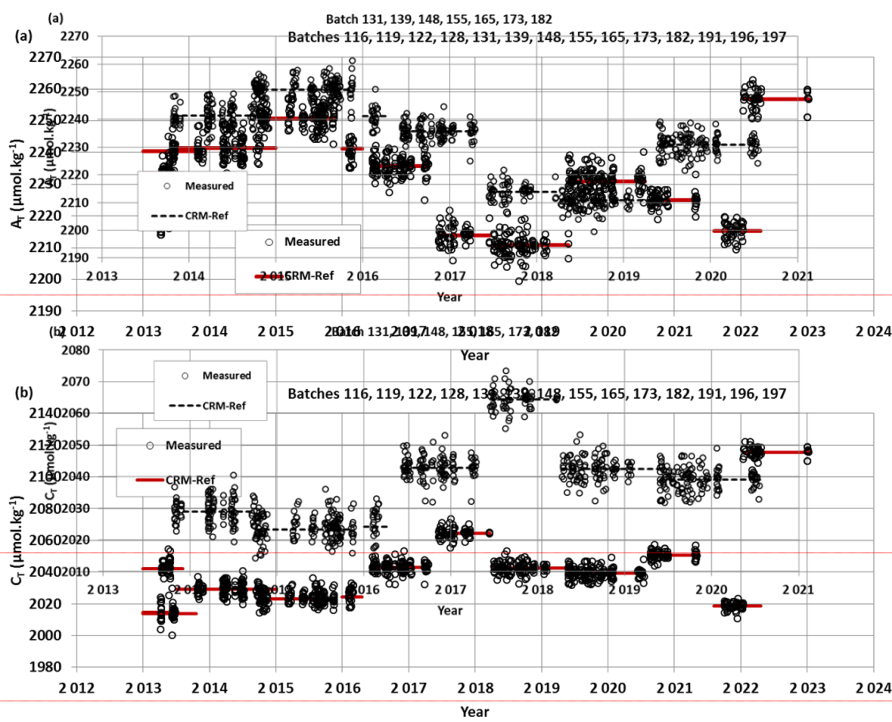
Mis en forme : Police :Gras

Since 2003, the discrete samples returned back at SNAPO-CO2 Service facilities (LOCEAN, Paris), were analyzed simultaneously for  $A_T$  and  $C_T$  by potentiometric titration using a closed cell (Edmond, 1970; Goyet et al., 1991). Except for the same technique was used at sea for surface water underway measurements during OISO and CLIM-EPARSEs cruises (indicated by \* in Table 1). For two time series, the dataset also includes measurements obtained before 2000 using other techniques: the DYFAMED time-series observations measured between in 1998 and 2000 in the Mediterranean Sea (Copin-Montégut and Bégovic, 2002; Coppola et al., 2020; Lange et al., 2023) and the SURATLANT time-series values acquired from 1993 to 1997 in the North Atlantic subpolar gyre (Reverdin et al., 2018) and samples measured. We also include  $A_T$  data in the river Penzé (Brittany) in 2019-2020 (Yann Bozec, SBR/Roscoff, pers. comm.), all discrete samples were measured at LOCEAN laboratory in Paris (SNAPO-CO2 Service facilities) using the same technique.  $A_T$  and  $C_T$  were analyzed simultaneously (comm.).

by potentiometric titration using a closed cell (Edmond, 1970; Goyet et al., 1991). In the late 1980s the so-called “JGOFS-IOC Advisory Panel on Ocean CO2” recommended the need for standard analysis protocols and for developing Certified Reference Materials (CRMs) for inorganic carbon measurements (Poisson et al., 1990; UNESCO, 1990, 1991). The CRMs were provided to international laboratories by Pr. A. Dickson (Scripps Institution of Oceanography, San Diego, USA), starting in 1990 for  $C_T$  and 1996 for  $A_T$ , respectively. These CRMs were thus always available to us and used to calibrate the measurements (CRM Batch numbers used for each cruise are listed in Supplementary file (Table S2). The concentrations of CRMs we used vary between 2193 and 2426  $\mu\text{mol kg}^{-1}$  for  $A_T$  and between 1968 and 2115  $\mu\text{mol kg}^{-1}$  for  $C_T$  corresponding to the range of

264 concentrations observed in open ocean water. The CRMs accuracy, as indicated in the certificate for each Batch,  
 265 is around  $\pm 0.5 \mu\text{mol kg}^{-1}$  for both  $A_T$  and  $C_T$  ([www.nodc.noaa.gov/ocads/oceans/Dickson\\_CRM/batches.html](http://www.nodc.noaa.gov/ocads/oceans/Dickson_CRM/batches.html)).

266 Results of analyses performed on 724965 CRM bottles (different Batches) in 2013-20202023 are  
 267 presented in Figure 2. The standard-deviations of the differences of measurements were on average around  $\pm 3.5$   
 268  $\mu\text{mol kg}^{-1}$  for both  $A_T$  and  $C_T$ . For unknown reasons, the differences were occasionally up to 10-15  $\mu\text{mol kg}^{-1}$   
 269 (0.8% of the data, Figure S2). These few CRM measurements were discarded for the data processing. On  
 270 average, and excluding some outliers, standard-deviations of the differences for 9851090 CRM analyses were  
 271  $\pm 2.9571 \mu\text{mol kg}^{-1}$  for  $A_T$  and  $\pm 3.30286 \mu\text{mol kg}^{-1}$  for  $C_T$ , respectively. We did not detect any specific signal for  
 272 these CRM analyses (e.g., larger uncertainty depending on the Batch number or temporal drifts during analyses,  
 273 Figure 2) but for some cruises and specific series of samples analyzed over 2 to 7 consecutive days, the accuracy  
 274 based on CRMs could be slightly better than  $3 \mu\text{mol kg}^{-1}$  ( $\pm 2.5 \mu\text{mol kg}^{-1}$  for both  $A_T$  and  $C_T$ , (e.g. Marrec et al.,  
 275 2014; Touratier et al., 2016; Ganachaud et al., 2017; Wimart-Rousseau et al., 2020a).



Mis en forme : Police :11 pt, Gras  
 Mis en forme : Gauche, Interligne :  
 Multiple 1,15 li

Mis en forme : Police :10 pt

Mis en forme : Couleur de police :  
 Violet

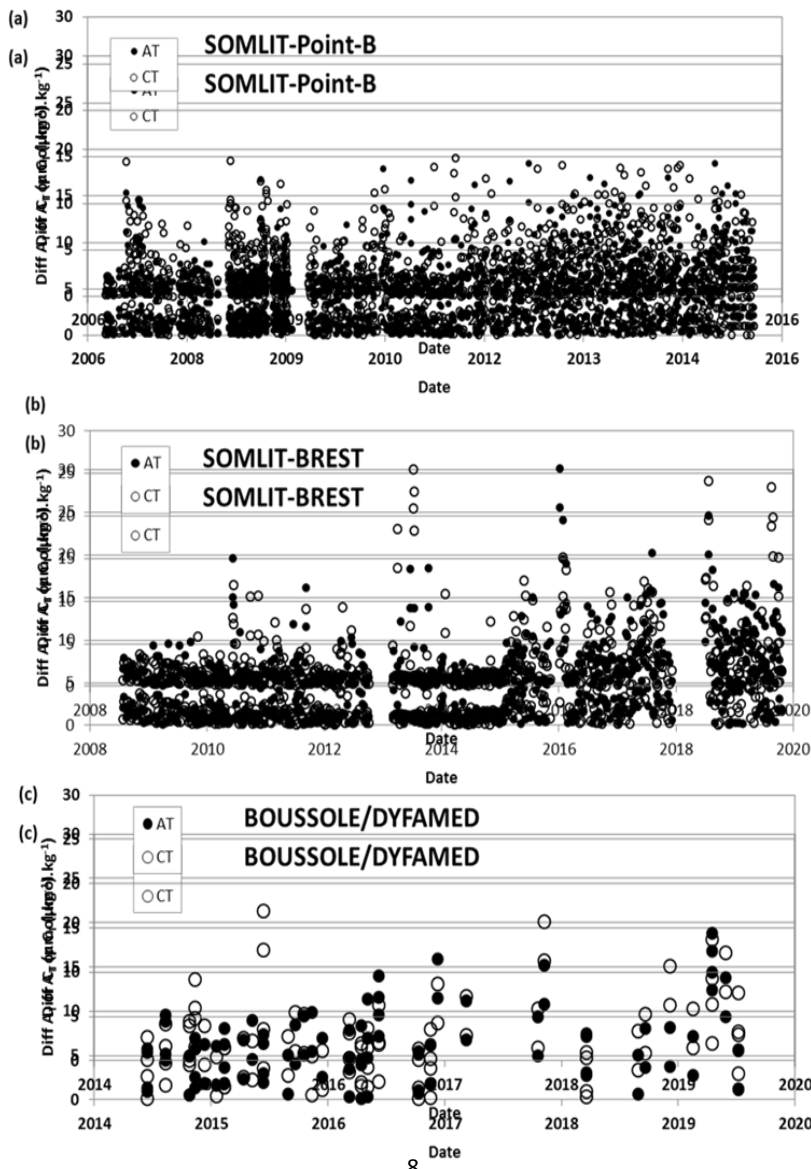
299 **Figure 2:**  $A_T$  (a) and  $C_T$  (b) analyses for different CRM Batches measured in 2013-20202023. For these 724965  
 300 analyses the mean and standard-deviations of the differences with the CRM reference were  $-0.081 (\pm 3.354)$   
 301  $\mu\text{mol.kg}^{-1}$  for  $A_T$  and  $0.451 (\pm 3.647) \mu\text{mol.kg}^{-1}$  for  $C_T$ .

### 3.2 Reproducibility and repeatability

#### 3.2 Repeatability

307 For some projects, duplicates have been regularly sampled (SOMLIT-Point-B, SOMLIT-BREST,  
 308 BOUSSOLE/DYFAMED) or replicate bottles sampled at selected depths at fixed stations during the cruises (e.g.  
 309 OUTPACE-2015, Wagener et al., 2018; SOMBA-2014, Keraghel et al., 2020). Results of  $A_T$  and  $C_T$

310 reproducibility or repeatability are synthesized in Table 2. and Figure 3 shows example of regular duplicates  
 311 from the times-series SOMLIT-Point-B in the coastal Mediterranean Sea (Kapsenberg et al., 2017), SOMLIT-  
 312 Brest in the Bay of Brest, coastal Iroise Sea (Salt et al., 2016) and BOUSSOLE/DYFAMED in the Ligurian Sea  
 313 (Merlivat et al., 2018; Golbol et al., 2000, 2020). For the 26 OISO cruises conducted between 1998 and 2018  
 314 and the CLIM-EPARSES cruise in April 2019 (Lo Monaco et al., 2020, 2021), the repeatability was evaluated  
 315 from duplicate analyses (within 20 minutes time) of continuous sea surface underway sampling at the same  
 316 location (when the ship was stopped). Similarly to what was found for the CRM measurements (Figure S2),  
 317 differences in duplicates are occasionally higher than 10-15  $\mu\text{mol kg}^{-1}$  (Figure 3) but most of the duplicates for  
 318 all projects are within 0 to 3  $\mu\text{mol kg}^{-1}$ . Based on the CRM analyses and replicates for different projects,  
 319 different regions and different periods, we estimated the accuracy for both  $A_T$  and  $C_T$  of  $\pm$  data to be consistent to  
 320 better than 4  $\mu\text{mol kg}^{-1}$ .





359  
360  
361  
362  
363  
364  
365  
366  
367

**Figure 3:** Results of duplicate  $A_T$  and  $C_T$  analyses from the time-series (a) SOMLIT-Point-B in the coastal Mediterranean Sea (Kapsenberg et al., 2017), (b) SOMLIT-BREST in the Bay of Brest, coastal Iroise Sea (Salt et al., 2016 and unpublished) and (c) BOUSSOLE/DYFAMED in the Ligurian Sea (Merlivat et al., 2018; Golbol et al., 2020). The plots show differences in duplicates for both  $A_T$  (filled circles) and  $C_T$  (open circles). Standard-deviations of these duplicates are listed in Table 2.

368  
 369 | **Table 2: Reproducibility/Repeatability** of  $A_T$  and  $C_T$  analyses for cruises with duplicate analysis. The results are  
 370 | expressed as the standard-deviations (Std) of the analysis of replicated samples. Nb = the number of replicates  
 371 | for each Time-series or Cruise. See Figure 4 for the results of regular duplicates for 3 Time-series (SOMLIT-  
 372 | Point-B, SOMLIT-BREST, and BOUSSOLE). For OISO and CLIM-EPARSEs cruises the results correspond to  
 373 | repeated measurements from continuous sea surface underway sampling at the same location (i.e. within 20  
 374 | minutes time and when the ship was stopped): (a). For the 26 OISO cruises (1998-2018) and for simplicity we  
 375 | list the mean repeatability obtained for all cruises. Detail for each OISO cruise could be consulted in the  
 376 | associated metadata online at NCEI/OCADS, [www.nodc.noaa.gov/ocads/oceans/VOS\\_Program/OISO.html](http://www.nodc.noaa.gov/ocads/oceans/VOS_Program/OISO.html)  
 377

Project-Cruise	Nb	Std $A_T$ $\mu\text{mol kg}^{-1}$	Std $C_T$ $\mu\text{mol kg}^{-1}$	Reference
OUTPACE	12	3.64	3.68	Wagener et al. (2018)
SOMBA	13	2.00	3.30	Keraghel et al. (2020)
SOMLIT-Point-B	786	2.63	3.10	Kapsenberg et al. (2017)
SOMLIT-Brest	446	3.34	3.67	Salt et al. (2016) + unpub
BOUSSOLE	48	3.47	4.02	Merlivat et al. (2018); Golbol et al. (2020)
CLIM-EPARSEs	122	2.20	2.30	Lo Monaco et al. (2020, 2021)
OISO 1998-2018	1162	2.06	2.28	Metzl et al. (2006) and (*) <b>(b)</b>

391  
 392 | ~~(\*) Data (a) See Figure 3 for the results of regular duplicates for 3 time-series (SOMLIT-Point-B, SOMLIT-BREST,~~  
 393 | ~~and BOUSSOLE).~~  
 394 | ~~(b) Metadata and data available at [www.nodc.noaa.gov/ocads/oceans/VOS\\_Program/OISO.html](http://www.nodc.noaa.gov/ocads/oceans/VOS_Program/OISO.html)~~  
 395

### 396 3.3 Inter-comparisons

397  
 398 | Inter-comparisons of measurements performed with different technics help to evaluate the quality of the  
 399 | data and detect potential ~~shifts (if any) biases~~ when merging the data in the same region obtained by different  
 400 | laboratories at different periods. This is especially important to interpret long-term trends of  $A_T$  and  $C_T$  as well as  
 401 | for  $p\text{CO}_2$  and pH calculated with  $A_T/C_T$  pairs. For ocean acidification studies, this also refers to the “climate  
 402 | goal” for which an accuracy for  $A_T$  and  $C_T$  better than  $\pm 2 \mu\text{mol kg}^{-1}$  is needed (Newton et al., 2015; Tilbrook et  
 403 | al., 2019). ~~Such inter-comparison thus helps to reflect the quality of the data to achieve either the so-called~~  
 404 | ~~“weather goal” (for  $A_T$  and  $C_T$ ,  $\pm 10 \mu\text{mol kg}^{-1}$ ) or the “climate goal” ( $\pm 2 \mu\text{mol kg}^{-1}$ ) (Bockmon and Dickson,~~  
 405 | ~~2015).~~ For the projects in this data synthesis, inter-laboratory comparisons were performed occasionally and  
 406 | summarized below.

#### 408 3.3.1 CHANNEL project

409  
 410 | As part of the time-series CHANNEL (2012-2015) in the Western English Channel, Marrec et al.  
 411 | (2014) analyzed surface samples collected bi-monthly in 2011-2013.  $A_T$  analyses were performed with a TA-  
 412 | ALK-2 system (Appolo SciTech.) while  $C_T$  measurements were acquired with an AIRICA system (Marianda  
 413 | Inc.) Based on CRM analyses (Batch #92) the accuracy was estimated  $\pm 3 \mu\text{mol kg}^{-1}$  for  $A_T$  and  $\pm 1.5 \mu\text{mol kg}^{-1}$   
 414 | for  $C_T$  (Marrec et al., 2014). When comparing with the samples measured at LOCEAN/Paris for the year 2012,  
 415 | Marrec et al. (2014) concluded that between the two methods the concentrations were within  $\pm 2 \mu\text{mol kg}^{-1}$  and  
 416 |  $\pm 3 \mu\text{mol kg}^{-1}$  for  $A_T$  and  $C_T$  respectively. This is close to the “climate goal” offering confident results for long-  
 417 | term trend analysis of the carbonate system in this region.  
 418

Mis en forme : Couleur de police : Automatique

Mis en forme : Couleur de police : Automatique

Mis en forme : Police : Italique

### 419 3.3.2 SURATLANT project

420

421 In the frame of the SURATLANT project in the ~~Sub-Polar~~subpolar North Atlantic gyre, some samples  
422 collected at the same time (in 2005, 2006, 2010, 2015, and 2016) were also analyzed onshore for  $A_T$  and/or  $C_T$  by  
423 other laboratories using different technics (e.g. coulometric method) and the results summarized by Reverdin et  
424 al. (2018). For  $C_T$ , the mean (and STD) differences between LOCEAN values and from 4 other laboratories  
425 range between  $-0.7 (\pm 4.6)$  and  $-6.5 (\pm 3.4) \mu\text{mol kg}^{-1}$  depending on the cruise. For  $A_T$  the mean differences with 2  
426 other laboratories range from  $-0.6 (\pm 4.1) \mu\text{mol kg}^{-1}$  to  $+2.3 (\pm 4.8) \mu\text{mol kg}^{-1}$ . ~~These results range between the~~  
427 ~~“climate goal” and the “weather goal”. See Reverdin et al. (2018) for details on these inter-comparisons.~~

428

### 429 3.3.3 OVIDE project

430

431 During OVIDE cruises conducted since 2002 in the North Atlantic along a section from Greenland to  
432 Portugal (Lherminier et al., 2007; Mercier et al., 2015) samples have been taken (since 2006) to complement, for  
433 summer, the SURATLANT time-series in the North Atlantic ~~Sub-Polar~~subpolar gyre (NASPG). The OVIDE  
434 samples at the surface and along the water-column at a few stations were measured back at LOCEAN for  $A_T$  and  
435  $C_T$  (Metzl et al., 2018). This enables us to compare our data with the measurements performed on-board by the  
436 IIM group in Vigo/Spain (e.g. Pérez et al., 2010, 2013, 2018; Vazquez-Rodriguez et al., 2012). The OVIDE data  
437 have been regularly quality controlled in CARINA and GLODAP data products (Velo et al., 2009; Key et al.,  
438 2010; Olsen et al., 2016, 2019, 2020). The results of inter-comparisons are gathered in Table 3. For OVIDE in  
439 2006 we identified (for unknown reason) a large difference between our original  $A_T$  values compared to the  $A_T$   
440 data qualified in GLODAP and we thus corrected our  $A_T$  data by  $+7.2 \mu\text{mol kg}^{-1}$ . However, no correction was  
441 applied for  $C_T$ . For other OVIDE cruises, differences for  $A_T$  range between  $-4.5 (\pm 4.11) \mu\text{mol kg}^{-1}$  and  $-0.05$   
442  $(\pm 3.43) \mu\text{mol kg}^{-1}$  depending on the cruise (i.e.  $A_T$  measured at LOCEAN was always slightly lower than  
443 onboard measurements). For  $C_T$ , we compared our measurements onshore with  $C_T$  values calculated with  $A_T$  and  
444 pH measured onboard. Most of the mean  $C_T$  differences are slightly positive (i.e.  $C_T$  measured at LOCEAN was  
445 always higher, except for 2010). Taking into account all errors associated with the sampling, the transport of  
446 samples, the instrumentations, the data processing, or the calculations for  $C_T$ , ~~using  $A_T$ /pH pairs (around 8.8~~  
447  ~~$\mu\text{mol kg}^{-1}$ , Orr et al., 2018),~~ the comparisons between LOCEAN and IIM data for OVIDE cruises are deemed  
448 acceptable and large differences for both  $A_T$  and  $C_T$  ( $> 4 \mu\text{mol kg}^{-1}$ ) are far from being systematic (Table 3). The  
449 data from SURATLANT and OVIDE can then be merged to complete the time-series in the NASPG in summer  
450 and to better describe the seasonality of the oceanic carbonate system. For example, in 2010, when the North  
451 Atlantic Oscillation (NAO) was strongly negative, the SURATLANT data showed a rapid decrease of  $C_T$   
452 concentrations in the NASPG between early June and August (Figure 4), with  $C_T$  concentrations in August much  
453 lower than other years (Racapé et al., 2014). This leads to a rapid drop in  $f\text{CO}_2$  in 2009-2010, such that the  
454 NASPG was a strong  $\text{CO}_2$  sink (Leseurre et al., 2020). The winter-to-summer seasonal decrease of  $C_T$  in 2010 in  
455 the north NASPG was on average  $-77 \mu\text{mol kg}^{-1}$  (Figure 4) much larger than in the climatology (range  $-50$  to  $-55$   
456  $\mu\text{mol kg}^{-1}$ , Takahashi et al., 2014; Reverdin et al., 2018). The OVIDE data in late June 2010 and SURATLANT  
457 in August 2010 confirmed this signal that was linked to a pronounced primary productivity in that period (Figure  
458 4, Henson et al., 2013; Racapé et al., 2014; Mc Kinley et al., 2018). Notice that for this period no  $\text{pCO}_2/\text{CO}_2$   
459 observations were available in July-September 2010 in SOCAT data-product and the  $A_T/C_T$  data presented here

Mis en forme : Police :Italique

Mis en forme : Police :Italique

460 | could be used to calculate  $p\text{CO}_2/\text{CO}_2$  to complement the  $p\text{CO}_2/\text{CO}_2$  dataset in this region like was done for other  
461 | periods (Mc Kinley et al., 2011).  
462

463  
464  
465  
466  
467  
468  
469  
470  
471  
472  
473  
474  
475  
476  
477  
478  
479  
480  
481  
482  
483  
484

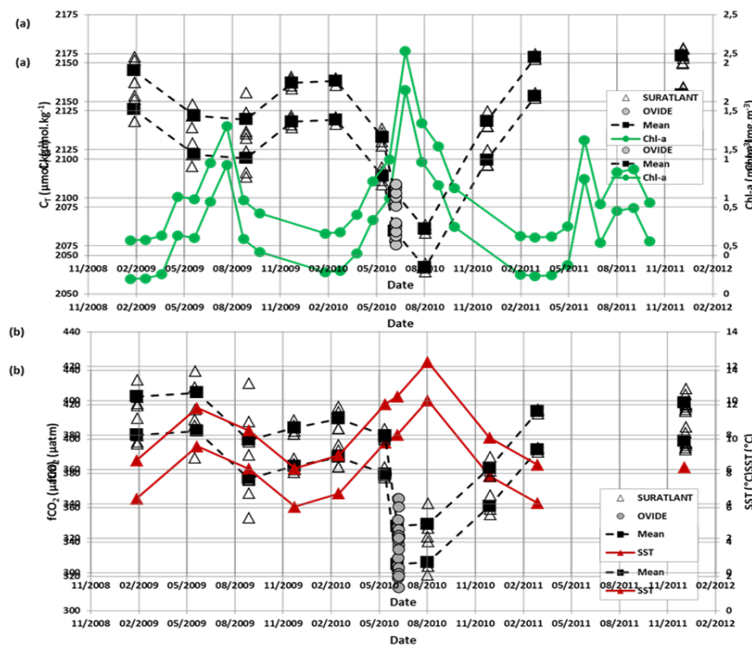


**Figure 4:** (a) Time-series of  $C_T$  concentrations ( $\mu\text{mol.kg}^{-1}$ ) for 2009-2011 in surface waters in the North Atlantic Sub-Polar-subpolar gyre (zone  $59^{\circ}\text{N}$ - $33^{\circ}\text{W}$ ) based on SURATLANT (open triangles) and OVIDE-2010 (grey circles) data. In 2009, SURATLANT data were available in February, June, September and December, while in 2010 data available in March, June, August and December and in 2011 data only available for March and December. The OVIDE data in late June 2010 completed the temporal cycle and confirmed the strong seasonal signal and low  $C_T$  concentrations in summer 2010 not seen in 2009 (or in 2011 as there is no data in summer). The mean observations for each period describe the  $C_T$  seasonal cycles in 2009 and 2010 (Black squares, dashed line). The monthly surface chlorophyll-a concentrations (Chl-a,  $\text{mg.m}^{-3}$ ) averaged in the same region based on MODIS are also shown (Green dots and line) highlighting the high productivity during the summer 2010. Chl-a monthly data extracted from MODIS (Giovanni/NASA, last access 3/5/19). (b): Time-series of  $f\text{CO}_2$  ( $\mu\text{atm}$ ) for the same cruises (same symbols) calculated with  $A_T - C_T / C_T$  and using the  $K_1$ ,  $K_2$  constants from Lueker et al (2000). Mean SST ( $^{\circ}\text{C}$ ) indicated (red triangles). In June 2010 oceanic  $f\text{CO}_2$  decreased by  $53 \mu\text{atm}$  in 2 weeks.

Mis en forme : Police :Italique  
Mis en forme : Police :Italique  
Mis en forme : Police :Italique  
Mis en forme : Police :Italique

**Table 3:** Comparisons of  $A_T$  and  $C_T$  samples measured back at LOCEAN with measurements onboard by IIM Laboratory (F. Pérez, Vigo, Spain) for OVIDE cruises in the North Atlantic. Nb= Number of samples. ND= No Data. The results listed indicate the mean and standard-deviations of the differences (LOCEAN-IIM). For  $A_T$ , IIM values were measured on-board. For  $C_T$ , IIM values were calculated from  $A_T$  and pH both measured onboard. The IIM data were quality controlled and here taken from the GLODAP data-products (Olsen et al, 2016, 2019).

Cruise Year	Nb $A_T$	$A_T$ (LOCEAN) - $A_T$ (IIM) $\mu\text{mol kg}^{-1}$	Nb $C_T$	$C_T$ (LOCEAN) - $C_T$ (IIM) $\mu\text{mol kg}^{-1}$
OVIDE-2006	14	-2.040 ( $\pm 5.849$ ) (*)	14	1.121 ( $\pm 2.495$ )
OVIDE-2008	29	-4.535 ( $\pm 4.111$ )	29	3.768 ( $\pm 3.111$ )
OVIDE-2010	41	-1.96 ( $\pm 2.260$ ) ( $\pm 2.3$ )	41	-2.424 ( $\pm 3.353$ )
OVIDE-2012	37	-0.121 ( $\pm 8.858$ )	ND	ND
GEOVIDE-2014	57	-0.051 ( $\pm 3.434$ )	54	2.364 ( $\pm 7.899$ )

(\*) for the OVIDE 2006 cruise original difference for  $A_T$  was  $-9.0 (\pm 5.8) \mu\text{mol kg}^{-1}$  and LOCEAN  $A_T$  data were corrected by  $+7.2 \mu\text{mol kg}^{-1}$  based on the mean concentrations in deep layers. No corrections were applied for  $A_T$  and  $C_T$  for other cruises.

519

### 520 3.3.4 PENZE river

521

522

523

524

525

526

527

528

529

530

531

532

533

534

535

536

537

538

539

540

541

542

543

544

545

546

547

548

549

550

551

552

553

554

555

556

557

558

559

560

561

562

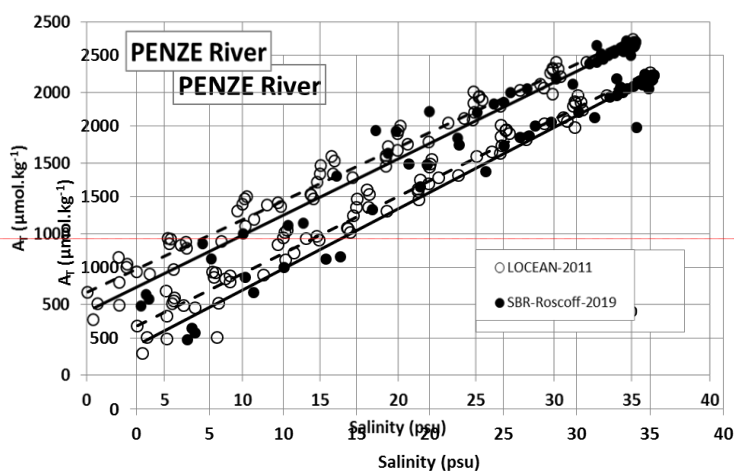
563

The comparisons described above concern the open ocean region with  $A_T$  and  $C_T$  concentrations in a range of concentrations close to the CRM references (used by the different laboratories). Another example of comparison is presented here for samples obtained along a river and thus for waters with low salinity and  $A_T$  concentrations (river Penzé in North Brittany). In 2019-2020,  $A_T$  was measured at SBR laboratory (Station Biologique de Roscoff) by a potentiometric method (using a Titrino-847 plus Metrohm) calibrated with CRM (Batch #131) for a final accuracy of  $\pm 2.1 \mu\text{mol kg}^{-1}$  (Gac et al., 2020). Although the samples were measured with different technics the  $A_T$ /Salinity relationships are very coherent for both datasets (Figure 5). The regressions for each period are for  $A_T$  (in  $\mu\text{mol kg}^{-1}$ ):

In 2011 (78 samples):  $A_T = 51.525 (\pm 0.944) S + 583.95 (\pm 19.94) (r^2 = 0.975)$

In 2019-2020 (70 samples):  $A_T = 54.022 (\pm 1.018) S + 450.23 (\pm 31.53) (r^2 = 0.976)$

Therefore we added the  $A_T$  data measured in 2019-2020 to complete the synthesis for this location (river Penzé).



Mis en forme : Retrait : Première ligne : 0 cm  
Mis en forme : Police : Italice

Mis en forme : Police : Non Gras, Couleur de police : Rouge foncé  
Mis en forme : Gauche, Interligne : 1,5 ligne

**Figure 5:** Total alkalinity ( $A_T$ ) versus salinity for samples measured in 2011 and 2019 in the river Penzé, North Brittany (Gac et al., 2020).  $A_T$  samples were measured at LOCEAN in 2011 (open circles, dashed-line) and at SBR laboratory (Roscoff) in 2019 (filled circles, black line).

### 3.4 Quality control and assigned flags

Identifying each data with an appropriate flag is very convenient for selecting the data (good, questionable or bad). Here we used 4 Flags flags for each property (Flags flags 2 = good, 3 = questionable, 4 = bad, and 9 = no data) following the WOCE program and used in other data products such as SOCAT (Bakker et al., 2016) or GLODAP (Olsen et al., 2016, 2019, 2020; Lauvset et al., 2021). During the data-processing, we first assigned a flag for each  $A_T$  and  $C_T$  data based on the standard error in the calculation of  $A_T$  and  $C_T$  concentrations (non-linear regression, Dickson et al. 2007). By default, if the standard-deviation on the regression is  $> 1 \mu\text{mol kg}^{-1}$ , we assigned a flag 3 (questionable) although the data could be acceptable and then used for interpretations.

564 Flag 3 was also assigned when salinity was doubtful or when differences of duplicates were large (e.g.  $\pm 20 \mu\text{mol}$   
565  $\text{kg}^{-1}$ ). Flags 4 (bad or certainly bad) were assigned when clear anomalies were detected for unknown reason (e.g.  
566 a sample probably not fixed with  $\text{HgCl}_2$ ). A secondary quality control was performed by the PIs of each project  
567 based on data inspection, duplicates,  $A_T$ /Salinity relationship, or the mean observations in deep layers where  
568 large variability in  $A_T$  and  $C_T$  is unlikely to occur from year to year. An example presents all data from the  
569 MOOSE-GE cruises conducted in 2010-2019 in the Mediterranean Sea (Coppola et al., 2020; Testor et al., 2010)  
570 where clear outliers have been identified (Figure S3). For the 10 MOOSE-GE cruises and a total of 1847  $A_T$  and  
571  $C_T$  analyses, 26 were identified flagged as bad (flag 4), 139 for  $A_T$  and 141 for  $C_T$  listed as questionable (flag 3)  
572 and 1682 for  $A_T$  and 1680 for  $C_T$  considered as good data (flag 2, i.e. more than 90%). Similar control was  
573 performed for each project.

574 The synthesis of various cruises in the same region and period also offers verification and secondary  
575 control of the data. For example, several cruises were conducted in the Mediterranean Sea in 2014 (MOOSE-GE,  
576 SOMBA, ANTARES and DYFAMED). The mean values of  $C_T$  and  $A_T$  in the deep layers ( $> 1800\text{m}$ ) for each  
577 cruise confirmed the coherence of the data (Table 4). This enabled to merge the different datasets for  
578 interpretations of the temporal trends and processes driving the  $\text{CO}_2$  cycle (Coppola et al., 2019, 2020; Ulses et  
579 al., 2022) or to train and validate a regional neural network to reconstruct the carbonate system (e.g.  
580 CANYON-MED, Fourier et al., 2020, 2022).

581  
582  
583 **Table 4:** Mean observations in the deep layers ( $> 1800\text{m}$ ) of the ~~western~~Western Mediterranean Sea for different  
584 cruises conducted in 2014. Results in deep layers ( $> 1800\text{m}$ ) for the DEWEX cruise in 2013 and the  
585 PEACETIME cruise in 2017 in the same region are also listed. N- $A_T$  and N- $C_T$  are  $A_T$  and  $C_T$  normalized at  
586 ~~Salinity~~salinity = 38. Nb = number of data (with flag 2). Standard-deviations are in brackets. References for  
587 these cruises are listed in Supplementary Material.

588  
589

Cruise	Period	Nb	Pot. Temp ( $^{\circ}\text{C}$ )	Salinity ( $\mu\text{mol kg}^{-1}$ )	N- $A_T$ (PSU)	N- $C_T$ ( $\mu\text{mol kg}^{-1}$ )
All cruises	Feb/Dec-2014	76	12.905 (0.007)	38.486 (0.005)	2562.9 (5.3)	2303.7 (4.7)
ANTARES	Feb/Nov-2014	14	12.913 (0.004)	38.488 (0.006)	2564.0 (3.8)	2301.9 (3.5)
DYFAMED	Mar/Dec-2014	9	12.905 (0.0016)	38.487 (0.004)	2560.1 (5.0)	2304.3 (6.8)
MOOSE-GE	Jul-2014	21	12.909 (0.004)	38.487 (0.005)	2565.6 (4.6)	2303.5 (4.1)
SOMBA	Aug/Sep-2014	32	12.899 (0.005)	38.483 (0.005)	2561.5 (5.6)	2304.6 (4.8)
DEWEX	Feb/Apr-2013	44	12.903 (0.010)	38.588 (0.006)	2556.0 (4.3)	2294.0 (5.7)
PEACETIME	May/Jun-2017	7	12.904 (0.002)	38.486 (0.003)	2567.2 (10.6)	2308.1 (8.9)

590  
591  
592  
593  
594  
595  
596  
597  
598  
599  
600  
601  
602  
603  
604  
605  
606  
607  
608  
609  
610  
611  
612  
613  
614  
615  
616  
617

Mis en forme : Couleur de police :  
Automatique

618 The total number of data for the Global Ocean and the Mediterranean Sea are gathered in Table 5 with  
 619 corresponding flags for each property. Overall, the synthesis includes more than 94% of good data for both  $A_T$   
 620 and  $C_T$ . About 5% are questionable and 2% are likely bad. Overall, we believe that all data (with **Flagflag 2**) in  
 621 this synthesis have an accuracy better than  $4 \mu\text{mol kg}^{-1}$  for both  $A_T$  and  $C_T$ , the same as for quality-controlled  
 622 data in GLODAP (Olsen et al., 2020; Lauvset et al., 2021). The uncertainty ranges between the “Climate goal”  
 623 ( $2 \mu\text{mol kg}^{-1}$ ) and the “Weather Goal” ( $10 \mu\text{mol kg}^{-1}$ ) for ocean acidification studies (Newton et al., 2015;  
 624 Tilbrook et al., 2019). This accuracy is also relevant to validate or constraint data-based methods that reconstruct  
 625  $A_T$  and  $C_T$  fields with an error of around 10-15  $\mu\text{mol kg}^{-1}$  for both properties (Bittig et al., 2018; Broullón et al.,  
 626 2019, 2020; Fourrier et al., 2020; Chau et al., 2023).

627 **Table 5:** Number of Temperature, Salinity,  $A_T$  and  $C_T$  data in the synthesis identified for **Flagsflags** 2, 3, 4, 9.  
 628 The data are given for the full data-set Global Ocean and for the Mediterranean Sea. Last column is the  
 629 percentage of **Flagflag 2** (Good).  
 630

	Flag 2	Flag 3	Flag 4	Flag 9	% Flag 2
Global Ocean					
Temperature	43538	410	0	478	<u>0.990799.07</u>
Salinity	44033	319	2	71	<u>0.992899.28</u>
$A_T$	39331	2144	1165	1787	<u>0.922492.24</u>
$C_T$	39921	2091	1148	1279	<u>0.925092.50</u>
Mediterranean Sea					
Temperature	9843	1	0	65	<u>0.999999.99</u>
Salinity	9879	8	2	20	<u>0.999999.99</u>
$A_T$	8853	425	411	220	<u>0.913791.37</u>
$C_T$	8854	451	389	211	<u>0.913391.33</u>

### 653 3.5 Using $A_T$ -and $C_T$ to calculate $p\text{CO}_2/f\text{CO}_2$ and pH and compare with $p\text{CO}_2/f\text{CO}_2$ and pH measurements

655 For some projects, the  $A_T$ -and  $C_T$  data presented in this synthesis were used to calibrate or validate in  
 656 situ  $p\text{CO}_2/f\text{CO}_2$  sensors (Bozec et al., 2011; Marrec et al., 2014; Merlivat et al., 2018). The  $A_T$ -and  $C_T$  data were  
 657 also used to calculate  $p\text{CO}_2/f\text{CO}_2$  and to derive associated air-sea  $\text{CO}_2$  fluxes, especially during periods when no  
 658 direct  $p\text{CO}_2/f\text{CO}_2$  measurements were available (e.g. in the North Atlantic, Figure 4, Watson et al., 2009; Mc  
 659 Kinley et al., 2011). For example, Marrec et al. (2014) successfully used the calculated  $p\text{CO}_2$  (with  $A_T/C_T$  pairs)  
 660 to adjust the drift of the  $p\text{CO}_2$  data recorded with a Contros-HydroC/CO2 FT sensor mounted on a FerryBox for  
 661 regularly sampling the Western English Channel- (CHANNEL project). Here we show the results for the period  
 662 2012-2014 (Figure 6). In this region the total alkalinity is relatively constant over time; the average of  $A_T$  for 528  
 663 samples at different seasons and years is  $2334.4 (\pm 7.2) \mu\text{mol kg}^{-1}$ . On the opposite, the  $C_T$  concentrations show  
 664 distinctive seasonality, with higher concentrations in winter and lower in summer when biological activity is  
 665 pronounced (Marrec et al., 2013, 2014; Kitidis et al., 2019). This controls the seasonal  $p\text{CO}_2$  distribution  
 666 revealed each year in both measured and calculated  $p\text{CO}_2$  (Figure 6). For 528 co-located samples the mean

Mis en forme : Police :Italique

Mis en forme : Police :Italique

Mis en forme : Police :Italique

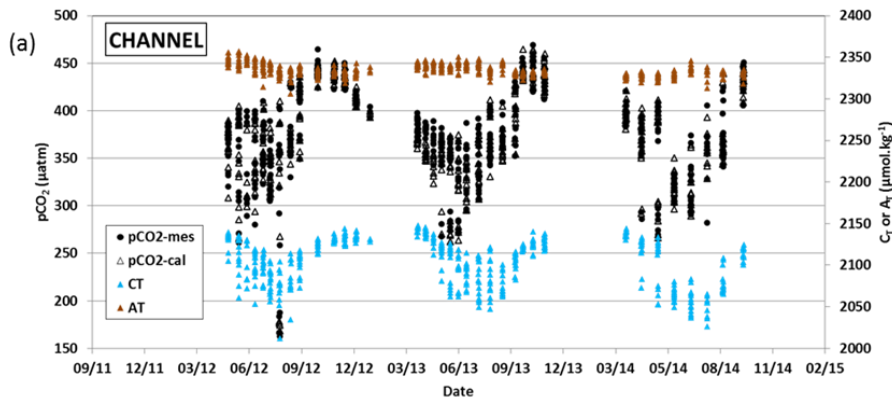
Mis en forme : Police :Italique



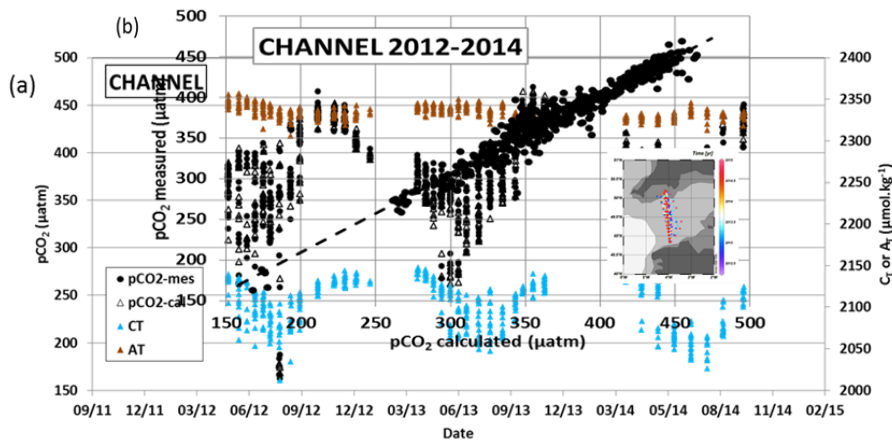
667 | difference between calculated and measured  $p\text{CO}_2$  is  $-1.9 (\pm 11.9) \mu\text{atm}$  with no distinct differences depending on  
668 | the season and year.  
669

**Mis en forme :** Police :Italique

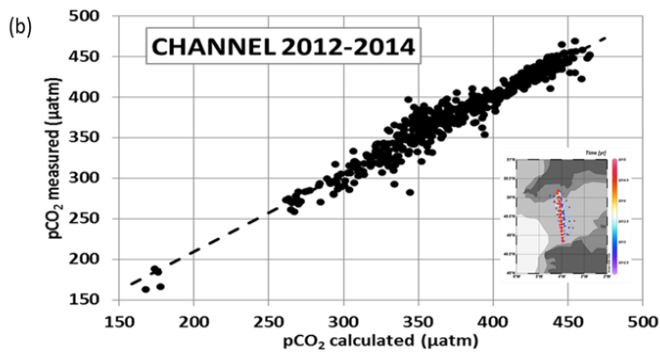
670  
671  
672  
673  
674  
675  
676  
677  
678  
679  
680  
681  
682



683  
684  
685  
686  
687  
688  
689  
690  
691  
692  
693  
694  
695  
696



697  
698  
699  
700  
701  
702  
703  
704  
705  
706  
707  
708  
709



710 **Figure 6:** (a): Time-series of  $A_T$  (brown triangles, right Y-axis),  $C_T$  (blue triangles, right Y-axis),  $pCO_2$   
711 calculated (open triangles, left Y-axis) and  $pCO_2$  measured (filled circles) in the Western English Channel in  
712 2012-2014 (Marrec et al., 2014). (b): Measured  $pCO_2$  versus calculated  $pCO_2$  for the same samples. The mean  
713 difference ( $pCO_{2cal} - pCO_{2mes}$ ) for 528 samples is  $-1.9 \mu atm (\pm 11.9) \mu atm$ . Data from Marrec and Bozec (2016  
714 a,b; 2017). Localization of the samples is shown in the inserted map.

716 In the Ligurian Sea, following the first high frequency in situ  $fCO_2$  measurements in 1995-1997 at the  
717 DYFAMED time-series station (Hood and Merlivat, 2001), a new CARIOCA  $fCO_2$  sensor was deployed at that  
718 location in 2013 (BOUSSOLE project, Merlivat et al., 2018). The CARIOCA sensor was calibrated with regular  
719  $A_T - C_T$  analyses performed at LOCEAN. Based on these data, the mean difference between CARIOCA- $fCO_2$

- Mis en forme : Police :Italique
- Mis en forme : Police :Italique
- Mis en forme : Police :Italique
- Mis en forme : Police :Italique
- Mis en forme : Police :Italique
- Mis en forme : Police :Italique
- Mis en forme : Retrait : Première ligne : 0 cm
- Mis en forme : Police :Italique
- Mis en forme : Police :Italique
- Mis en forme : Police :Italique

720 | measurements and calculated  $f\text{CO}_2$  data was estimated to be around  $\pm 4.4 \mu\text{atm}$  for 2013-2015, i.e. the same order  
721 | than the precision of the CARIOCA sensor ( $\pm 5 \mu\text{atm}$ , Merlivat et al., 2018). Here we extend the results for the  
722 | period 2013-2018 (Golbol et al., 2020; data also in SOCAT version v2021, Bakker et al., 2016) and compared  
723 | the CARIOCA  $f\text{CO}_2$  time-series with  $A_T$  and  $C_T$  data from different cruises (BOUSSOLE, DYFAMED and  
724 | MOOSE-GE) selected in the layer 0-20m at that location (Figure S4). For 67 co-located samples at different  
725 | seasons and years, the mean difference between calculated and measured  $f\text{CO}_2$  ( $f\text{CO}_{2\text{cal}} - f\text{CO}_{2\text{mes}}$ ) was  $-3.7 \mu\text{atm}$   
726 | ( $\pm 10.8$ )  $\mu\text{atm}$ - where  $f\text{CO}_2$  was calculated from  $A_T/C_T$  pairs using the constant from Lueker et al (2000). At that  
727 | location, the alkalinity is relatively constant over 2013-2018 with an average concentration of  $2569.8 (\pm 13.2)$   
728 |  $\mu\text{mol kg}^{-1}$ .  $C_T$  concentrations show a clear seasonality, decreasing by around  $50 \mu\text{mol kg}^{-1}$  from winter to late  
729 | summer driving the large seasonal cycle of  $f\text{CO}_2$  (range  $80 \mu\text{atm}$ ) revealed in both measured and calculated  
730 | values (here  $f\text{CO}_2$  is normalized at  $13^\circ\text{C}$ , Figure S4). In addition to calibration purposes, a regional  $A_T$ /Salinity  
731 | relationship was derived from the  $A_T$  data measured at that location and successfully used to construct time-  
732 | series of  $C_T$  and pH calculated from the high-frequency CARIOCA  $f\text{CO}_2$  data to investigate and interpret the  
733 | long-term change of  $f\text{CO}_2$  and acidification in the Ligurian Sea (Merlivat et al., 2018; Coppola et al., 2020).

734 | A CARIOCA sensor was also deployed in 2003 near the SOMLIT-Brest time-series site in the Bay of  
735 | Brest (Bozec et al., 2011; Salt et al., 2016). As for BOUSSOLE in the Ligurian Sea, samples collected for  $A_T$ -  
736 | and  $C_T$  were used for validation of the  $p\text{CO}_2$  recorded by the CARIOCA sensor and the comparison with  
737 | calculated  $p\text{CO}_2$  showed a good agreement, i.e.  $p\text{CO}_{2\text{cal}} = 0.98 * p\text{CO}_{2\text{mes}} + 7 \mu\text{atm}$  (Bozec et al., 2011).  
738 | CARIOCA sensors were also deployed on moorings in the Tropical Atlantic (PIRATA project, e.g. Lefèvre et  
739 | al., 2008, 2016; Parard et al., 2010). With the discrete  $A_T$  and  $C_T$  data included in this synthesis (EGEE and  
740 | PIRATA-FR cruises), the  $f\text{CO}_2$  data from CARIOCA sensor associated with an adapted  $A_T$ /Salinity relationship  
741 | were used to derive pH (Lefèvre et al., 2016) or  $C_T$  time-series to evaluate net community production in the  
742 | easternEastern tropical Atlantic (Parard et al., 2010; Lefèvre and Merlivat 2012).

743 | Although this is not a direct instrumental inter-comparison, differences between  $p\text{CO}_2$  (or  $f\text{CO}_2$ )  
744 | calculated using  $A_T/C_T$  pairs with direct  $p\text{CO}_2$  measurements give a glimpse of the quality of  $A_T$  and  $C_T$  data in  
745 | this synthesis given the uncertainty attached to the  $p\text{CO}_2$  or pH calculations (Orr et al., 2015). For example, in  
746 | the frame of the SURATLANT project in the North Atlantic, calculated  $f\text{CO}_2$  data were compared with co-  
747 | located  $f\text{CO}_2$  measurements for different seasons and years (Figure S5). The mean differences ( $f\text{CO}_{2\text{cal}} - f\text{CO}_{2\text{mes}}$ )  
748 | ranged between  $-4.3 \mu\text{atm} (\pm 12.9) \mu\text{atm}$  (2004-2007, 74 co-located samples) and  $-3.0 (\pm 12.1) \mu\text{atm}$  (2014-2015,  
749 | 98 co-located samples). The differences are almost the same for different years (and seasons) and are thus  
750 | attributed to method uncertainties (including sampling time, measurement errors, and data processing). Based on  
751 | these comparisons and the consistency between data we are confident that the  $A_T$ - and  $C_T$  data presented in this  
752 | synthesis could be used to calculate  $f\text{CO}_2$  (and pH) and interpret temporal changes and drivers of these  
753 | parameters as well as to estimate air-sea  $\text{CO}_2$  fluxes in the North Atlantic (e.g. Corbière et al., 2007; Schuster et  
754 | al., 2009, 2013; Watson et al., 2009; Metzl et al., 2010; Mc Kinley et al., 2011; Reverdin et al., 2018, Kitidis et  
755 | al., 2019; Leseurre et al., 2020).

756 | The  $A_T$ - and  $C_T$  data in this synthesis have been also successfully used for  $f\text{CO}_2$  and air-sea  $\text{CO}_2$  fluxes  
757 | calculations in other regions: the tropical Atlantic (Koffi et al., 2010), the tropical Pacific (Moutin et al., 2018;  
758 | Wagener et al., 2018), the Solomon sea (Ganachaud et al., 2017) or the Mediterranean sea and coastal zones (De  
759 | Carlo et al., 2013; Marrec et al., 2015; Kapsenberg et al., 2017; Coppola et al., 2020; Keraghel et al., 2020;  
760 | Wimart-Rousseau et al., 2020a; Gattuso et al., 2023).

Mis en forme : Police :Italique

Mis en forme : Police :Italique

Mis en forme : Police :Italique

Mis en forme : Police :Italique

Mis en forme : Police :Italique

Mis en forme : Police :Italique

Mis en forme : Police :Italique

Mis en forme : Police :Italique

Mis en forme : Police :Italique

Mis en forme : Police :Italique

Mis en forme : Indice

Mis en forme : Police :Italique

Mis en forme : Police :Italique

Mis en forme : Indice

Mis en forme : Police :Italique

Mis en forme : Indice

Mis en forme : Police :Italique

Mis en forme : Police :Italique

Mis en forme : Police :Italique

Mis en forme : Police :Italique

Mis en forme : Police :Italique

Mis en forme : Police :Italique

Mis en forme : Police :Italique

Mis en forme : Police :Italique

Mis en forme : Police :Non Italique

Mis en forme : Police :Non Italique

Mis en forme : Police :Italique

Mis en forme : Police :Italique

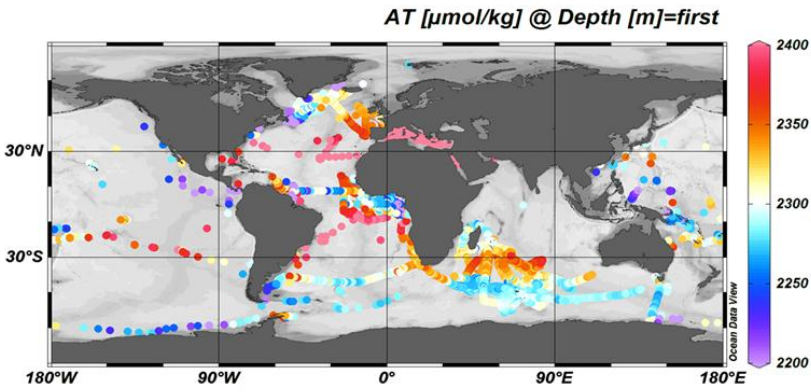
761 In addition,  $A_T$  and  $C_T$  data in the surface and the water-column are also relevant to calculate pH and  
 762 evaluate its rate of change for addressing ocean acidification topic in different regions (Kapsenberg et al., 2017;  
 763 Ganachaud et al., 2017; Wagener et al., 2018; Coppola et al., 2020; Leseurre et al., 2020; Lo Monaco et al.,  
 764 2021). At the time-series station ECOSCOPA in the Bay of Brest (Fleury et al., 2023; Petton et al., 2023), pH  
 765 calculated with  $A_T$ / $C_T$  data were compared with direct pH measurements (Figure S6). In 2017-2019, pH (at  
 766 standard temperature 25°C, pH-25C) was always lower than 8 and presented a large seasonal signal of 0.3 (high  
 767 pH values in spring, low in winter). The mean difference between calculated and measured pH-25C for 46  
 768 samples was equal to +0.013 ( $\pm$  0.010) which is in the range of the pH uncertainty evaluated by error  
 769 propagation when calculated from  $A_T$ / $C_T$  pairs ( $A_T$  and  $C_T$  error of  $\pm 3 \mu\text{mol kg}^{-1}$  leads to pH error of  $\pm 0.0144$ ).  
 770 Part of these  $A_T$  and  $C_T$  data used to calculate pH also helped for interpreting the response of marine species to  
 771 acidification, e.g. pteropodes or coccolithophores (*Emiliana huxleyi*) in the Mediterranean Sea (Howes et al.,  
 772 2015, 2017; Meier et al., 2014) or in the Southern Ocean (Beaufort et al., 2011). The  $A_T$  and  $C_T$  data were also  
 773 supporting environmental analysis in coral reef ecosystems in the tropical Pacific (TARA Expedition, Douville  
 774 et al., 2022; Lombard et al., 2023; Canesi et al., 2023).

775  
 776 **4 SpatialGlobal distribution of and relationships from  $A_T$  and  $C_T$ : a global view from based on the**  
 777 **SNAPO-CO2 dataset**

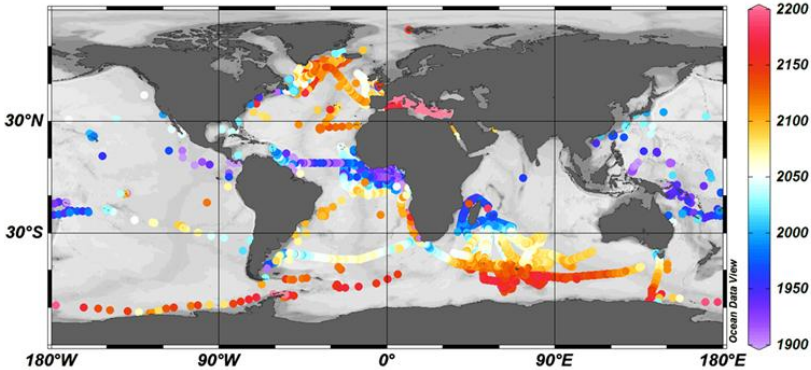
Mis en forme : Retrait : Première ligne : 0 cm  
 Mis en forme : Barré

779 The surface distribution in the global ocean based on the SNAPO-CO2 dataset is presented in Figure 7  
 780 for  $A_T$  and  $C_T$ . In the open ocean, high  $A_T$  concentrations are identified in the subtropics in all basins (Jiang et al.,  
 781 2014; Takahashi et al., 2014) with highest concentrations up to 2484  $\mu\text{mol kg}^{-1}$  in the central North Atlantic  
 782 (STRASSE cruise in August 2012, 26°N/36°W). In surface and at depth, the  $A_T$ /Salinity and  $A_T$ / $C_T$  relationships  
 783 are clearly identified and structured at regional scale (Figure 8).

784  
 785  **$A_T$  [ $\mu\text{mol/kg}$ ] @ Depth [m]=first**



797  
 798  **$C_T$  [ $\mu\text{mol/kg}$ ] @ Depth [m]=first**



800  
 801  
 802  
 803  
 804  
 805

806  
807  
808  
809  
810  
811  
812  
813

**Figure 7:** Distribution of  $A_T$  (top) and  $C_T$  (bottom) concentrations ( $\mu\text{mol}\cdot\text{kg}^{-1}$ ) in surface waters (0-10m). Only data with flag 2 are presented in these figures. Figures produced with ODV (Schlitzer, 2018).

814  
815  
816  
817  
818  
819  
820  
821  
822  
823  
824  
825  
826  
827  
828  
829  
830  
831  
832  
833  
834  
835  
836  
837  
838  
839  
840  
841  
842  
843  
844  
845  
846  
847  
848  
849  
850  
851  
852

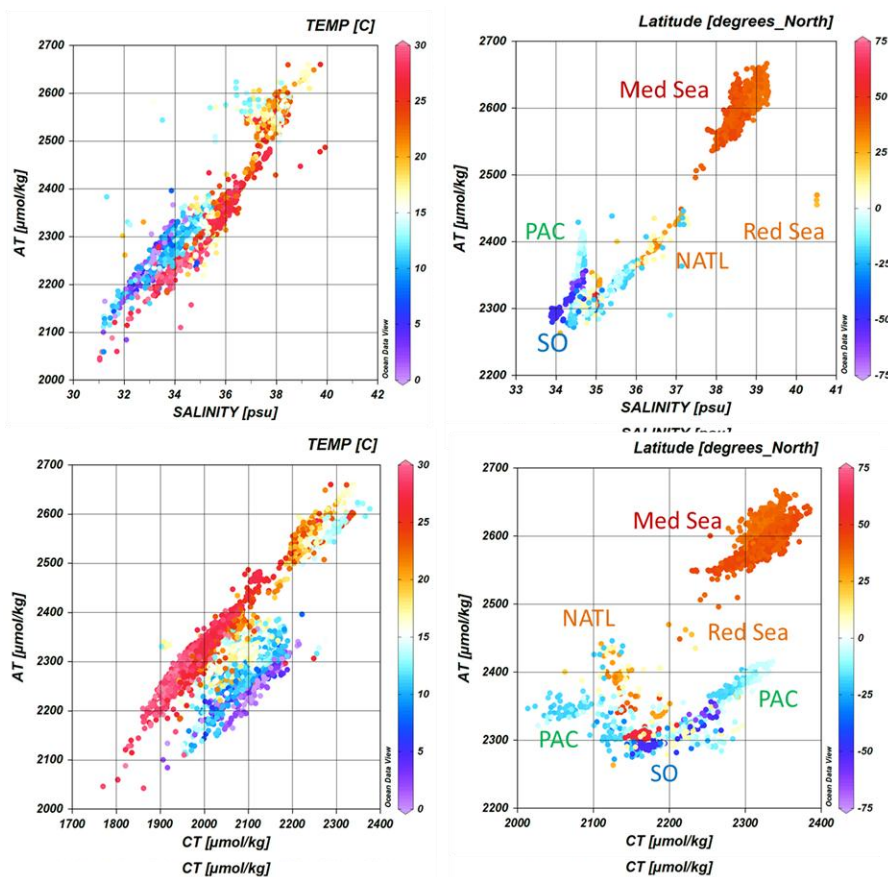


**Figure 8:** Relationships between  $A_T$  and Salinity (upper panel) and  $A_T$  versus  $C_T$  (lower panel) for samples in surface waters (0-10m and SSS > 31) (left) and in the water column below 100m (right). Only data with flag 2 are presented. The color scales correspond to the temperature (left) or the latitude (right). Some location of data are identified: Mediterranean Sea (Med Sea), Red Sea, Tropical Pacific (PAC), North Atlantic (NATL) and Southern Ocean (SO). Figures produced with ODV (Schlitzer, 2018).

853  
854  
855  
856  
857  
858  
859  
860  
861  
862  
863

In the ~~eastern~~Eastern tropical Atlantic (ETA) where the Congo River impacts the salinity field (Vangriesheim et al., 2009),  $A_T$  concentrations range between 2100 and 2400  $\mu\text{mol}\cdot\text{kg}^{-1}$ . The regional  $A_T$ /Salinity relationship in the ETA based on data from the EGEE cruises in 2005-2007 (Koffi et al., 2010) is robust and validated with more recent measurements from PIRATA-FR cruises in 2010-2019 (Lefevre et al., 2021). The strong  $A_T$ /Salinity relationship in the ETA was also recognized using data from the TARA-MICROBIOME

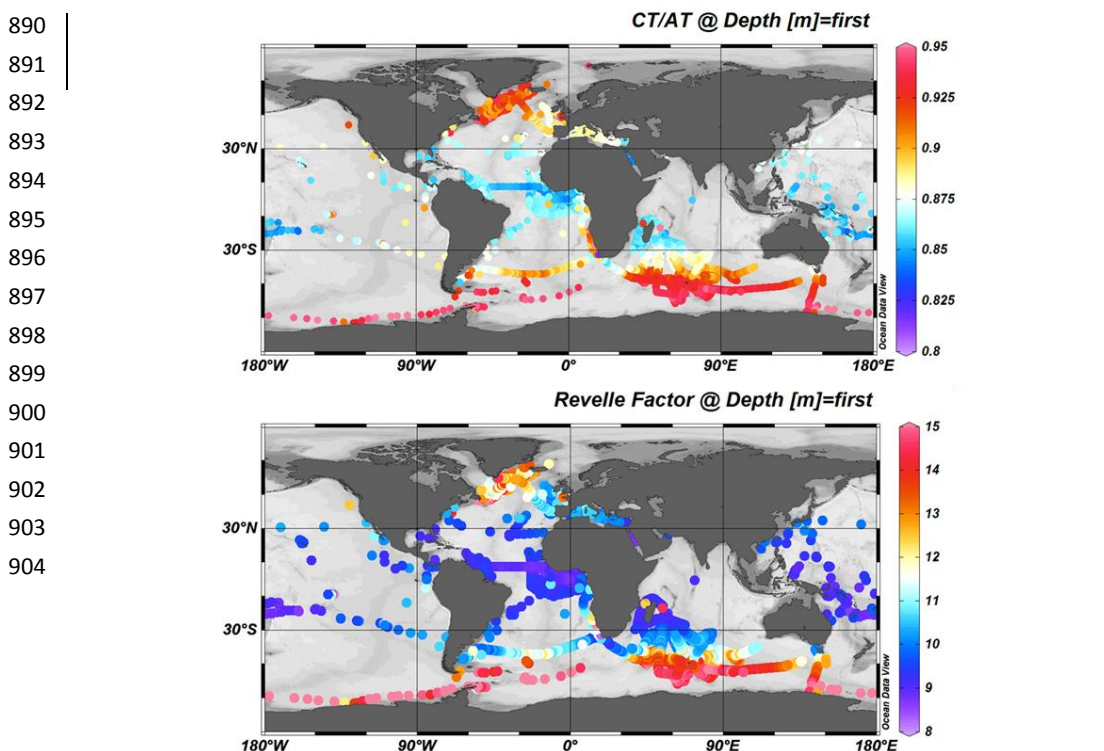
864 cruise in May-July 2022 (Figure S7). Low salinity ( $< 30$ ) and low  $A_T$  ( $1700-2200 \mu\text{mol kg}^{-1}$ ) are also observed in  
865 the ~~western~~Western tropical Atlantic near the Amazon River plume. The  $A_T$ /Salinity relationships in both river  
866 plume regions are very similar (Figure S7).

867 For  $C_T$ , the lowest concentrations were observed in the coastal regions of the Tropical Atlantic, on the  
868 eastern side in the Gulf of Guinea (BIOZAIRE cruise in 2003,  $6^\circ\text{S}/11^\circ\text{E}$ ,  $C_T=1390 \mu\text{mol kg}^{-1}$ , Vangriesheim et  
869 al., 2009) and on the ~~western~~Western side in coastal zone off French Guyana (PLUMAND cruise in 2007,  
870  $5^\circ\text{N}/51^\circ\text{W}$ ,  $C_T=1512 \mu\text{mol kg}^{-1}$ , Lefèvre et al., 2010). Such low  $C_T$  concentrations were also observed around  
871  $5^\circ\text{N}/51^\circ\text{W}$  in the Amazon River plume during the recent EUREC4A-OA cruise in 2020 and the TARA-  
872 MICROBIOME cruise in 2021 ( $C_T=1451 \mu\text{mol kg}^{-1}$ ) leading to low oceanic  $f\text{CO}_2$  ( $< 350 \mu\text{atm}$ ) and a  $\text{CO}_2$  sink  
873 in this region (Olivier et al., 2022).

Mis en forme : Police :Italique

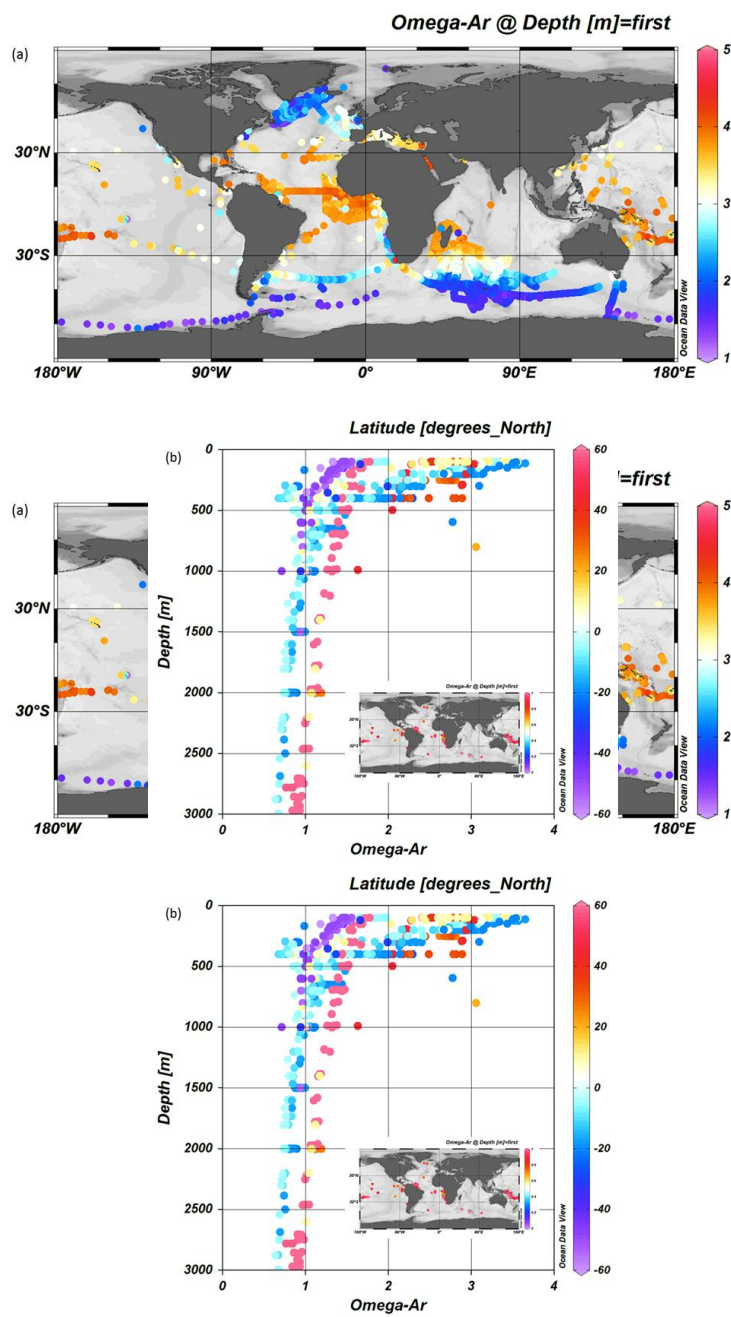
874 The high  $C_T$  concentrations were mainly observed in the Southern Ocean (OISO and ACE cruises)  
875 south of the Polar Front around  $50^\circ\text{S}$  linked to the upwelling of  $C_T$ -rich deep water (Figure 7, Metzl et al., 2006;  
876 Wu et al., 2019; Chen et al., 2022). This leads to a high  $C_T/A_T$  ratio and a high Revelle factor in the Southern  
877 Ocean (Figure 9, Fassbender et al., 2017). The high  $C_T$  content and low temperature in the Southern Ocean also  
878 lead to low calcite and aragonite saturation state ( $\Omega$ ) (Takahashi et al., 2014; Jiang et al., 2015) ~~but at~~. We  
879 calculate  $\Omega$  from  $A_T$  and  $C_T$  data at insitu temperature, salinity and pressure. At present the surface ocean is not  
880 under-saturated with regard to aragonite (Figure 10); however, under-saturation levels ( $\Omega\text{-Ar}<1$ ) were found  
881 around 500 m in the Southern Ocean (ACE cruise in 2017, MODYDICK cruise in 2018), 1000 m in the Tropical  
882 Pacific (PANDORA 2012 and OUTPACE 2015 cruises) and 2200 m in the North Atlantic (OVIDE 2012 and  
883 2014 cruises, see also Turk et al., 2017) (Figure 10). Samples at 400 m from the TARA-Oceans cruise in 2009-  
884 2012 also indicated aragonite under-saturation in the Equatorial Atlantic, Equatorial Pacific, as well as off South  
885 America ( $73^\circ\text{W}-34^\circ\text{S}$ , Chile) associated to equatorial or eastern boundary upwelling systems (Feely et al., 2012;  
886 Lauvset et al., 2020).

887 In surface,  $\Omega\text{-Ar}>3$  is found in the latitudinal band  $45^\circ\text{S}-54^\circ\text{N}$  and  $\Omega\text{-Ar}<3$ , below the critical  
888 threshold of  $\Omega\text{-Ar}=3.25$  that represents a limit for distribution of tropical coral reefs (Hoegh-Guldberg et al.,  
889 2007) is observed at very few locations in the tropics.



905  
906  
907  
908  
909  
910  
911  
912  
913  
914  
915  
916  
917  
918  
919  
920  
921  
922  
923  
924  
925  
926  
927  
928  
929  
930  
931  
932  
933  
934  
935  
936  
937  
938  
939  
940  
941  
942  
943  
944  
945  
946  
947  
948  
949  
950  
951  
952  
953  
954  
955  
956

**Figure 9:** Distribution of the  $C_T/A_T$  ratio (top) and the Revelle factor (bottom) in surface waters (0-10m). Only data with flag 2 were used. Figures produced with ODV (Schlitzer, 2018).



957  
958  
959  
960  
961  
962  
963  
964

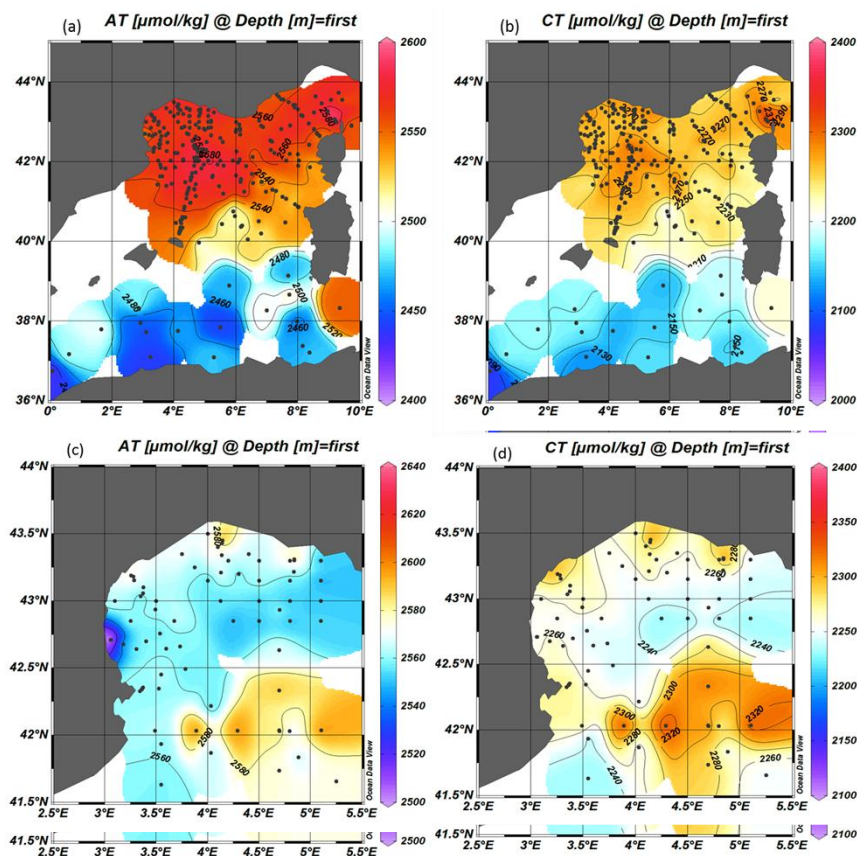
**Figure 10:** (a): Distribution of the aragonite saturation state ( $\Omega$ -Ar) in surface waters (0-10m). Only data with flag 2 were used. (b): Depth profiles (100-3000m) of  $\Omega$ -Ar at few locations in the Tropical Pacific, Atlantic and Southern Oceans. Stations where under-saturation is detected ( $\Omega$ -Ar<1) at depth are identified in the inserted map. Figures produced with ODV (Schlitzer, 2018).

Mis en forme : Police :10 pt

965  
966  
967  
968  
969  
970  
971  
972  
973  
974

Compared to the open ocean,  $A_T$  concentrations are much higher in the Mediterranean Sea (Copin-Montégut, 1993; Schneider et al., 2007; Álvarez et al., 2023) with values up to  $2600 \mu\text{mol kg}^{-1}$  (Figure 8). The  $A_T$  and  $C_T$  data obtained in 1998-2019 show on average a clear contrast between the northern and southern regions of the ~~western~~Western Mediterranean sea (Figure 11 a, b) with higher concentration in the Ligurian Sea and the Gulf of Lion (Gemayel et al., 2015). However, the basin scale average distribution view smoothed the meso-scale signals recognized in the Mediterranean Sea (e.g. Bosse et al., 2017; Petrenko et al., 2017). In the Gulf of Lion the synthesis of 11 cruises conducted from May 2010 to June 2011 (CARBORHONE, CASCADE, LATEX, MOLA, MOOSE-GE) highlights the contrasting distributions of  $A_T$  and  $C_T$  in the coastal zones and off shore (Figure 11 c, d). The averaging of all data in 1998-2019 also smoothed the seasonal signal and the inter-annual variability described below.

975  
976  
977  
978  
979  
980  
981  
982  
983  
984  
985  
986  
987  
988  
989  
990  
991  
992  
993  
994  
995  
996  
997  
998  
999





1000  
1001

1002 **Figure 11:** Distribution of  $A_T$  (a) and  $C_T$  (b) in  $\mu\text{mol}\cdot\text{kg}^{-1}$  in surface waters of the **western** Mediterranean  
1003 Sea (0-10m) from all data for 1998-2019. Detailed distribution of  $A_T$  (c) and  $C_T$  (d) in  $\mu\text{mol}\cdot\text{kg}^{-1}$  in surface  
1004 waters of the Gulf of Lion for the period 2010-2011 only (cruises CARBORHONE, CASCADE, LATEX,  
1005 MOLA, MOOSE-GE). Figures produced with ODV (Schlitzer, 2018).  
1006

### 1007 5 Temporal variations of $A_T$ and $C_T$ : examples from the SNAPO-CO2 dataset

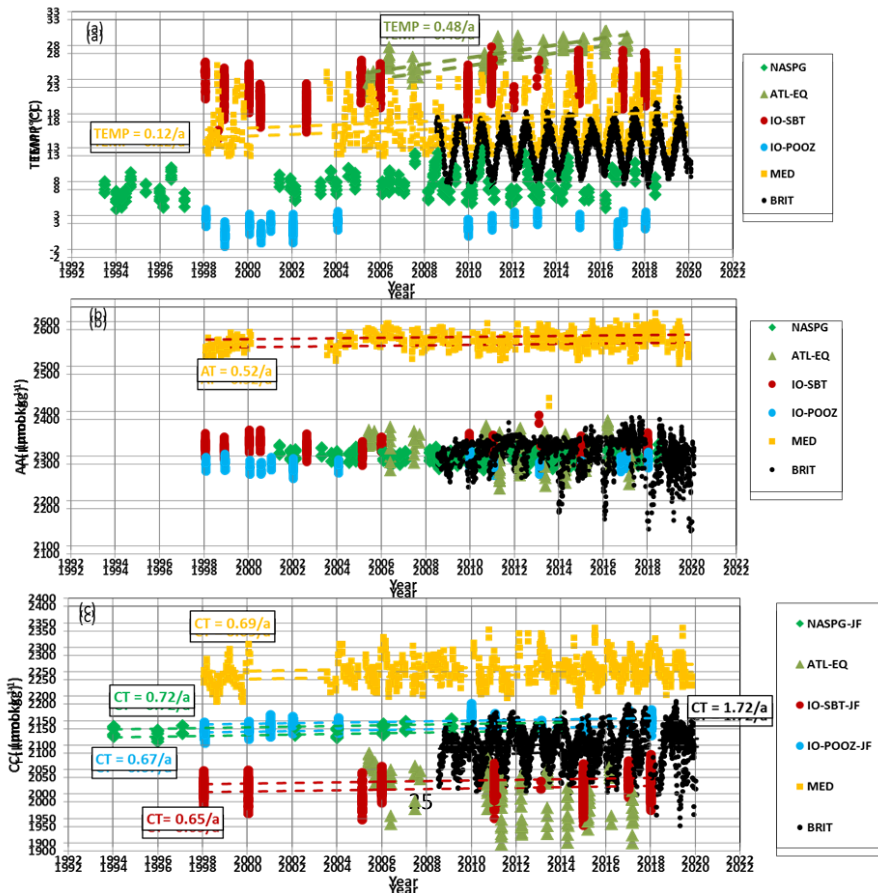
1008

1009 Time-series stations such as BATS, ESTOC, HOT, **in the subtropics and stations** in the Irminger Sea or  
1010 in the Iceland Sea are the only way to detect the long-term change in the ocean carbonate system in the surface  
1011 and the water column (Bates et al., 2014). These important time-series help to understand driving processes (e.g.  
1012 Hagens and Middelburg, 2016) and are often used to validate the  $p\text{CO}_2$ ,  $A_T$ ,  $C_T$ , or pH reconstructed fields (e.g.  
1013 Rödenbeck et al., 2013; Broullón et al., 2019, 2020; Keppler et al., 2020; Gregor and Gruber, 2021; Chau et al.,  
1014 2023; Ma et al., 2023).

Mis en forme : Police :Italique

1015 Here we show examples of the temporal surface variations at locations where data were obtained for  
1016 more than 10 years (Figure 12). We thus selected the following contrasting regions: the North Atlantic **Subpolar**  
1017 **Gyresubpolar gyre** (NASPG around  $60^\circ\text{N}/30^\circ\text{W}$ , period 1993-2018), the Equatorial Atlantic (at  $2^\circ\text{N}-$   
1018  $2^\circ\text{S}/12^\circ\text{W}-8^\circ\text{W}$ , period 2005-2017), the Indian Ocean subtropical sector ( $26-35^\circ\text{S}/50-56^\circ\text{E}$ , period 1998-2018),  
1019 the Indian Ocean high latitude ( $54-60^\circ\text{S}/60-70^\circ\text{E}$ , period 1998-2018), the Ligurian Sea (around DYFAMED  
1020 station,  $43.5-42.5^\circ\text{N}/5.5-9^\circ\text{E}$ , period 1998-2019) and times-series stations in the coastal zones off Brittany  
1021 (period 2008-2019).  
1022

1023  
1024



1025  
1026  
1027  
1028  
1029  
1030  
1031  
1032  
1033  
1034  
1035  
1036  
1037  
1038  
1039  
1040  
1041  
1042

1043  
 1044  
 1045  
 1046  
 1047

1048 **Figure 12:** Time-series of (a) sea surface temperature (°C), (b)  $A_T$  ( $\mu\text{mol} \cdot \text{kg}^{-1}$ ) and (c)  $C_T$  ( $\mu\text{mol} \cdot \text{kg}^{-1}$ ) in 6  
 1049 regions: the North Atlantic ~~Subpolar Gyre~~ subpolar gyre (NASPG 1993-2018, green diamond), the Equatorial  
 1050 Atlantic (ATL-EQ, 2005-2017, green triangle), the Indian subtropical sector (IO-SBT, red circle) and high  
 1051 latitude (IO-POOZ, blue circle) (1998-2018), the Ligurian Sea (MED, 1998-2019, orange square) and times-  
 1052 series stations in the coastal zones off Brittany (BRIT, period 2008-2019, black dots). Trends (dashed lines and  
 1053 values) are shown when relevant for the discussion ( $C_T$  trends listed in Table 6).

1054  
 1055  
 1056 **Table 6:** Trend of  $C_T$  ( $\mu\text{mol} \cdot \text{kg}^{-1} \cdot \text{yr}^{-1}$ ) and corresponding standard error in 5 selected regions where data were  
 1057 available for more than 10 years (data are shown in Figure 12). The projects/cruises for selection of the data in  
 1058 each domain are indicated.

Region (acronym)	Period	$C_T$ trend ( $\mu\text{mol} \cdot \text{kg}^{-1} \cdot \text{yr}^{-1}$ )	Season	Projects/Cruises
North Atlantic (NASPG)	1994-2014	+0.71972 (0.16817)	Jan-Feb	SURATLANT
Indian Subtropic (IO-SBT)	1998-2018	+0.64665 (0.11712)	Jan-Feb	OISO
Indian High LatSouth (IO-POOZ)	1998-2018	+0.66867 (0.04204)	Jan-Feb	OISO
Ligurian Sea (MED) DYFAMED, BOUSSOLE, MOOSE-GE	1998-2019	+0.68668 (0.18118)	All seasons	
Coast Brittany (BRIT) PENZE	2008-2019	+1.72072 (0.28128)	All seasons	Brest, Roscoff, ECOSCOPA,

1060  
 1061  
 1062  
 1063  
 1064  
 1065  
 1066  
 1067  
 1068  
 1069  
 1070  
 1071  
 1072  
 1073  
 1074  
 1075  
 1076  
 1077  
 1078  
 1079

1080 In the 6 regions, there was a progressive warming most clearly detected in the Mediterranean Sea (e.g.  
 1081 Nykjaer, 2009). From 1998 to 2019 the warming in the Ligurian Sea was  $+0.1208^\circ\text{C} \cdot \text{yr}^{-1}$  ( $\pm 0.0227$ ) (Figure 12).  
 1082 In the equatorial Atlantic, the apparent rapid increase of temperature of  $+0.48^\circ\text{C} \cdot \text{yr}^{-1}$  ( $\pm 0.04$ ) in 2005-2017 from  
 1083 the selected data indicated a change in water masses and circulation. The colder sea surface in 2005 was  
 1084 associated with the so-called Atlantic Cold Tongue (ACT) which was one of the most intense ATC since 1982  
 1085 (Caniaux et al., 2011). The ACT also leads to significant changes in oceanic  $f\text{CO}_2$  and air-sea  $\text{CO}_2$  fluxes (Parard  
 1086 et al., 2010; Koseki et al., 2023) and explained the high  $C_T$  concentrations observed in 2005 in this region  
 1087 (Figure 12, Koffi et al., 2010).

1088 **Total alkalinity** presents rather homogenous concentrations in the NASGP and the south  
 1089 Indian Ocean. Inter-annual variability of  $A_T$  is pronounced in the equatorial Atlantic ranging between 2245 and  
 1090  $2378 \mu\text{mol} \cdot \text{kg}^{-1}$ . This is mainly related to salinity as normalized  $A_T$  values ( $N-A_T$ , for salinity= 35) do not show  
 1091 such inter-annual variability (Mean  $N-A_T = 2295.7 \pm 4.6 \mu\text{mol} \cdot \text{kg}^{-1}$ ,  $n = 67$  for 2005-2017, not shown). In the  
 1092 coastal zones off Brittany, the  $A_T$  is also highly variable (Salt et al., 2016; Gac et al., 2021) ranging between  
 1093 2150 and  $2386 \mu\text{mol} \cdot \text{kg}^{-1}$  (Figure 12).

- Mis en forme : Police :8 pt
- Mis en forme : Police :8 pt
- Mis en forme : Police :8 pt
- Mis en forme : Police :8 pt
- Mis en forme : Police :8 pt
- Mis en forme : Police :8 pt
- Mis en forme : Police :8 pt
- Mis en forme : Police :8 pt
- Mis en forme : Police :8 pt
- Mis en forme : Police :8 pt
- Mis en forme : Police :8 pt
- Mis en forme : Police :8 pt
- Mis en forme : Police :8 pt
- Mis en forme : Police :8 pt
- Mis en forme : Police :8 pt
- Mis en forme : Police :8 pt
- Mis en forme : Police :8 pt
- Mis en forme : Police :8 pt
- Mis en forme : Police :8 pt
- Mis en forme : Police :8 pt
- Mis en forme : Justifié, Interligne : 1,5 ligne, Ne pas ajuster l'espace entre le texte latin et asiatique, Ne pas ajuster l'espace entre le texte et les nombres asiatiques
- Mis en forme : Retrait : Première ligne : 1,25 cm
- Mis en forme : Police :Italique

1094 An interesting signal is the progressive increase of  $A_T$  in the Mediterranean Sea. The positive  $A_T$  trend  
1095 of  $+0.53 (\pm 0.11) \mu\text{mol kg}^{-1} \text{yr}^{-1}$  ( $n=538$ ) in 1998-2019 in the region offshore was also observed at the coastal  
1096 station SOMLIT-Point-B in 2007-2015 but with a faster increase of  $+2.08 (\pm 0.19) \mu\text{mol kg}^{-1} \text{yr}^{-1}$  (Kapsenberg et  
1097 al., 2017). Close to the DYFAMED site, at station SOMLIT-Point-B, the  $A_T$  trend was not linked to salinity  
1098 temporal changes as a positive  $N-A_T$  trend was also reported,  $+0.52 (\pm 0.07) \mu\text{mol kg}^{-1} \text{yr}^{-1}$  (not shown). Based  
1099 on data from the PERLE cruises in 2018-2021 a significant increase in  $A_T$  was also identified in the Eastern  
1100 Mediterranean Sea (Wimart-Rousseau et al., 2021). Along with the increase of  $C_T$  and the warming, the  $A_T$   
1101 increase would impact on the  $f\text{CO}_2$ , air-sea  $\text{CO}_2$  fluxes and pH temporal changes (Merlivat et al., 2018).  
1102 Processes explaining the  $A_T$  increase in the Mediterranean Sea are still unexplained and deserve further  
1103 investigations (Coppola et al., 2019).

Mis en forme : Police :Italique

1104 As expected, because of the anthropogenic  $\text{CO}_2$  uptake the  $C_T$  concentrations increased in most regions  
1105 (Figure 12, Table 6). This is identified in the Indian Ocean (in the subtropics and the high latitude), in the  
1106 Mediterranean Sea, and in coastal waters off Brittany. However, the signal is more complex in the NASPG. As  
1107 previously shown the  $C_T$  trend in the NASPG depends on seasons and decades (Metzl et al., 2010; Reverdin et  
1108 al., 2018; Fröb et al., 2019; Leseurre et al., 2020). Here we selected only the data in January-February from the  
1109 SURATLANT cruises leading a  $C_T$  trend of  $+0.71972 (\pm 0.16817) \mu\text{mol kg}^{-1} \text{yr}^{-1}$ . Compared to the regions  
1110 further north the  $C_T$  trend in the NASPG is about half the  $C_T$  trends of  $+1.44 (\pm 0.23) \mu\text{mol kg}^{-1} \text{yr}^{-1}$  observed in  
1111 the Iceland Sea (Olafsson et al., 2009) or  $+1.48 (\pm 0.22) \mu\text{mol kg}^{-1} \text{yr}^{-1}$  at station M in the Norwegian Sea  
1112 (Skjelvan et al., 2022).

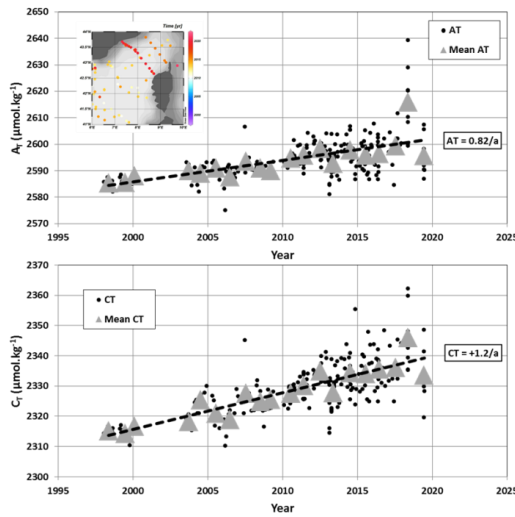
1113 In the coastal zones off Brittany, although there are large seasonal and inter-annual variabilities (Gac et  
1114 al., 2021), an annual  $C_T$  trend of  $+1.72 (\pm 0.28) \mu\text{mol kg}^{-1} \text{yr}^{-1}$  is detected over 10 years (2009 to 2019). The same  
1115 is observed in the Mediterranean Sea where the  $C_T$  offshore trend of  $+0.69 (\pm 0.18) \mu\text{mol kg}^{-1} \text{yr}^{-1}$  is low  
1116 compared to what was observed in the coastal zone (SOMLIT-Point-B,  $+2.97 (\pm 0.20) \mu\text{mol kg}^{-1} \text{yr}^{-1}$ , Kapsenberg  
1117 et al., 2017).

1118 In the southern Indian Ocean,  $C_T$  concentrations also increased in both subtropical and high latitudes,  
1119 two regions where the primary productivity is relatively low (oligotrophic regime in the subtropics and High  
1120 Nutrient Low Chlorophyll regime, HNLC, south of the Polar Front). With the data selected for austral summer  
1121 (January-February) the  $C_T$  trends appeared almost similar in these two regions, around  $+0.65 \mu\text{mol kg}^{-1} \text{yr}^{-1}$   
1122 (Table 6).

1123 Finally, in the Equatorial Atlantic the selected data around  $0^\circ$ - $10^\circ\text{W}$  highlighted the large variability  
1124 linked to the oceanic circulation. Detecting a  $C_T$  trend as well as a possible link with anthropogenic carbon  
1125 uptake, at least with the data available in 2005-2017, appears to be intricate as it has been previously discussed  
1126 for the period 2006-2013 (Lefèvre et al., 2016). However, the signal of the  $C_T$  increase is better identified north  
1127 or south of the Equator in the eastern tropical Atlantic sector (Lefèvre et al., 2021).

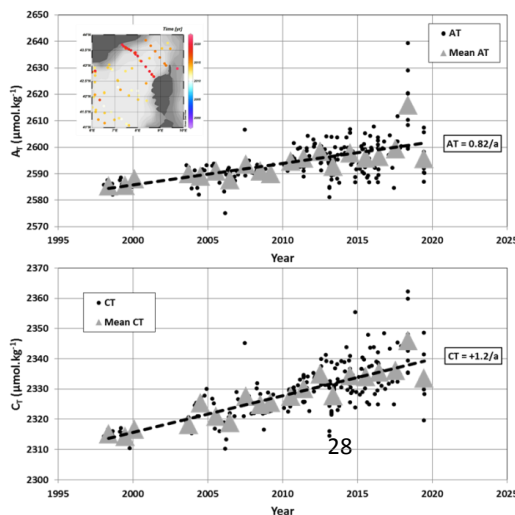
1128 In the water column  $A_T$ - and  $C_T$  data from dedicated cruises were used to evaluate the anthropogenic  
1129  $\text{CO}_2$  ( $C_{\text{ant}}$ ) distribution and pH change since pre-industrial era (e.g. PANDORA cruise, Ganachaud et al., 2017;  
1130 OUTPACE cruise, Wagener et al., 2018; SOMBA cruise, Keraghel et al., 2020). Time-series at DYFAMED  
1131 station also enabled to investigate the temporal variability of  $C_T$ ,  $A_T$  and  $C_{\text{ant}}$  in the water column (Touratier and  
1132 Goyet, 2009; Coppola et al., 2020; Fourrier et al., 2022). As an example of the observed temporal variations at  
1133 depth we selected the data in the layer 950-1050m in the Ligurian Sea from different cruises (Figure 13). At that  
1134 depth both  $A_T$  and  $C_T$  present some large anomalies especially noticed in 2013 (lower  $A_T$  and  $C_T$  in February  
1135 2013, DEWEX cruise) and in 2018 (lower  $A_T$  and  $C_T$  in May 2018, MOOSE-GE cruise) the later probably

1136 linked to episodic convective process that occurred in winter 2018 (Fourrier et al., 2022; Coppola et al., 2023).  
 1137 During the strong convection event in 2013 the positive anomalies of  $A_T$  and  $C_T$  were mostly identified in the  
 1138 upper layers (Figure 12c, Ulses et al, 2023).  
 1139



1140  
 1141  
 1142  
 1143  
 1144  
 1145  
 1146  
 1147  
 1148  
 1149  
 1150  
 1151  
 1152  
 1153  
 1154  
 1155  
 1156  
 1157  
 1158 **Figure 13:** Time-series of  $A_T$  ( $\mu\text{mol kg}^{-1}$ ) and  $C_T$  ( $\mu\text{mol kg}^{-1}$ ) in the Ligurian Sea (1998-2019) in the layer 950-  
 1159 1050m. Annual mean (grey triangles) was calculated from all data each year (black dots). The trends (dashed  
 1160 line) based on annual mean are  $+0.82 (\pm 0.15) \mu\text{mol kg}^{-1} \text{yr}^{-1}$  for  $A_T$  and  $+1.20 (\pm 0.12) \mu\text{mol kg}^{-1} \text{yr}^{-1}$  for  $C_T$ . In  
 1161 this layer data selected are from cruises ANTARES, CASCADE, DEWEX, DYFAMED, MOOSE-GE and  
 1162 PEACETIME (location of stations shown in the inserted map).  
 1163 ↗

1164 In this region the long-term increase of  $A_T$  indicates that in addition to the anthropogenic  $\text{CO}_2$  signal  
 1165 ~~another process isother processes are~~ at play to explain the rapid  $C_T$  trend of  $+1.20 (\pm 0.12) \mu\text{mol kg}^{-1} \text{yr}^{-1}$  at  
 1166 depth compared to that observed in surface (Figure 12). The signal at depth is probably linked to the variations  
 1167 of the deep convection and mixing with Levantine intermediate water (LIW, Margirier et al., 2020) with higher  
 1168  $A_T$  and  $C_T$  concentrations. The long-term increase of  $A_T$  and  $C_T$  at depth (here at 1000m, Figure 13) was also  
 1169 observed below 2000m (Coppola et al., 2020) a signal that has to be investigated in dedicated analysis using  
 1170 other properties ( $\text{O}_2$ , nutrients, following Fourrier et al. (2022) for the period 2012-2020) and a larger dataset in  
 1171 the Mediterranean Sea (e.g. CARIMEDGLODAP).



1185  
1186  
1187  
1188  
1189  
1190  
1191  
1192  
1193  
1194  
1195

~~Figure 13: Time-series of  $A_T$  ( $\mu\text{mol.kg}^{-1}$ ) and  $C_T$  ( $\mu\text{mol.kg}^{-1}$ ) in the Ligurian Sea (1998-2019) in the layer 950-1050m. Annual mean (grey triangles) was calculated from all data each year (black dots). The trends (dashed line) based on annual mean are  $-0.82 (\pm 0.15) \mu\text{mol.kg}^{-1}.\text{yr}^{-1}$  for  $A_T$  and  $+1.20 (\pm 0.12) \mu\text{mol.kg}^{-1}.\text{yr}^{-1}$  for  $C_T$ . In this layer data selected are from cruises ANTARES, CASCADE, DEWEX, DYFAMED, MOOSE GE and PEACETIME (location of stations shown in the inserted map).~~

## 1196 6 Using $A_T$ and $C_T$ data to validate observations from autonomous instruments

1197  
1198

The dataset presented in this synthesis would also offer interesting observations to validate properties ( $A_T$  and  $C_T$ ) derived from [BG-ARGOBGC-Argo](#) floats equipped with pH sensors (e.g. Bushinsky et al., 2019; Mazloff et al., 2023; Mignot et al., 2023). The water column in situ  $A_T$  and  $C_T$  data obtained during the Antarctic Circumpolar Expedition (ACE) in 2016-2017 were collected at location where SOCCOM floats were launched (Walton and Thomas, 2018). A SOCCOM float (WMO ID 5905069) was launched on January 11<sup>th</sup> 2017 at 55°S-96°E south of the Polar Front in the southern Indian Ocean. The pH, temperature and salinity data from the float were then used to derive  $A_T$  and  $C_T$  profiles (here using [the a multiple linear regression \(MLR method\) algorithm](#), Williams et al., 2016, 2017). In the top layers the discrete ACE data (Figure 14) present large variability of  $A_T$  and  $C_T$  concentrations not captured in the records derived from the float (MLR method somehow smooth the profiles). However, given the uncertainty in reconstructed  $A_T$  from float data ( $5.6 \mu\text{mol.kg}^{-1}$ ) the average values in the first 100m were almost identical ( $A_{T-ACE} = 2285.1 (\pm 4.4) \mu\text{mol.kg}^{-1}$  and  $A_{T-float} = 2278.3 (\pm 0.7) \mu\text{mol.kg}^{-1}$ ;  $C_{T-ACE} = 2139.7 (\pm 9.2) \mu\text{mol.kg}^{-1}$  and  $C_{T-float} = 2141.1 (\pm 3.2) \mu\text{mol.kg}^{-1}$ ). Moreover below 200m, profiles from the float are coherent compared to the  $A_T$  and  $C_T$  measurements (Figure 14). This is encouraging for using float data to explore the seasonal variability of  $A_T$  and  $C_T$  in the Southern Ocean (e.g. Williams et al., 2018; Johnson et al., 2022) and the estimation of anthropogenic  $\text{CO}_2$  in the water column in this sector (Figure 14). Here the  $C_{ant}$  concentrations were calculated below 200m (corresponding to the temperature minimum of the winter in the SO and using the TrOCA method, Touratier et al., 2007). The float data suggest that  $C_{ant}$  concentrations are positive down to about 1000m, with maximum values in subsurface. In 2017 the mean  $C_{ant}$  concentration at 200m was  $49.1 (\pm 9.0) \mu\text{mol.kg}^{-1}$ . Below that depth,  $C_{ant}$  decreased and reduced to  $+29.8 (\pm 8.5) \mu\text{mol.kg}^{-1}$  in the layer 300-400m. To complement the  $C_{ant}$  inventories based on GLODAP data-product (e.g. Gruber et al., 2019)  $C_{ant}$  estimates derived from [BG-ARGOBGC-Argo](#) floats as evaluated here in the Southern Ocean could be applied in other locations as was previously tested in the North Pacific (Li et al., 2019).

In surface water as the  $A_T$  derived from the float data are deduced using MLR or LIAR methods (Williams et al., 2017; Carter et al., 2016), the  $A_T$  data in the SNAPO-CO2 synthesis could also be used to identify  $A_T$  anomalies not always captured from floats. This is particularly relevant in coccolithophores blooms areas when low  $A_T$  concentrations and high  $p\text{CO}_2$  are observed (e.g. Balch et al., 2016 in the Southern Ocean; Robertson et al., 1994 in the North Atlantic).

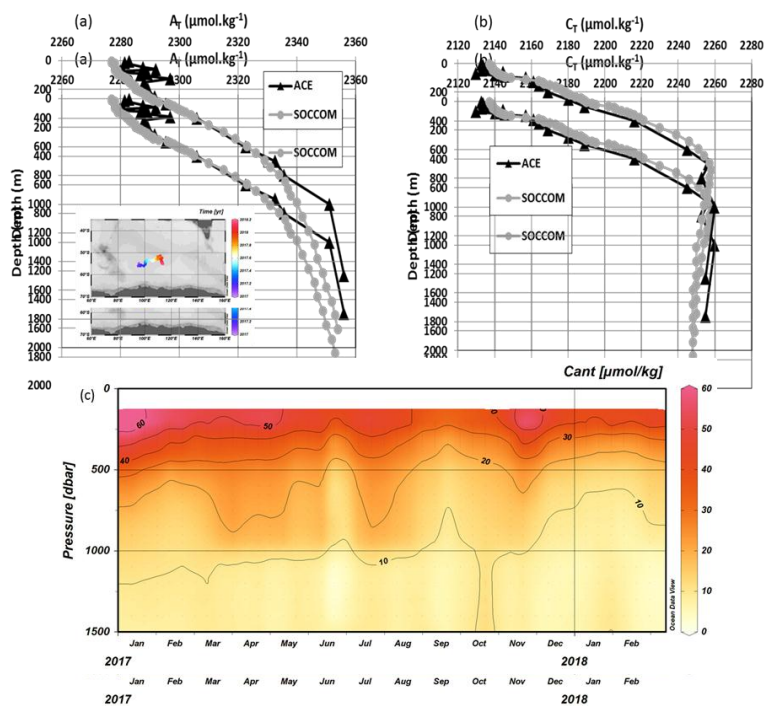
1226  
1227  
1228

## 7 Summary and suggestions

Mis en forme : Police :Italique

Mis en forme : Indice

1229 The ocean data synthesized in this product are based on measurements of  $A_T$  and  $C_T$  performed  
 1230 ~~in~~ between the period 1993- and 2022 with an accuracy of  $\pm 4 \mu\text{mol kg}^{-1}$ . It offers a large data set of  $A_T$  and  $C_T$  for  
 1231 the global ocean and regional biogeochemical studies. It includes more than 44 400 surface and water column  
 1232 observations in all oceanic basins, in the Mediterranean Sea, in the coastal zones, near coral ~~reef~~reefs, and in  
 1233 rivers. For the open ocean this complements the SOCAT and GLODAP data-products (Bakker et al., 2016;  
 1234 Lauvset et al., 2021) and for the Mediterranean Sea the ongoing CARIMED dataset. For the coastal sites  
 1235 this also complements the synthesis of coastal time-series only done around North America (Fassbender et al.,  
 1236 2018; Jiang et al., 20202021; OCADS, 2023).



1258 **Figure 14:** Profiles of (a)  $A_T$  ( $\mu\text{mol kg}^{-1}$ ) and (b)  $C_T$  ( $\mu\text{mol kg}^{-1}$ ) observed at station ACE-20 (55°S-95°E,  
 1259 11/1/17, black triangles) compared with the profiles deduced from the SOCCOM float (WMO code 5905069)  
 1260 launched at that location (first data on January 12<sup>th</sup> 2017, grey circles). The location/drift of the float in 2017-  
 1261 2018 is shown on the inserted map. (c) Hovmoller section (Pressure/time) of anthropogenic CO<sub>2</sub> concentrations  
 1262 ( $C_{ant}$  in  $\mu\text{mol kg}^{-1}$ ) estimated from the float data ( $A_T$ ,  $C_T$ ,  $O_2$ , T) below 200m (period January 2017-February  
 1263 2018). Section produced with ODV (Schlitzer, 2018).

Mis en forme : Indice

1265 The SNAPO-CO<sub>2</sub> dataset enables to investigate seasonal variations to decadal trends of  $A_T$  and  $C_T$  in  
 1266 various oceanic provinces. In regions where data are available for more than 2 decades in surface water (North  
 1267 Atlantic, Ligurian Sea, Southern Indian Ocean, and coastal regions), all time-series show an increase in  $C_T$ .  
 1268 Excepted in the Mediterranean Sea,  $A_T$  appears relatively constant over time, although the  $A_T$  content present  
 1269 significant inter-annual variability such as in the NASPG or in the coastal zones including near the Congo and  
 1270 Amazon Rivers plumes.

1271 This dataset represents independent data for validation of reconstructed  $A_T$  or  $C_T$  fields using various  
 1272 methods (e.g. Rödenbeck et al., 2013, 2015; Sauzède et al., 2017; Turk et al., 2017; Bittig et al., 2018; Broullón

1273 et al., 2019, 2020; Land et al., 2019; Keppler et al., 2020; Fourier et al., 2020; Gregor and Gruber, 2021; Sims et  
1274 al., 2023; Chau et al., 2023). It is also useful to validate Earth System Models (ESM) that currently present bias  
1275 to reproduce the seasonal cycle of  $C_T$  and  $A_T$  due to inadequate representation of biogeochemical cycles,  
1276 including the coupling of biological and physical processes (e.g. Pilcher et al., 2015; Mongwe et al., 2018;  
1277 Lerner et al., 2021). This should be resolved for confident in future projections of the productivity, ocean  
1278 acidification, and the responses of the marine ecosystems (e.g. Kwiatowkki et al., 2020). Recall that OBGm or  
1279 ESM models calculate  $pCO_2$  from  $A_T/C_T$  pairs and the simulated annual  $CO_2$  flux might be correct when  
1280 compared to observations but for wrong reasons (e.g. Goris et al., 2018, Lerner et al., 2021). For example, it has  
1281 been shown that biases in  $A_T$  in ESM models led to an overestimation of the oceanic  $fCO_2$  trend and thus  
1282 uncertainty when predicting the oceanic anthropogenic  $CO_2$  uptake (Lebehot et al., 2019). The simulated  
1283 seasonal cycle of  $pCO_2/CO_2$  is also uncertain in ESM models especially in high latitudes (e.g. Joos et al., 2023).  
1284 It is thus important to attempt validating ESM models with  $A_T$  and  $C_T$  data such as presented in this synthesis.

Mis en forme : Police :Italique

1285 This dataset would also serve for validating autonomous platforms capable of measuring pH and  
1286  $pCO_2/CO_2$  variables and, along with SOCAT and GLODAP datasets, provides an additional reference dataset for  
1287 the development and validation of regional biogeochemical models for simulating air-sea  $CO_2$  fluxes. It is also  
1288 essential for training and validating neural networks capable of predicting variables in the carbonate system,  
1289 thereby enhancing observations of marine  $CO_2$  at different spatial and temporal scales.

1290 The data presented here are available online on the Seanoë server (Metzl et al., 2023,  
1291 <https://doi.org/10.17882/95414>) and is divided in two files: one for the Global Ocean, and one for the  
1292 Mediterranean Sea. The sources of the original datasets (doi) with the associated references are listed in the  
1293 Supplementary Material (Table S3, S4). We invite the users to comment on any anomaly that would have not  
1294 been detected or to suggest potential misqualification of data in the present product (e.g. data probably good  
1295 although assigned with **Flagflag** 3, probably wrong). The SNAPO-CO2 dataset will be regularly updated on  
1296 Seanoë data server with new observations controlled and archived.

Mis en forme : Couleur de police :  
Automatique

## 1297 **8 Data availability**

Mis en forme : Couleur de police :  
Automatique

1299 Data presented in this study are available at Seanoë: <https://www.seanoë.org>, <https://doi.org/10.17882/95414>  
1300 (Metzl et al., 2023).

1301  
1302 *Author contributions.* NM prepared the data synthesis, the figures and wrote the draft of the manuscript with  
1303 contributions from all authors. JF measured the discrete samples since 2014, with the help from CM and CLM,  
1304 and prepared the individual reports for each project. NM and JF pre-qualified the discrete  $A_T/C_T$  data. CLM and  
1305 NM are co-Is of the ongoing OISO project and qualified the underway  $A_T/C_T$  data from OISO and CLIM-  
1306 **EPARSES** cruises. All authors have contributed either to organizing cruises, sample collection and/or data  
1307 qualification, and reviewed the manuscript.

1308  
1309 *Competing interest.* The authors declare that they have no conflict of interest.

1310  
1311 *Acknowledgments.* The  $A_T$  and  $C_T$  data presented in this study were measured at the SNAPO-CO2 facility  
1312 (Service National d'Analyse des Paramètres Océaniques du CO2) housed by the LOCEAN laboratory and part of  
1313 the OSU ECCE Terra at Sorbonne University and INSU/CNRS analytical services. Support by INSU/CNRS, by  
1314 OSU ECCE Terra and by LOCEAN, is gratefully acknowledged as well as support by different French "Services

1315 nationaux d'Observations", such as OISO/CARAUS, SOMLIT, PIRATA, SSS and MOOSE. We thank the  
1316 research infrastructure ICOS (Integrated Carbon Observation System) France for funding a large part of the  
1317 analyses. We thank the French oceanographic fleet ("Flotte océanographique française") for financial and  
1318 logistic support for most cruises listed in this synthesis and for the OISO program  
1319 (<https://campagnes.flotteoceanographique.fr/series/228/>). We acknowledge the MOOSE program (Mediterranean  
1320 Ocean Observing System for the Environment, <https://campagnes.flotteoceanographique.fr/series/235/fr/>)  
1321 coordinated by CNRS-INSU and the Research Infrastructure ILICO (CNRS-IFREMER). AWIPEV-CO2 was  
1322 supported by the Coastal Observing System for Northern and Arctic Seas (COSYNA), the two Helmholtz large-  
1323 scale infrastructure projects ACROSS and MOSES, the French Polar Institute (IPEV) as well as the European  
1324 Union's Horizon 2020 research and innovation projects Jericho-Next (No 871153 and 951799), INTAROS (No  
1325 727890) and FACE-IT (No 869154). ~~Support from~~ The BOUSSOLE time series project was funded by the  
1326 Centre National d'Etudes Spatiales (CNES) and the European Space Agency (ESA ESRIN contract  
1327 4000119096/17/I-BG), and the first three years of the CO2 time series at that site were funded by the French  
1328 Agence Nationale de la Recherche (ANR) is also acknowledged through their funding of the BIOCAREX  
1329 project. The EURECA4-OA cruise was also supported by the EUREC4A-OA JPI Ocean and Climate program.  
1330 We thank Tara Ocean Foundation and many institutes and funding agencies for supporting TARA cruises since  
1331 2009. The OISO program was supported by the French institutes INSU (Institut National des Sciences de  
1332 l'Univers) and IPEV (Institut Polaire Paul-Emile Victor), OSU Ecce-Terra (at Sorbonne Université), and the  
1333 French program SOERE/Great-Gases. ~~We thank the French oceanographic fleet ("Flotte océanographique~~  
1334 ~~française") for financial and logistic support for all cruises listed in this synthesis and for the OISO program~~  
1335 ~~(<https://campagnes.flotteoceanographique.fr/series/228/>).~~ The CLIM-EPARSES cruise was supported by TAAF  
1336 (Terres Australes et Antarctiques Françaises), Fondation du Prince Albert II de Monaco, IRD, OSU Ecce-Terra,  
1337 CNRS, MNHN, LOCEAN and LSCE laboratory. Data from the float launched during the ACE cruise were made  
1338 freely available by the Southern Ocean Carbon and Climate Observations and Modeling (SOCCOM) Project  
1339 funded by the National Science Foundation, Division of Polar Programs (NSF PLR -1425989), supplemented by  
1340 NASA, and by the International Argo Program and the NOAA programs that contribute to it. The Argo Program  
1341 is part of the Global Ocean Observing System (<http://doi.org/10.17882/42182>, <http://argo.jcompos.org>). We  
1342 thank Frédéric Merceur (IFREMER) for preparing the page and data availability on Seanoe. We thank Patrick  
1343 Raimbault (retired, former at MIO, Marseille) for managing the MOOSE project until 2019. We thank all  
1344 colleagues and students who participated to the cruises and have carefully collected the precious seawater  
1345 samples. We warmly acknowledge our colleague Christian Brunet (retired) for his supportive help for the  
1346 analysis since the start of the Service facility SNAPO-CO2. We would like to pay tribute to our late colleague  
1347 Frédéric Diaz who contributed to the LATEX cruise in 2010. We thank the associated editor Xingchen Wang to  
1348 manage this manuscript, Marta Álvarez and a (more or less) anonymous reviewer for their suggestions that  
1349 helped to improve this article.

Mis en forme : Police :Non Italique

## 1351 References

1352  
1353 Álvarez, M., Catalá, T. S., Civitarese, G., Coppola, L., Hassoun, A. E.R., Ibello, V., Lazzari, P., Lefevre, D.,  
1354 Macías, D., Santinelli, C. and Ulses, C.: Chapter 11 - Mediterranean Sea general biogeochemistry, Editor(s):  
1355 Katrin Schroeder, Jacopo Chiggiato, Oceanography of the Mediterranean Sea, Elsevier, Pages 387-451,  
1356 <https://doi.org/10.1016/B978-0-12-823692-5.00004-2>, 2023.

Mis en forme : Police :10 pt, Non  
Gras, Non souligné

Mis en forme : Normal



1358 Bakker, D. C. E., Pfeil, B., Smith, K., Hankin, S., Olsen, A., Alin, S. R., Cosca, C., Harasawa, S., Kozyr, A.,  
1359 Nojiri, Y., O'Brien, K. M., Schuster, U., Telszewski, M., Tilbrook, B., Wada, C., Akl, J., Barbero, L., Bates, N.  
1360 R., Boutin, J., Bozec, Y., Cai, W.-J., Castle, R. D., Chavez, F. P., Chen, L., Chierici, M., Currie, K., De Baar, H.  
1361 J. W., Evans, W., Feely, R. A., Fransson, A., Gao, Z., Hales, B., Hardman-Mountford, N. J., Hoppema, M.,  
1362 Huang, W.-J., Hunt, C. W., Huss, B., Ichikawa, T., Johannessen, T., Jones, E. M., Jones, S., Jutterström, S.,  
1363 Kitidis, V., Körtzinger, A., Landschützer, P., Lauvset, S. K., Lefèvre, N., Manke, A. B., Mathis, J. T., Merlivat,  
1364 L., Metzl, N., Murata, A., Newberger, T., Omar, A. M., Ono, T., Park, G.-H., Paterson, K., Pierrot, D., Ríos, A.  
1365 F., Sabine, C. L., Saito, S., Salisbury, J., Sarma, V. V. S. S., Schlitzer, R., Sieger, R., Skjelvan, I., Steinhoff, T.,  
1366 Sullivan, K. F., Sun, H., Sutton, A. J., Suzuki, T., Sweeney, C., Takahashi, T., Tjiputra, J., Tsurushima, N., Van  
1367 Heuven, S. M. A. C., Vandemark, D., Vlahos, P., Wallace, D. W. R., Wanninkhof, R. and Watson, A. J.: An  
1368 update to the Surface Ocean CO<sub>2</sub> Atlas (SOCAT version 2). *Earth System Science Data*, 6, 69-90.  
1369 doi:10.5194/essd-6-69-2014. 2014  
1370  
1371 Bakker, D. C. E., Pfeil, B., Landa, C. S., Metzl, N., O'Brien, K. M., Olsen, A., Smith, K., Cosca, C., Harasawa,  
1372 S., Jones, S. D., Nakaoka, S.-I., Nojiri, Y., Schuster, U., Steinhoff, T., Sweeney, C., Takahashi, T., Tilbrook, B.,  
1373 Wada, C., Wanninkhof, R., Alin, S. R., Balestrini, C. F., Barbero, L., Bates, N. R., Bianchi, A. A., Bonou, F.,  
1374 Boutin, J., Bozec, Y., Burger, E. F., Cai, W.-J., Castle, R. D., Chen, L., Chierici, M., Currie, K., Evans, W.,  
1375 Featherstone, C., Feely, R. A., Fransson, A., Goyet, C., Greenwood, N., Gregor, L., Hankin, S., Hardman-  
1376 Mountford, N. J., Harlay, J., Hauck, J., Hoppema, M., Humphreys, M. P., Hunt, C. W., Huss, B., Ibáñez, J. S.  
1377 P., Johannessen, T., Keeling, R., Kitidis, V., Körtzinger, A., Kozyr, A., Krasakopoulou, E., Kuwata, A.,  
1378 Landschützer, P., Lauvset, S. K., Lefèvre, N., Lo Monaco, C., Manke, A., Mathis, J. T., Merlivat, L., Millero, F.  
1379 J., Monteiro, P. M. S., Munro, D. R., Murata, A., Newberger, T., Omar, A. M., Ono, T., Paterson, K., Pearce, D.,  
1380 Pierrot, D., Robbins, L. L., Saito, S., Salisbury, J., Schlitzer, R., Schneider, B., Schweitzer, R., Sieger, R.,  
1381 Skjelvan, I., Sullivan, K. F., Sutherland, S. C., Sutton, A. J., Tadokoro, K., Telszewski, M., Tuma, M., Van  
1382 Heuven, S. M. A. C., Vandemark, D., Ward, B., Watson, A. J., and Xu, S.: A multi-decade record of high-quality  
1383 fCO<sub>2</sub> data in version 3 of the Surface Ocean CO<sub>2</sub> Atlas (SOCAT), *Earth Syst. Sci. Data*, 8, 383-413,  
1384 doi:10.5194/essd-8-383-2016. 2016.  
1385  
1386 Bakker, D.C.E., Alin, S.R., Bates, N.R., Becker, M., Feely, R. A., Gritzalis, T. , Jones, S. D., Kozyr, A., Lauvset,  
1387 S. K., Metzl, N., Munro, D.R., Nakaoka, S.-I., Nojiri, Y., O'Brien, K., Olsen, A., Pierrot, D., Rehder, G.,  
1388 Steinhoff, T., Sutton, A., Sweeney, C., Tilbrook, B., Wada, C., Wanninkhof, R., and all >100 SOCAT  
1389 contributors: An alarming decline in the ocean CO<sub>2</sub> observing capacity. Available at [www.socat.info](http://www.socat.info), 2023.  
1390  
1391 Balch, W.M., Bates, N.R., Lam, P.J., Twining, B.S., Rosengard, S. Z., Bowler, B.C., Drapeau, D.T., Garley, R.,  
1392 Lubelczyk, L.C., Mitchell, C. and Rauschenberg S.: Factors regulating the Great Calcite Belt in the Southern  
1393 Ocean and its biogeochemical significance. *Global Biogeochem. Cycles*, 30, doi:10.1002/2016GB005414, 2016  
1394  
1395 Beaufort, L., Probert, I., de Garidel-Thoron, T., Bendif, E.M., Ruiz-Pino, D., Metzl, N., Goyet, C., Buchet, N.,  
1396 Coupel, P., Grelaud, M., Rost, B., Rickaby, R.E.M., and de Vargas C.: Sensitivity of coccolithophores to  
1397 carbonate chemistry and ocean acidification. *Nature*, doi:10.1038/nature10295. 2011  
1398  
1399 Bittig, H.C., Steinhoff, T., Claustre, H., Fiedler, B., Williams, N.L., Sauzède, R., Körtzinger, A. and Gattuso, J.-  
1400 P.: An Alternative to Static Climatologies: Robust Estimation of Open Ocean CO<sub>2</sub> Variables and Nutrient  
1401 Concentrations From T, S, and O<sub>2</sub> Data Using Bayesian Neural Networks. *Front. Mar. Sci.* 5:328. doi:  
1402 10.3389/fmars.2018.00328, 2018  
1403  
1404 Bockmon, E. E., and Dickson, A. G.: An inter-laboratory comparison assessing the quality of seawater carbon  
1405 dioxide measurements. *Marine Chemistry*, 171, 36-43, doi:10.1016/j.marchem.2015.02.002, 2015.  
1406  
1407 Bosse, A., Testor, P., Mayot, N., Prieur, L., D'Ortenzio, F., Mortier, L., Le Goff, H., Gourcuff, C., Coppola, L.,  
1408 Lavigne, H. and Raimbault, P.: A submesoscale coherent vortex in the Ligurian Sea: From dynamical barriers to  
1409 biological implications. *J. Geophys. Res. Oceans*, 122, doi:10.1002/2016JC012634., 2017.  
1410

Code de champ modifié

1411 Bozec, Y., Merlivat, L., Baudoux, A.-C., Beaumont, L., Blain, S., Bucciarelli, E., Danguy, T., Grossteffan, E.,  
1412 Guillot, A., Guillou, J., Répécaud, M., and Tréguer, P.: Diurnal to inter-annual dynamics of pCO<sub>2</sub> recorded by a  
1413 CARIOCA sensor in a temperate coastal ecosystem (2003–2009). *Marine Chemistry*, 126, 1-4, 13-26,  
1414 10.1016/j.marchem.2011.03.003. 2011

1415  
1416 Broullón, D., Pérez, F. F., Velo, A., Hoppema, M., Olsen, A., Takahashi, T., Key, R. M., Tanhua, T., González-  
1417 Dávila, M., Jeansson, E., Kozyr, A., and van Heuven, S. M. A. C.: A global monthly climatology of total  
1418 alkalinity: a neural network approach, *Earth Syst. Sci. Data*, 11, 1109–1127, [https://doi.org/10.5194/essd-11-](https://doi.org/10.5194/essd-11-1109-2019)  
1419 1109-2019. 2019

1420  
1421 Broullón, D., Pérez, F. F., Velo, A., Hoppema, M., Olsen, A., Takahashi, T., Key, R. M., Tanhua, T., Santana-  
1422 Casiano, J. M., and Kozyr, A.: A global monthly climatology of oceanic total dissolved inorganic carbon: a  
1423 neural network approach, *Earth Syst. Sci. Data*, 12, 1725–1743, <https://doi.org/10.5194/essd-12-1725-2020>.  
1424 2020

1425  
1426 Bushinsky, S. M., Landschützer, P., Rödenbeck, C., Gray, A. R., Baker, D., Mazloff, M. R., Resplandy L.,  
1427 Johnson K. S., and Sarmiento, J. L.: Reassessing Southern Ocean air-sea CO<sub>2</sub> flux estimates with the addition of  
1428 biogeochemical float observations. *Global Biogeochemical Cycles*, 33. doi: 10.1029/2019GB006176, 2019.

1429  
1430 Canesi, M., Douville, E., Montagna, P., Taviani, M., Stolarski, J., Bordier, L., Dapoigny, A., Coulibaly, G. E. H.,  
1431 Simon, A.-C., Agelou, M., Fin, J., Metzl, N., Iwankow, G., Allemand, D., Planes, S., Moulin, C., Lombard, F.,  
1432 Bourdin, G., Troublé, R., Agostini, S., Banaigs, B., Boissin, E., Boss, E., Bowler, C., de Vargas, C., Flores, M.,  
1433 Forcioli, D., Furla, P., Gilson, E., Galand, P. E., Pesant, S., Sunagawa, S., Thomas, O., Thurber, R. V., Voolstra,  
1434 C. R., Wincker, P., Zoccola, D., and Reynaud, S.: Differences in carbonate chemistry up-regulation of long-lived  
1435 reef-building corals. *Sci. Rep.* 13, 11589, Doi: 10.1038/s41598-023-37598-9, 2023.

1436  
1437 Caniaux, G., Giordani, H., Redelsperger, J.-L., Guichard, F., Key, E. and Wade, M.: Coupling between the  
1438 Atlantic cold tongue and the West African monsoon in boreal spring and summer. *J. Geophys. Res.*, 119,  
1439 C04003, doi:10.1029/2010JC006570., 2011.

1440  
1441 Cariou, T., and Bozec, Y.: COMOR-CARBORHONE 1 cruise, RV L'Europe,  
1442 <https://doi.org/10.17600/11060060>, 2011a.

1443  
1444 Cariou, T., and Bozec, Y.: COMOR-CARBORHONE 2 cruise, RV Téthys II,  
1445 <https://doi.org/10.17600/11450150>, 2011b.

1446  
1447 Cariou, T., and Bozec, Y.: CARBORHONE 3 cruise, RV Téthys II, <https://doi.org/10.17600/12450020>, 2012a.

1448  
1449 Cariou, T., and Bozec, Y.: CARBORHONE 4 cruise, RV Téthys II, <https://doi.org/10.17600/12450140>, 2012b.

1450  
1451 Carter, B. R., Williams, N. L., Gray, A. R., and Feely, R. A.: Locally interpolated alkalinity regression for global  
1452 alkalinity estimation, *Limnol. Oceanogr. Methods*, 14(4), 268–277, doi:10.1002/lom3.10087, 2016.

1453  
1454 Chau, T.-T.-T., Gehlen, M., Metzl, N., and Chevallier, F.: CMEMS-LSCE: A global 0.25-degree, monthly  
1455 reconstruction of the surface ocean carbonate system, *Earth Syst. Sci. Data Discuss.* [preprint],  
1456 <https://doi.org/10.5194/essd-2023-146>, in review, 2023.

1457  
1458 Chen, H., Haumann, F. A., Talley, L. D., Johnson, K. S., and Sarmiento, J. L.: The deep ocean's carbon exhaust.  
1459 *Global Biogeochemical Cycles*. doi: <https://doi.org/10.1002/essoar.10507757.1>, 2022

1460  
1461 Cheng, L. J., Abraham, J., Zhu, J., Trenberth, K. E., Fasullo, J., Boyer, T., Locarnini, R., Zhang, B., Yu, F. J.,  
1462 Wan, L. Y., Chen, X. R., Song, X. Z., Liu, Y. L., and Mann, M. E.: Record-setting ocean warmth continued in  
1463 2019, *Adv. Atmos. Sci.*, 37, 137-142. <https://doi.org/10.1007/s00376-020-9283-7>, 2020

1464

1465 Claustre, H., Johnson, K. S., and Takeshita, Y.: Observing the Global Ocean with Biogeochemical-Argo. *Annual*  
1466 *Review of Marine Science*, 12: 23-48 | DOI: [10.1146/annurev-marine-010419-010956](https://doi.org/10.1146/annurev-marine-010419-010956), 2020.  
1467  
1468 Conan, P., Guieux, A., and Vuillemin, R.: MOOSE (MOLA), <https://doi.org/10.18142/234>, 2020.  
1469  
1470 Copin-Montégut, C.: Alkalinity and carbon budgets in the Mediterranean Sea, *Global Biogeochemical Cycles*,  
1471 vol. 7, pp. 915–925, 1993.  
1472  
1473 Copin-Montégut, C., and Bégovic, M.: Distributions of carbonate properties and oxygen along the water column  
1474 (0–2000 m) in the central part of the NW Mediterranean Sea (Dyfamed site): influence of the winter vertical  
1475 mixing on air–sea CO<sub>2</sub> and O<sub>2</sub> exchanges. *Deep-Sea Research II* 49, 2049–2066, [https://doi.org/10.1016/S0967-](https://doi.org/10.1016/S0967-0645(02)00027-9)  
1476 [0645\(02\)00027-9](https://doi.org/10.1016/S0967-0645(02)00027-9), 2002.  
1477  
1478 Coppola, L., and Diamond-Riquier, E.: MOOSE (DYFAMED), <https://doi.org/10.18142/131>, 2008.  
1479  
1480 Coppola, L., Raimbault, P., Mortier, L., and Testor, P.: Monitoring the environment in the northwestern  
1481 Mediterranean Sea, *Eos*, 100, <https://doi.org/10.1029/2019EO125951>. Published on 25 July 2019.  
1482  
1483 Coppola, L., Boutin, J., Gattuso, J.-P., Lefèvre, D., and Metzl, N.: The Carbonate System in the Ligurian Sea. In  
1484 *The Mediterranean Sea in the Era of Global Change: Evidence from 30 years of multidisciplinary study of the*  
1485 *Ligurian Sea*, C. Migon, P. Nival, A. Sciandra, Eds. (ISTE Science Publishing LTD, London, UK, 2020), vol. 1,  
1486 chap. 4, pp. 79-104. ISBN: 9781786304285. <https://doi.org/10.1002/9781119706960.ch4>, 2020.  
1487  
1488 [Coppola, L., Fourier, M., Pasqueron de Fommervault, O., Poteau, A., Riquier, E. D. and Béguery, L.:](#)  
1489 [Highresolution study of the air-sea CO2 flux and net community oxygen production in the Ligurian Sea by a](#)  
1490 [fleet of gliders. \*Front. Mar. Sci.\* 10:1233845. doi: 10.3389/fmars.2023.1233845, 2023](#)  
1491  
1492 Corbière, A., Metzl, N., Reverdin, G., Brunet, C., and Takahashi, T.: Interannual and decadal variability of the  
1493 oceanic carbon sink in the North Atlantic subpolar gyre. *Tellus B*, Vol. 59, issue 2, 168-179, DOI:  
1494 [10.1111/j.1600-0889.2006.00232, 2007](https://doi.org/10.1111/j.1600-0889.2006.00232.2007).  
1495  
1496 D'Ortenzio, F. and Taillandier, V.: BIO-ARGO-MED-2018 cruise, RV Téthys II,  
1497 <https://doi.org/10.17600/18000550>, 2018.  
1498  
1499 De Carlo, E. H., Mousseau, L., Passafiume, O., Drupp, P. and Gattuso J.-P.: Carbonate chemistry and air-sea  
1500 CO<sub>2</sub> flux in a NW Mediterranean bay over a four-year period: 2007-2011. *Aquatic Geochemistry*  
1501 doi:10.1007/s10498-013-9217-4, 2013.  
1502  
1503 Dickson, A. G., Sabine, C. L., and Christian, J. R.: Guide to best practices for ocean CO<sub>2</sub> measurements, North  
1504 Pacific Marine Science Organization, Sidney, British Columbia, 191, <https://doi.org/10.25607/OBP-1342>, 2007.  
1505  
1506 Division Plans de DMI – SHOM: PROTEUS2010\_LEG1 cruise, RV Pourquoi pas ?,  
1507 <https://doi.org/10.17600/10030040>, 2010.  
1508  
1509 Division Plans de DMI – SHOM: PROTEVSMED\_PERLE\_2018 cruise, RV L'Atalante,  
1510 <https://campagnes.flotteoceanographique.fr/campaign>, 2018.  
1511  
1512 Doney, S. C., Fabry, V. J., Feely, R. A., and Kleypas, J. A., Ocean acidification: The other CO<sub>2</sub> problem. *Annual*  
1513 *Review of Marine Science*, 1(1), 169–192. [10.1146/annurev.marine.010908.163834](https://doi.org/10.1146/annurev.marine.010908.163834), 2009  
1514  
1515 Doney, S. C., Busch, D. S., Cooley, S. R., and Kroeker, K. J.: The Impacts of Ocean Acidification on Marine  
1516 Ecosystems and Reliant Human Communities. *Annual Review of Environment and Resources* 45:1,  
1517 <https://doi.org/10.1146/annurev-environ-012320-083019>. 2020  
1518

Code de champ modifié

1519 Douville, E., Bourdin, G., Lombard, F., Gorsky, G., Fin, J., Metzl, N., Pesant, S., and Tara Pacific Consortium:  
1520 Seawater carbonate chemistry dataset collected during the Tara Pacific Expedition 2016-2018. PANGAEA,  
1521 <https://doi.org/10.1594/PANGAEA.944420>, 2022.

1522

1523 Durrieu de Madron, X.: CASCADE cruise, RV L'Atalante, <https://doi.org/10.17600/11010020>, 2011.

1524

1525 Durrieu de Madron, X., and Conan, P.: PERLE2 cruise, RV Pourquoi pas ?, <https://doi.org/10.17600/18000865>,  
1526 2018

1527

1528 Edmond, J. M.: High precision determination of titration alkalinity and total carbon dioxide content of sea water  
1529 by potentiometric titration, *Deep-Sea Res.*, 17, 737–750, [https://doi.org/10.1016/0011-7471\(70\)90038-0](https://doi.org/10.1016/0011-7471(70)90038-0), 1970.

1530

1531 Eldin, G. : PANDORA cruise, RV L'Atalante, <https://doi.org/10.17600/12010050>, 2012.

1532

1533 Eyring, V., Righi, M., Lauer, A., Evaldsson, M., Wenzel, S., Jones, C., Anav, A., Andrews, O., Cionni, I., Davin,  
1534 E. L., Deser, C., Ehbrecht, C., Friedlingstein, P., Gleckler, P., Gottschaldt, K.-D., Hagemann, S., Jukes, M.,  
1535 Kindermann, S., Krasting, J., Kunert, D., Levine, R., Loew, A., Mäkelä, J., Martin, G., Mason, E., Phillips, A. S.,  
1536 Read, S., Rio, C., Roehrig, R., Senfleben, D., Sterl, A., van Ulft, L. H., Walton, J., Wang, S., and Williams, K.  
1537 D.: ESMValTool (v1.0) – a community diagnostic and performance metrics tool for routine evaluation of Earth  
1538 system models in CMIP, *Geosci. Model Dev.*, 9, 1747-1802, doi:10.5194/gmd-9-1747-2016, 2016.

1539

1540 Fabry, V. J., Seibel, B. A., Feely, R. A. and Orr, J. C.: Impacts of ocean acidification on marine fauna and  
1541 ecosystem processes. *ICES J. Mar. Sci.* 65, 414–432. <https://doi.org/10.1093/icesjms/fsn048>, 2008.

1542

1543 Fassbender, A. J., Sabine, C. L., and Palevsky, H. I.: Nonuniform ocean acidification and attenuation of the  
1544 ocean carbon sink, *Geophys. Res. Lett.*, 44, 8404–8413, doi:10.1002/2017GL074389., 2017.

1545

1546 Fassbender, A. J., Alin, S. R., Feely, R. A., Sutton, A. J., Newton, J. A., Krembs, C., Bos, J., Keyzers, M., Devol,  
1547 A., Ruef, W., and Pelletier, G.: Seasonal carbonate chemistry variability in marine surface waters of the US  
1548 Pacific Northwest, *Earth Syst. Sci. Data*, 10, 1367–1401, <https://doi.org/10.5194/essd-10-1367-2018>, 2018.

1549

1550 Feely, R. A., Sabine, C. L., Byrne, R. H., Millero, F. J., Dickson, A. G., Wanninkhof, R., et al.: Decadal changes  
1551 in the aragonite and calcite saturation state of the Pacific Ocean. *Global Biogeochemical Cycles*, 26, GB3001.  
1552 <https://doi.org/10.1029/2011GB004157>, 2012.

1553

1554 [Feely, R. A., Jiang, L.-Q., Wanninkhof, R., Carter, B. R., Alin, S. R., Bednaršek, N., and Cosca, C. E.:  
1555 Acidification of the global surface ocean: What we have learned from observations. \*Oceanography\*,  
1556 <https://doi.org/10.5670/oceanog.2023.222>, 2023](https://doi.org/10.5670/oceanog.2023.222)

1557

1558 Fleury, E., Petton, S., Benabdelmouna, A., and Pouvreau, S., (coord.): Observatoire national du cycle de vie de  
1559 l'huître creuse en France. Rapport annuel ECOSCOPA 2022. R.INT.BREST RBE/PFOM/PI 2023-1, 2023.

1560

1561 Fourrier, M., Coppola, L., Claustre, H., D'Ortenzio, F., Sauzède, R. and Gattuso, J.-P.: A regional neural  
1562 network approach to estimate water-column nutrient concentrations and carbonate system variables in the  
1563 Mediterranean Sea: CANYON-MED. *Frontiers in Marine Science*, 7:620,  
1564 <https://www.frontiersin.org/articles/10.3389/fmars.2020.00620>, 2020.

1565

1566 Fourrier, M., Coppola, L., D'Ortenzio, F., Migon, C., and Gattuso, J.-P.: Impact of intermittent convection in the  
1567 northwestern Mediterranean Sea on oxygen content, nutrients, and the carbonate system. *Journal of Geophysical  
1568 Research: Oceans*, 127, e2022JC018615. <https://doi.org/10.1029/2022JC018615>, 2022

1569

1570 Friedlingstein, P., O'Sullivan, M., Jones, M. W., Andrew, R. M., Gregor, L., Hauck, J., Le Quéré, C., Luijckx, I.  
1571 T., Olsen, A., Peters, G. P., Peters, W., Pongratz, J., Schwingshackl, C., Sitch, S., Canadell, J. G., Ciais, P.,  
1572 Jackson, R. B., Alin, S. R., Alkama, R., Arneeth, A., Arora, V. K., Bates, N. R., Becker, M., Bellouin, N., Bittig,  
1573 H. C., Bopp, L., Chevallier, F., Chini, L. P., Cronin, M., Evans, W., Falk, S., Feely, R. A., Gasser, T., Gehlen,

1574 M., Gkritzalis, T., Gloege, L., Grassi, G., Gruber, N., Gürses, Ö., Harris, I., Hefner, M., Houghton, R. A., Hurtt,  
1575 G. C., Iida, Y., Ilyina, T., Jain, A. K., Jersild, A., Kadono, K., Kato, E., Kennedy, D., Klein Goldewijk, K.,  
1576 Knauer, J., Korsbakken, J. I., Landschützer, P., Lefèvre, N., Lindsay, K., Liu, J., Liu, Z., Marland, G., Mayot, N.,  
1577 McGrath, M. J., Metzl, N., Monacci, N. M., Munro, D. R., Nakaoka, S.-I., Niwa, Y., O'Brien, K., Ono, T.,  
1578 Palmer, P. I., Pan, N., Pierrot, D., Pocock, K., Poulter, B., Resplandy, L., Robertson, E., Rödenbeck, C.,  
1579 Rodriguez, C., Rosan, T. M., Schwinger, J., Séférian, R., Shutler, J. D., Skjelvan, I., Steinhoff, T., Sun, Q.,  
1580 Sutton, A. J., Sweeney, C., Takao, S., Tanhua, T., Tans, P. P., Tian, X., Tian, H., Tilbrook, B., Tsujino, H.,  
1581 Tubiello, F., van der Werf, G. R., Walker, A. P., Wanninkhof, R., Whitehead, C., Willstrand Wranne, A.,  
1582 Wright, R., Yuan, W., Yue, C., Yue, X., Zaehle, S., Zeng, J., and Zheng, B.: Global Carbon Budget 2022, *Earth*  
1583 *Syst. Sci. Data*, 14, 4811–4900, <https://doi.org/10.5194/essd-14-4811-2022>, 2022.

1584

1585 Fröb, F., Olsen, A., Becker, M., Chafik, L., Johannessen, T., Reverdin, G., and Omar, A.: Wintertime fCO<sub>2</sub>  
1586 variability in the subpolar North Atlantic since 2004. *Geophysical Research Letters*, 46,  
1587 <https://doi.org/10.1029/2018GL080554>, 2019.

1588

1589 Gac, J.-P., Marrec, P., Cariou, T., Guillerm, C., Macé, E., Vernet, M., and Bozec, Y.: Cardinal buoys: An  
1590 opportunity for the study of air-sea CO<sub>2</sub> fluxes in coastal ecosystems. *Front. Mar. Sci.* doi:  
1591 10.3389/fmars.2020.00712. 2020.

1592

1593 Gac, J.-P., Marrec, P., Cariou, T., Grosstefan, E., Macé, E., Rimmelin-Maury, P., Vernet, M., and Bozec, Y.:  
1594 Decadal Dynamics of the CO<sub>2</sub> System and Associated Ocean Acidification in Coastal Ecosystems of the North  
1595 East Atlantic Ocean. *Front. Mar. Sci.* 8:688008. doi:10.3389/fmars.2021.688008, 2021.

1596

1597 Ganachaud, A., Cravatte, S., Sprintall, J., Germineaud, C., Albery, M., Jeandel, C., Eldin, G., Metzl, N., Bonnet,  
1598 S., Benavides, M., Heimbürger, L.-E., Lefèvre, J., Michael, S., Resing, J., Quéroué, F., Sarthou, G., Rodier, M.,  
1599 Berthelot, H., Baurand, F., Grelet, J., Hasegawa, T., Kessler, W., Kilepak, M., Lacan, F., Privat, E., Send, U.,  
1600 Van Beek, P., Souhaut, M. and Sonke, J. E.: The Solomon Sea: its circulation, chemistry, geochemistry and  
1601 biology explored during two oceanographic cruises. *Elem Sci Anth*, 5: 33, DOI:  
1602 <https://doi.org/10.1525/elementa.221>, 2017.

1603

1604 Gattuso, J.-P., Magnan, A., Billé, R., Cheung, W. W. L., Howes, E. L., Joos, F., Allemand, D., Bopp, L., Cooley,  
1605 S., Eakin, M., Hoegh-Guldberg, O., Kelly, R. P., Pörtner, H.-O., Rogers, A. D., Baxter, J. M., Laffoley, D.,  
1606 Osborn, D., Rankovic, A., Rochette, J., Sumaila, U. R., Treyer, S., and Turley, C.: Contrasting futures for ocean  
1607 and society from different anthropogenic CO<sub>2</sub> emissions scenarios. *Science* 349:aac4722.doi:  
1608 10.1126/science.aac4722, 2015.

1609

1610 Gattuso, J.-P., Alliouane, S., and Mousseau, L.: Seawater carbonate chemistry in the Bay of Villefranche, Point  
1611 B (France), January 2007 - September 2020. PANGAEA, <https://doi.org/10.1594/PANGAEA.727120>, 2021.

1612

1613 Gattuso, J.-P., Alliouane, S., and Fischer, P.: High-frequency, year-round time series of the carbonate chemistry  
1614 in a high-Arctic fjord (Svalbard), *Earth Syst. Sci. Data*, 15, 2809–2825, [https://doi.org/10.5194/essd-15-2809-](https://doi.org/10.5194/essd-15-2809-2023)  
1615 [2023](https://doi.org/10.5194/essd-15-2809-2023), 2023.

1616

1617 Gattuso, J.-P., Alliouane, S., and Fischer, P.: High-frequency, year-round time series of the carbonate chemistry  
1618 in a high-Arctic fjord (Svalbard) v2. PANGAEA, <https://doi.org/10.1594/PANGAEA.960131>, 2023.

1619

1620 Gemayel, E., Hassoun, A. E. R., Benallal, M. A., Goyet, C., Rivaro, P., Abboud-Abi Saab, M., Krasakopoulou,  
1621 E., Touratier, F., and Ziveri, P.: Climatological variations of total alkalinity and total inorganic carbon in the  
1622 Mediterranean Sea surface waters. *Earth Syst. Dynam.*, 6, 789–800, doi:10.5194/esd-6-789-2015. 2015.

1623

1624 Golbol, M., Vellucci, V., and Antoine, D.: BOUSSOLE, <https://doi.org/10.18142/1>, 2000.

1625

1626 Golbol M., Boutin J., Merlivat L., Vellucci, V., and Antoine, D.: Dissolved Inorganic Carbon and Total  
1627 Alkalinity sampled at Boussole site in the Mediterranean Sea. SEANO. <https://doi.org/10.17882/71911>, 2020.

Code de champ modifié

Code de champ modifié

1628  
1629 Goris, N., Tjiputra, J. F., Olsen, A., Schwinger, J., Lauvset, S. K. and Jeansson, E.: Constraining projection-  
1630 based estimates of the future North Atlantic carbon uptake, *J. Climate*, 31, 3959–3978,  
1631 <https://doi.org/10.1175/JCLI-D-17-0564.1>, 2018.  
1632  
1633 Goyet, C., Beauverger, C., Brunet, C., and Poisson, A.: Distribution of carbon dioxide partial pressure in surface  
1634 waters of the Southwest Indian Ocean, *Tellus B: Chemical and Physical Meteorology*, 43:1, 1-11, DOI:  
1635 [10.3402/tellusb.v43i1.15242](https://doi.org/10.3402/tellusb.v43i1.15242), 1991.  
1636  
1637 Gregor, L. and Gruber, N.: OceanSODA-ETHZ: a global gridded data set of the surface ocean carbonate system  
1638 for seasonal to decadal studies of ocean acidification, *Earth Syst. Sci. Data*, 13, 777–808,  
1639 <https://doi.org/10.5194/essd-13-777-2021>, 2021.  
1640  
1641 Gruber, N., Clement, D. , Carter, B. R., Feely, R. A., van Heuven, S., Hoppema, M., Ishii, M., Key, R. M.,  
1642 Kozyr, A., Lauvset, S. K., Lo Monaco, C. , Mathis, J. T., Murata, A., Olsen, A., Perez, F. F., Sabine, C. L.,  
1643 Tanhua, T., and Wanninkhof, R.: The oceanic sink for anthropogenic CO<sub>2</sub> from 1994 to 2007, *Science* vol. 363  
1644 (issue 6432), pp. 1193-1199. DOI: 10.1126/science.aau5153, 2019.  
1645  
1646 Guieu, C., Desboeufs, K., Albani, S., et al.: BIOGEOCHEMICAL dataset collected during the PEACETIME  
1647 cruise. SEANOE. <https://doi.org/10.17882/75747>, 2020.  
1648  
1649 Hagens, M., and Middelburg, J. J.: Attributing seasonal pH variability in surface ocean waters to governing  
1650 factors, *Geophys. Res. Lett.*, 43, doi:10.1002/2016GL071719. 2016.  
1651  
1652 Henson, S. A., Painter, S. C., Holliday, N. P., Stinchcombe, M. C., and Giering, S. L. C.: Unusual subpolar  
1653 North Atlantic phytoplankton bloom in 2010: Volcanic fertilization or North Atlantic Oscillation?, *J. Geophys.*  
1654 *Res. Oceans*, 118, 4771–4780, doi:10.1002/jgrc.20363, 2013.  
1655  
1656 Hoegh-Guldberg, O., Mumby, P.J., Hooten, A.J., Steneck, R.S., Greenfield, P., Gomez, E., Harvell, C.D., Sale,  
1657 P.F., Edwards, A.J., Caldeira, K., Knowlton, N., Eakin, C.M., Iglesias-Prieto, R., Muthiga, N., Bradbury, R.H.,  
1658 Dubi, A., and Hatziolos, M.E.: Coral reefs under rapid climate change and ocean acidification. *Science* 14,  
1659 1737–1742. <https://doi.org/10.1126/science.1152509>, 2007.  
1660  
1661 Hood, E.M., and Merlivat, L.: Annual to interannual variations of fCO<sub>2</sub> in the northwestern Mediterranean  
1662 Sea: Results from hourly measurements made by CARIOCA buoys, 1995-1997, *Journal Of Marine Research*,  
1663 59, 113-131, doi: 10.1357/002224001321237399. 2001  
1664  
1665 Howes, E., Stemmann, L., Assailly, C., Irissou, J.-O., Dima, M., Bijma, J., Gattuso, J.-P.: Pteropod time series  
1666 from the North Western Mediterranean (1967-2003): impacts of pH and climate variability. *Mar Ecol Prog Ser*  
1667 531: 193-206, doi: 10.3354/meps11322. 2015.  
1668  
1669 Howes, E. L., Eagle, R., Gattuso, J.-P., and Bijma, J.: Comparison of Mediterranean pteropod shell biometrics  
1670 and ultrastructure from historical (1910 and 1921) and present day (2012) samples provides baseline for  
1671 monitoring effects of global change. *PLoS ONE* 12:e0167891. 2017.  
1672  
1673 IPCC. Changing Ocean, Marine Ecosystems, and Dependent Communities. in *The Ocean and Cryosphere in a*  
1674 *Changing Climate* 447–588 (Cambridge University Press, 2022). doi:10.1017/9781009157964.007. 2022  
1675  
1676 Jiang, Z.-P., Tyrrell, T., Hydes, D. J., Dai, M., and Hartman, S. E.: Variability of alkalinity and the alkalinity-  
1677 salinity relationship in the tropical and subtropical surface ocean, *Global Biogeochem. Cycles*, 28, 729–742,  
1678 doi:10.1002/2013GB004678, 2014.  
1679

Mis en forme : Anglais (États Unis)

1680 Jiang, L.-Q., Feely, R. A., Carter, B. R., Greeley, D. J., Gledhill, D. K., and Arzayus K. M.: Climatological  
1681 distribution of aragonite saturation state in the global oceans, *Global Biogeochem. Cycles*, 29, 1656–1673,  
1682 doi:10.1002/2015GB005198, 2015.

1683

1684 Jiang, L.-Q., Carter, B. R., Feely, R. A., Lauvset, S. K. and Olsen, A.: Surface ocean pH and buffer capacity:  
1685 past, present and future, *Sci Rep*, 9(1), 1–11, doi:10.1038/s41598-019-55039-4. 2019.

1686

1687 Jiang, L.-Q., Feely, R. A., Wanninkhof, R., ~~et al~~Greeley, D., Barbero, L., Alin, S., Carter, B. R., Pierrot, D.,  
1688 Featherstone, C., Hooper, J., Melrose, C., Monacchi, N., Sharp, J. D., Shellito, S., Xu, Y.-Y., Kozyr, A., Byrne, R.  
1689 H., Cai, W.-J., Cross, J., Johnson, G. C., Hales, B., Langdon, C., Mathis, J., Salisbury, J., and Townsend, D. W.:  
1690 Coastal Ocean Data Analysis Product in North America (CODAP-NA, ~~Version 2021~~) (NCEI Accession  
1691 0219960). ~~[indicate subset used]~~. NOAA National Centers) – an internally consistent data product for  
1692 Environmental Information Dataset. ~~https://doi.org/10.25921/531n-e230~~. Accessed [date]. 2020-discrete  
1693 inorganic carbon, oxygen, and nutrients on the North American ocean margins. *Earth System Science Data*,  
1694 13(6), 2777–2799. <https://doi.org/10.5194/essd-13-2777-2021>, 2021

1695

1696 Jiang, L.-Q., Dunne, J., Carter, B. R., Tjiputra, J. F., Terhaar, J., Sharp, J. D., et al.: Global surface ocean  
1697 acidification indicators from 1750 to 2100. *Journal of Advances in Modeling Earth Systems*, 15,  
1698 e2022MS003563. <https://doi.org/10.1029/2022MS003563>, 2023a

1699

1700 Jiang, L.Q., Kozyr, A., Relph, J.M. *et al.* The Ocean Carbon and Acidification Data System. *Sci Data* 10, 136.  
1701 <https://doi.org/10.1038/s41597-023-02042-0>, 2023b

1702

1703 Johnson, K. S., Mazloff, M. R., Bif, M. B., Takeshita, Y., Jannasch, H. W., Maurer, T. L., et al.: Carbon to  
1704 nitrogen uptake ratios observed across the Southern Ocean by the SOCCOM profiling float array. *Journal of*  
1705 *Geophysical Research: Oceans*, 127, e2022JC018859. <https://doi.org/10.1029/2022JC018859>, 2022.

1706

1707 Joos, F., Hameau, A., Frölicher, T. L., and Stephenson, D. B.: Anthropogenic attribution of the  
1708 increasing seasonal amplitude in surface ocean pCO<sub>2</sub>. *Geophysical Research Letters*, 50, e2023GL102857.  
1709 <https://doi.org/10.1029/2023GL102857>, 2023.

1710

1711 Joyce, T. and Corry, C., eds: Requirements for WOCE Hydrographic Programme Data Reporting. WHPO  
1712 Publication 90-1 Revision 2, WOCE Report 67/91, Woods Hole, Mass., USA, May 1994.

1713

1714 Kapsenberg, L., Alliouane, S., Gazeau, F., Mousseau, L., and Gattuso, J.-P.: Coastal ocean acidification and  
1715 increasing total alkalinity in the northwestern Mediterranean Sea, *Ocean Sci.*, 13, 411-426, doi:10.5194/os-13-  
1716 411-2017, 2017.

1717

1718 Keppler, L., Landschützer, P., Gruber, N., Lauvset, S. K., and Stemmler, I.: Seasonal carbon dynamics in the  
1719 near-global ocean. *Global Biogeochemical Cycles*, 34, e2020GB006571. doi:10.1029/2020GB006571, 2020.

1720

1721 Keppler, L., Landschützer, P., Lauvset, S.K., and Gruber, N.: Recent trends and variability in the oceanic storage  
1722 of dissolved inorganic carbon. *Global Biogeochemical Cycles*, 37, e2022GB007677. Doi:  
1723 10.1029/2022GB007677, 2023.

1724

1725 Keraghel, M. A., Louanchi, F., Zerrouki, M., Kaci, M. A., Aït-Ameur, N., Labaste, M., Legoff, H., Taillandier,  
1726 V., Harid, R., and Mortier, L.: Carbonate system properties and anthropogenic carbon inventory in the Algerian  
1727 Basin during SOMBA cruise (2014): Acidification estimate, *Marine Chemistry*,  
1728 <https://doi.org/10.1016/j.marchem.2020.103783>. 2020.

1729

1730 Key, R. M., Kozyr, A., Sabine, C. L., Lee, K., Wanninkhof, R., Bullister, J. L., Feely, R. A., Millero, F. J.,  
1731 Mordy, C., and Peng, T. H.: A global ocean carbon climatology: Results from Global Data Analysis Project  
1732 (GLODAP), *Global Biogeochemical Cycles*, 18, GB4031, <https://doi.org/10.1029/2004GB002247>, 2004.

1733

Mis en forme : Interligne : simple,  
Taquets de tabulation : Pas à 1,27 cm

1734 Key, R. M., Tanhua, T., Olsen, A., Hoppema, M., Jutterström, S., Schirnack, C., van Heuven, S., Kozyr, A., Lin,  
1735 X., Velo, A., Wallace, D. W. R., and Mintrop, L.: The CARINA data synthesis project: introduction and  
1736 overview, *Earth Syst. Sci. Data*, 2, 105–121, <https://doi.org/10.5194/essd-2-105-2010>, 2010.  
1737

1738 Khatiwala, S., Tanhua, T., Mikaloff Fletcher, S., Gerber, M., Doney, S. C., Graven, H. D., Gruber, N.,  
1739 McKinley, G. A., Murata, A., Ríos, A. F., and Sabine, C. L.: Global ocean storage of anthropogenic carbon,  
1740 *Biogeosciences*, 10, 2169–2191, <https://doi.org/10.5194/bg-10-2169-2013>, 2013.  
1741

1742 Kitidis, V., Shutler, J. D., Ashton, I., Warren, M., Brown, I., Findlay, H., Hartman, S. E., Sanders, R.,  
1743 Humphreys, M., Kivimäe, C., Greenwood, N., Hull, T., Pearce, D., McGrath, T., Stewart, B. M., Walsham, P.,  
1744 McGovern, E., Bozec, Y., Gac, J.-P., van Heuven, S., Hoppema, M., Schuster, U., Johannessen, T., Omar, A.,  
1745 Lauvset, S. K., Skjelvan, I., Olsen, A., Steinhoff, T., Körtzinger, A., Becker, M., Lefèvre, N., Diverrès, D.,  
1746 Gkritzalis, T., Catrijsse, A., Petersen, W., Voynova, Y., Chapron, B., Grouazel, A., Land, P. E., Sharples, J., and  
1747 Nightingale, P. D.: Winter weather controls net influx of atmospheric CO<sub>2</sub> on the north-west European shelf. *Sci*  
1748 *Rep* 9, 20153, doi:10.1038/s41598-019-56363-5. 2019.  
1749

1750 Koffi U., Lefevre, N., Kouadio, G., and Boutin, J.: Surface CO<sub>2</sub> parameters and air-sea CO<sub>2</sub> fluxes distribution  
1751 in the eastern equatorial Atlantic Ocean. *J. Marine Systems*, doi:10.1016/j.jmarsys/2010.04.010. 2010.  
1752

1753 Koffi, U., Georges, K., and Boutin, J.: Partial pressure (or fugacity) of carbon dioxide, dissolved inorganic  
1754 carbon, alkalinity, temperature, salinity and other variables collected from Surface underway, discrete sample  
1755 and profile observations using CTD, Carbon dioxide (CO<sub>2</sub>) gas analyzer and other instruments from ANTEA  
1756 and L'ATALANTE in the Gulf of Guinea, North Atlantic Ocean and South Atlantic Ocean from 2005-06-09 to  
1757 2007-09-30 (NCEI Accession 0108086). [indicate subset used]. NOAA National Centers for Environmental  
1758 Information. Dataset. [https://doi.org/10.3334/cdiac/otg.egee1\\_6](https://doi.org/10.3334/cdiac/otg.egee1_6). Accessed [date]., 2013  
1759

1760 Koseki, S., Tjiputra, J., Fransner, F. et al.: Disentangling the impact of Atlantic Niño on sea-air CO<sub>2</sub> flux. *Nat*  
1761 *Commun* 14, 3649. <https://doi.org/10.1038/s41467-023-38718-9>, 2023.  
1762

1763 Kwiatkowski, L., Torres, O., Bopp, L., Aumont, O., Chamberlain, M., Christian, J. R., Dunne, J. P., Gehlen, M.,  
1764 Ilyina, T., John, J. G., Lenton, A., Li, H., Lovenduski, N. S., Orr, J. C., Palmieri, J., Santana-Falcón, Y.,  
1765 Schwinger, J., Séférian, R., Stock, C. A., Tagliabue, A., Takano, Y., Tjiputra, J., Toyama, K., Tsujino, H.,  
1766 Watanabe, M., Yamamoto, A., Yool, A., and Ziehn, T.: Twenty-first century ocean warming, acidification,  
1767 deoxygenation, and upper-ocean nutrient and primary production decline from CMIP6 model projections,  
1768 *Biogeosciences*, 17, 3439–3470, <https://doi.org/10.5194/bg-17-3439-2020>, 2020.  
1769

1770 Land, P. E., Findlay, H. S., Shutler, J. D., Ashton, I. G., Holding, T., Grouazel, A., Girard-Arduin, F., Reul, N.,  
1771 Piolle, J. F., Chapron, B., and Quilfen, Y.: Optimum satellite remote sensing of the marine carbonate system  
1772 using empirical algorithms in the global ocean, the Greater Caribbean, the Amazon Plume and the Bay of  
1773 Bengal. *Remote Sensing of Environment*, 235, p.111469, doi: 10.1016/j.rse.2019.111469, 2019.  
1774

1775 Lange, N., Fiedler, B., Álvarez, M., Benoit-Cattin, A., Benway, H., Buttigieg, P. L., Coppola, L., Currie, K.,  
1776 Flecha, S., Honda, M., Huertas, I. E., Lauvset, S. K., Muller-Karger, F., Körtzinger, A., O'Brien, K. M.,  
1777 Ólafsdóttir, S. R., Pacheco, F. C., Rueda-Roa, D., Skjelvan, I., Wakita, M., White, A., and Tanhua, T.: Synthesis  
1778 Product for Ocean Time-Series (SPOTS) – A ship-based biogeochemical pilot, *Earth Syst. Sci. Data Discuss.*  
1779 [preprint], <https://doi.org/10.5194/essd-2023-238>, in review, 2023.  
1780

1781 Lauvset, S. K., Gruber, N., Landschützer, P., Olsen, A., and Tjiputra, J.: Trends and drivers in global surface  
1782 ocean pH over the past 3 decades. *Biogeosciences*, 12, 1285–1298, doi:10.5194/bg-12-1285-2015, 2015  
1783

1784 Lauvset, S. K., Carter, B. R., Perez, F. F., Jiang, L.-Q., Feely, R. A., Velo, A., and Olsen, A.: Processes Driving  
1785 Global Interior Ocean pH Distribution, *Global Biogeochem. Cycles*, 34, e2019GB006 229,  
1786 <https://doi.org/10.1029/2019GB006229>, 2020.  
1787

Mis en forme : Anglais (États Unis)



1788 Lauvset, S. K., Lange, N., Tanhua, T., Bittig, H. C., Olsen, A., Kozyr, A., Álvarez, M., Becker, S., Brown, P. J.,  
1789 Carter, B. R., Cotrim da Cunha, L., Feely, R. A., van Heuven, S., Hoppema, M., Ishii, M., Jeansson, E.,  
1790 Jutterström, S., Jones, S. D., Karlsen, M. K., Lo Monaco, C., Michaelis, P., Murata, A., Pérez, F. F., Pfeil, B.,  
1791 Schirnack, C., Steinfeldt, R., Suzuki, T., Tilbrook, B., Velo, A., Wanninkhof, R., Woosley, R. J., and Key, R. M.:  
1792 An updated version of the global interior ocean biogeochemical data product, GLODAPv2.2021, *Earth Syst. Sci.*  
1793 *Data*, 13, 5565–5589, <https://doi.org/10.5194/essd-13-5565-2021>, 2021.

1794

1795 [Lauvset, S. K., Lange, N., Tanhua, T., Bittig, H. C., Olsen, A., Kozyr, A., Alin, S., Álvarez, M., Azetsu-Scott,](#)  
1796 [K., Barbero, L., Becker, S., Brown, P. J., Carter, B. R., da Cunha, L. C., Feely, R. A., Hoppema, M., Humphreys,](#)  
1797 [M. P., Ishii, M., Jeansson, E., Jiang, L.-Q., Jones, S. D., Lo Monaco, C., Murata, A., Müller, J. D., Pérez, F. F.,](#)  
1798 [Pfeil, B., Schirnack, C., Steinfeldt, R., Suzuki, T., Tilbrook, B., Ulfso, A., Velo, A., Woosley, R. J., and Key, R.](#)  
1799 [M.: GLODAPv2.2022: the latest version of the global interior ocean biogeochemical data product. \*Earth Syst.\*](#)  
1800 [Sci. Data, 14, 5543–5572. <https://doi.org/10.5194/essd-14-5543-2022>, 2022.](#)

1801

1802 Lebehot, A. D., Halloran, P. R., Watson, A. J., McNeill, D., Ford, D. A., Landschützer, P., Lauvset, S. K.,  
1803 and Schuster, U.: Reconciling Observation and Model Trends in North Atlantic Surface CO<sub>2</sub>, *Global*  
1804 *Biogeochem. Cy.*, 33, 1204–1222, <https://doi.org/10.1029/2019GB006186>, 2019.

1805

1806 Lee, K., Wanninkhof, R., Feely, R. A., Millero, F. J., and Peng, T.-H.: Global relationships of total inorganic  
1807 carbon with temperature and nitrate in surface seawater, *Global Biogeochem. Cy.*, 14, 979–994,  
1808 <https://doi.org/10.1029/1998GB001087>, 2000.

1809

1810 Lee, K., Tong, L.T., Millero, F.J., Sabine, C.L., Dickson, A.G., Goyet, C., Park, G.H., Wanninkhof, R., Feely,  
1811 R.A., and Key, R.M.: Global relationships of total alkalinity with salinity and temperature in surface waters of  
1812 the world's oceans. *Geophys. Res. Lett.* 33, L19605. doi10.1029/2006GL027207. 2006.

1813

1814 Lefèvre, D.: MOOSE (ANTARES), <https://doi.org/10.18142/233>, 2010.

1815

1816 Lefèvre, N., Guillot, A., Beaumont, L., and Danguy, T.: Variability of fCO<sub>2</sub> in the Eastern Tropical Atlantic  
1817 from a moored buoy. *J. of Geophysical Research-Oceans*, Volume: 113 Issue: C1, DOI:  
1818 10.1029/2007JC004146. 2008.

1819

1820 Lefèvre N., and Merlivat, L.: Carbon and oxygen net community production in the eastern tropical Atlantic  
1821 estimated from a moored buoy. *Global biogeochemical cycles*, 26(1), 1-14.  
1822 <https://doi.org/10.1029/2010GB004018>. 2012.

1823

1824 Lefèvre, N., Diverres, D., and Gallois, F.: Origin of CO<sub>2</sub> undersaturation in the western tropical Atlantic: *Tellus*  
1825 *Series B Chemical and Physical Meteorology*. Volume: 62 Issue: 5 Special Issue: SI Pages: 595-607 DOI:  
1826 10.1111/j.1600-0889.2010.00475.x, 2010.

1827

1828 Lefèvre N.: Carbon parameters along a zonal transect. *SEANOE*. <https://doi.org/10.17882/58575>, 2010.

1829

1830 Lefèvre, N., Veleda, D., Araujo, M., Caniaux, G.: Variability and trends of carbon parameters at a time series in  
1831 the eastern tropical Atlantic. *Tellus B*, Co-Action Publishing, 68, pp.30305. 10.3402/tellusb.v68.30305. 2016.

1832

1833 Lefèvre, N., Mejia, C., Khvorostyanov, D., Beaumont, L., and Koffi, U.: Ocean Circulation Drives the  
1834 Variability of the Carbon System in the Eastern Tropical Atlantic. *Oceans*, 2021, 2, 126–148.  
1835 <https://doi.org/10.3390/oceans2010008>, 2021.

1836

1837 Lefèvre, N.: Discrete profile measurements of dissolved inorganic carbon, total alkalinity, temperature and  
1838 salinity collected from R/V Antea French PIRATA cruise in Eastern Tropical Atlantic Ocean from 2009-07-10  
1839 to 2010-10-01 (NCEI Accession 0171193), 2018a.

1840

1841 Lefèvre, N.: Discrete surface measurements of dissolved inorganic carbon, total alkalinity, temperature and  
1842 salinity collected from R/V Le Suroit French PIRATA cruise in Eastern Tropical Atlantic Ocean from 2011-05-  
1843 03 to 2011-05-25 (NCEI Accession 0171197), 2018b.

Mis en forme : Anglais (États Unis)

Code de champ modifié

1844  
1845 Lefèvre, N.: Discrete profile measurements of dissolved inorganic carbon, total alkalinity, temperature and  
1846 salinity collected from R/V Le Suroit French PIRATA cruise in Eastern Tropical Atlantic Ocean from 2012-03-  
1847 21 to 2012-04-30 (NCEI Accession 0171195), 2018c.  
1848  
1849 Lefèvre, N.: Discrete surface measurements of dissolved inorganic carbon, total alkalinity, temperature and  
1850 salinity collected from R/V Le Suroit French PIRATA cruise in Eastern Tropical Atlantic Ocean from 2013-05-  
1851 11 to 2013-06-18 (NCEI Accession 0171189), 2018d.  
1852  
1853 Lefèvre, N.: Discrete profile measurements of dissolved inorganic carbon, total alkalinity, temperature and  
1854 salinity collected from R/V Le Suroit French PIRATA cruise in Eastern Tropical Atlantic Ocean from 2014-04-  
1855 10 to 2014-05-19 (NCEI Accession 0171194), 2018e.  
1856  
1857 Lefèvre, N.: Discrete surface measurements of dissolved inorganic carbon, total alkalinity, temperature and  
1858 salinity collected from R/V Thalassa French PIRATA cruise in Eastern Tropical Atlantic Ocean from 2015-03-  
1859 18 to 2015-04-15 (NCEI Accession 0171196), 2018f.  
1860  
1861 Lefèvre, N.: Discrete surface measurements of dissolved inorganic carbon, total alkalinity, temperature and  
1862 salinity collected from R/V Thalassa French PIRATA cruise in Eastern Tropical Atlantic Ocean from 2016-03-  
1863 08 to 2016-04-11 (NCEI Accession 0171190), 2018g.  
1864  
1865 Lefèvre, N.: Discrete surface measurements of dissolved inorganic carbon, total alkalinity, temperature and  
1866 salinity collected from R/V Thalassa French PIRATA cruise in Eastern Tropical Atlantic Ocean from 2017-02-  
1867 26 to 2017-03-30 (NCEI Accession 0171191), 2018h.  
1868  
1869 Le Quéré, C., Moriarty, R., Andrew, R. M., Canadell, J. G., Sitch, S., Korsbakken, J. I., Friedlingstein, P., Peters,  
1870 G. P., Andres, R. J., Boden, T. A., Houghton, R. A., House, J. I., Keeling, R. F., Tans, P., Arneeth, A., Bakker, D.  
1871 C. E., Barbero, L., Bopp, L., Chang, J., Chevallier, F., Chini, L. P., Ciais, P., Fader, M., Feely, R. A., Gkritzalis,  
1872 T., Harris, I., Hauck, J., Ilyina, T., Jain, A. K., Kato, E., Kitidis, V., Klein Goldewijk, K., Koven, C.,  
1873 Landschützer, P., Lauvset, S. K., Lefèvre, N., Lenton, A., Lima, I. D., Metzl, N., Millero, F., Munro, D. R.,  
1874 Murata, A., Nabel, J. E. M. S., Nakaoka, S., Nojiri, Y., O'Brien, K., Olsen, A., Ono, T., Pérez, F. F., Pfeil, B.,  
1875 Pierrot, D., Poulter, B., Rehder, G., Rödenbeck, C., Saito, S., Schuster, U., Schwinger, J., Séférian, R., Steinhoff,  
1876 T., Stocker, B. D., Sutton, A. J., Takahashi, T., Tilbrook, B., van der Laan-Luijkx, I. T., van der Werf, G. R., van  
1877 Heuven, S., Vandemark, D., Viovy, N., Wiltshire, A., Zaehle, S., and Zeng, N.: Global Carbon Budget 2015,  
1878 *Earth Syst. Sci. Data*, 7, 349–396, <https://doi.org/10.5194/essd-7-349-2015>, 2015.  
1879  
1880 Lerner, P., Romanou, A., Kelley, M., Romanski, J., Ruedy, R., and Russell, G.: Drivers of Air-Sea CO<sub>2</sub> Flux  
1881 Seasonality and its Long-Term Changes in the NASA-GISS model CMIP6 submission. *Journal of Advances in*  
1882 *Modeling Earth Systems*, 13, e2019MS002028. [Doi:10.1029/2019MS002028](https://doi.org/10.1029/2019MS002028), 2021.  
1883  
1884 Leseurre, C., Lo Monaco, C., Reverdin, G., Metzl, N., Fin, J., Olafsdottir, S., and Racapé, V.: Ocean carbonate  
1885 system variability in the North Atlantic Subpolar surface water (1993–2017), *Biogeosciences*, 17, 2553–2577,  
1886 <https://doi.org/10.5194/bg-17-2553-2020>, 2020  
1887  
1888 Leseurre, C., Lo Monaco, C., Reverdin, G., Metzl, N., Fin, J., Mignon, C., and Benito, L.: Summer trends and  
1889 drivers of sea surface fCO<sub>2</sub> and pH changes observed in the southern Indian Ocean over the last two decades  
1890 (1998–2019), *Biogeosciences*, 19, 2599–2625, <https://doi.org/10.5194/bg-19-2599-2022>, 2022.  
1891  
1892 Lherminier, P., Mercier, H., Gourcuff, C., Alvarez, M., Bacon, S., and Kermabon, C.: Transports across the 2002  
1893 Greenland-Portugal OVIDE section and comparison with 1997. *J. Geophys. Res.*, 112(C7), C07003,  
1894 [doi:10.1029/2006JC003716](https://doi.org/10.1029/2006JC003716). 2007  
1895  
1896 Li, B. F., Watanabe, Y. W., Hosoda, S., Sato, K., and Nakano, Y.: Quasireal-time and high-resolution  
1897 spatiotemporal distribution of ocean anthropogenic CO<sub>2</sub>. *Geophysical Research Letters*, 46, 4836–4843.  
1898 <https://doi.org/10.1029/2018GL081639>, 2019.  
1899

Code de champ modifié

1900 Lo Monaco, C., Álvarez, M., Key, R. M., Lin, X., Tanhua, T., Tilbrook, B., Bakker, D. C. E., van Heuven, S.,  
1901 Hoppema, M., Metzl, N., Ríos, A. F., Sabine, C. L., and Velo, A.: Assessing the internal consistency of the  
1902 CARINA database in the Indian sector of the Southern Ocean, *Earth Syst. Sci. Data*, 2, 51–70,  
1903 <https://doi.org/10.5194/essd-2-51-2010>, 2010.

1904  
1905 Lo Monaco, C., Metzl, N., Fin, J., and Tribollet, A.: Sea surface measurements of dissolved inorganic carbon  
1906 (DIC) and total alkalinity (TALK), temperature and salinity during the R/V Marion-Dufresne cruise CLIM-  
1907 EPARSEs (EXPOCODE 35MV20190405) in the Indian Ocean and Mozambique Channel from 2019-04-04 to  
1908 2019-04-30. (NCEI Accession 0212218). [indicate subset used]. NOAA National Centers for Environmental  
1909 Information. Dataset. <https://doi.org/10.25921/26rw-w185>. Accessed [date]. 2020.

1910  
1911 Lo Monaco, C., Metzl, N., Fin, J., Mignon, C., Cuet, P., Douville, E., Gehlen, M., Trang Chau, T.T., and  
1912 Tribollet, A.: Distribution and long-term change of the sea surface carbonate system in the Mozambique Channel  
1913 (1963-2019), *Deep-Sea Research Part II*, <https://doi.org/10.1016/j.dsr2.2021.104936>, 2021

1914  
1915 Lombard, F., Bourdin, G., Pesant, S., Agostini, S., Baudena, A., Boissin, E., Cassar, N., Clampitt, M., Conan,  
1916 P., Da Silva, O., Dimier, C., Douville, E., Elineau, A., Fin, J., Flores, J.-M., Ghiglione, J.-F., Hume, B. C. C.,  
1917 Jalabert, L., John, S. G., Kelly, R. L., Koren, I., Lin, Y., Marie, D., McMinds, R., Mériguet, Z., Metzl, N., Paz-  
1918 García, D. A., Luiza Pedrotti, M., Poulain, J., Pujo-Pay, M., Ras, J., Reverdin, G., Romac, S., Röttinger, E.,  
1919 Vardi, A., Voolstra, C. R., Moulin, C., Iwankow, G., Banaigs, B., Bowler, C., de Vargas, C., Forcioli, D., Furla,  
1920 P., Galand, P. E., Gilson, E., Reynaud, S., Sunagawa, S., Thomas, O., Troublé, R., Vega Thurber, R., Wincker,  
1921 P., Zoccola, D., Allemand, D., Planes, S., Boss, E., and Gorsky, G.: Open science resources from the Tara  
1922 Pacific expedition across the surface ocean and coral reef ecosystems. *Sci Data* 10, 324 (2023).  
1923 <https://doi.org/10.1038/s41597-022-01757-w>, 2022.

1924  
1925 [Lueker, T. J., Dickson, A. G., and Keeling, C. D.: Ocean pCO<sub>2</sub> calculated from dissolved inorganic carbon,  
1926 alkalinity, and equations for K-1 and K-2: validation based on laboratory measurements of CO<sub>2</sub> in gas and  
1927 seawater at equilibrium. \*Marine Chemistry\* 70, 105-119. \[https://doi.org/10.1016/S0304-4203\\(00\\)00022-0\]\(https://doi.org/10.1016/S0304-4203\(00\)00022-0\), 2000.](#)

1928  
1929 Ma, D., Gregor, L., and Gruber, N: Four decades of trends and drivers of global surface ocean acidification.  
1930 *Global Biogeochemical Cycles*, 37, e2023GB007765. [10.1029/2023GB007765](https://doi.org/10.1029/2023GB007765), 2023.

1931  
1932 Maier, C., Watremez, P., Taviani, M., Weinbauer, M. G, and Gattuso, J-P.: Calcification rates and the effect of  
1933 ocean acidification on Mediterranean cold-water corals. *Proceedings of the Royal Society B-Biological Sciences*,  
1934 279(1734), 1716-1723, doi:10.1098/rspb.2011.1763. 2012.

1935  
1936 Margirier, F., Testor, P., Heslop, E. et al. : Abrupt warming and salinification of intermediate waters interplays  
1937 with decline of deep convection in the Northwestern Mediterranean Sea. *Sci Rep* 10, 20923. [10.1038/s41598-  
1938 020-77859-5](https://doi.org/10.1038/s41598-020-77859-5), 2020.

1939  
1940 Marrec, P., Cariou, T., Collin, E., Durand, A., Latimier, M., Macé, E., Morin, P., Raimund, S., Vernet, M., and  
1941 Bozec, Y.: Seasonal and latitudinal variability of the CO<sub>2</sub> system in the western English Channel based on  
1942 Voluntary Observing Ship (VOS) measurements. *Marine Chemistry*, 155 (2013): 29–41. 2013.

1943  
1944 Marrec, P., Cariou, T., Latimier, M., Macé, E., Morin, P., Vernet, M., and Bozec, Y.: Spatio-temporal dynamics  
1945 of biogeochemical processes and air–sea CO<sub>2</sub> fluxes in the Western English Channel based on two years of  
1946 FerryBox deployment. *Journal of Marine Systems*, Special Issue: 5<sup>th</sup> FerryBox Workshop.  
1947 [10.1016/j.jmarsys.2014.05.010](https://doi.org/10.1016/j.jmarsys.2014.05.010). 2014.

1948  
1949 Marrec, P., Cariou, T., Macé, E., Morin, P., Salt, L. A., Vernet, M., Taylor, B., Paxman, K., and Y. Bozec:  
1950 Dynamics of air–sea CO<sub>2</sub> fluxes in the northwestern European shelf based on voluntary observing ship and  
1951 satellite observations, *Biogeosciences*, 12, 5371-5391, doi:10.5194/bg-12-5371-2015. 2015

1952  
1953 Marrec, P., and Bozec, Y.: Partial pressure (or fugacity) of carbon dioxide, dissolved inorganic carbon, alkalinity  
1954 and salinity collected from Surface underway observations using Carbon dioxide (CO<sub>2</sub>) gas analyzer and other

1955 instruments from ARMORIQUE in the English Channel from 2012-04-25 to 2013-01-03 (NCEI Accession  
1956 0157472). Version 1.1. NOAA National Centers for Environmental Information. Dataset.  
1957 doi:10.3334/CDIAC/OTG.COAST\_FERRYBOX\_ROSCOFF\_PLYMOUTH\_2012 [access date]. 2016a.  
1958  
1959 Marrec, P., and Bozec, Y.: Partial pressure (or fugacity) of carbon dioxide, dissolved inorganic carbon, alkalinity  
1960 and salinity collected from Surface underway observations using Carbon dioxide (CO<sub>2</sub>) gas analyzer and other  
1961 instruments from ARMORIQUE in the English Channel from 2013-03-15 to 2013-12-22 (NCEI Accession  
1962 0157444). Version 1.1. NOAA National Centers for Environmental Information. Dataset.  
1963 doi:10.3334/CDIAC/OTG.COAST\_FERRYBOX\_ROSCOFF\_PLYMOUTH\_2013 [access date]. 2016b.  
1964  
1965 Marrec, P., and Bozec, Y.: Partial pressure (or fugacity) of carbon dioxide, dissolved inorganic carbon, alkalinity  
1966 and salinity collected from surface underway observations using Carbon dioxide (CO<sub>2</sub>) gas analyzer and other  
1967 instruments from ARMORIQUE in the English Channel from 2014-03-18 to 2014-10-09 (NCEI Accession  
1968 0163193). Version 1.1. NOAA National Centers for Environmental Information. Dataset.  
1969 doi:10.3334/CDIAC/OTG.COAST\_FERRYBOX\_ROSCOFF\_PLYMOUTH\_2014 [access date]. 2017.  
1970  
1971 Mazloff, M. R., Verdy, A., Gille, S. T., Johnson, K. S., Cornuelle, B. D., and Sarmiento, J.: Southern Ocean  
1972 acidification revealed by biogeochemical-Argo floats. *Journal of Geophysical Research: Oceans*, 128,  
1973 e2022JC019530. <https://doi.org/10.1029/2022JC019530>, 2023.  
1974  
1975 McCulloch, M., Trotter, J., Montagna, P., Falter, J., Dunbar, R., Freiwald, A., Försterra, G., López Correa, M.,  
1976 Maier, C., Rüggeberg, A., and Taviani, M.: Resilience of cold-water scleractinian corals to ocean acidification:  
1977 Boron isotopic systematics of pH and saturation state up-regulation. *Geochimica et Cosmochimica Acta*, Volume  
1978 87, 21-34. <http://dx.doi.org/10.1016/j.gca.2012.03.027>. 2012  
1979  
1980 McKinley, G. A., Fay, A. R., Takahashi, T., and Metzl, N.: Convergence of atmospheric and North Atlantic  
1981 carbon dioxide trends on multidecadal timescales. *Nature Geoscience*. doi:10.1038/NGEO1193. 2011.  
1982  
1983 McKinley, G. A., Ritzer, A. L. and Lovenduski, N. S.: Mechanisms of northern North Atlantic biomass  
1984 variability, *Biogeosciences*, 15(20), 6049–6066, doi:<https://doi.org/10.5194/bg-15-6049-2018>, 2018.  
1985  
1986 Meier, K. J. S., Beaufort, L., Heussner, S., and Ziveri, P.: The role of ocean acidification in *Emiliana huxleyi*  
1987 coccolith thinning in the Mediterranean Sea, *Biogeosciences*, 11, 2857–2869, [https://doi.org/10.5194/bg-11-](https://doi.org/10.5194/bg-11-2857-2014)  
1988 2857-2014, 2014.  
1989  
1990 Mercier, H., Lherminier, P., Sarafanov, A., Gaillard, F., Daniault, N., Desbruyères, D., Falina, A., Ferron, B.,  
1991 Huck, T., and Thierry, V.: Variability of the meridional overturning circulation at the Greenland-Portugal Ovide  
1992 section from 1993 to 2010. *Progress in Oceanography*, 132, 250-261, doi:10.1016/j.pocean.2013.11.001. 2015  
1993  
1994 Merlivat, L., Boutin, J., Antoine, D., Beaumont, L., Golbol, M., and Vellucci, V.: Increase of dissolved inorganic  
1995 carbon and decrease in pH in near-surface waters in the Mediterranean Sea during the past two decades,  
1996 *Biogeosciences*, 15, 5653-5662, <https://doi.org/10.5194/bg-15-5653-2018>, 2018.  
1997  
1998 Metzl, N., Brunet, C., Jabaud-Jan, A., Poisson, A., and Schauer, B.: Summer and winter air-sea CO<sub>2</sub> fluxes in  
1999 the Southern Ocean *Deep Sea Res I*, 53, 1548-1563, doi:10.1016/j.dsr.2006.07.006. 2006.  
2000  
2001 Metzl, N., Tilbrook, B., Bakker, D., Le Quéré, C., Doney, S., Feely, R., Hood M., and Dargaville, R.: Global  
2002 Changes in Ocean Carbon: Variability and Vulnerability. *Eos, Transactions of the American Geophysical Union*  
2003 88 (28): 286-287. doi: 10.1029/2007EO280005, 2007.  
2004  
2005 Metzl, N., Corbière, A., Reverdin, G., Lenton, A., Takahashi, T., Olsen, A., Johannessen, T., Pierrot, D.,  
2006 Wanninkhof, R., Ólafsdóttir, S. R., Ólafsson, J., and Ramonet, M.: Recent acceleration of the sea surface fCO<sub>2</sub>  
2007 growth rate in the North Atlantic subpolar gyre (1993-2008) revealed by winter observations, *Global*  
2008 *Biogeochem. Cycles*, 24, GB4004, doi:10.1029/2009GB003658, 2010.

2009  
2010 Metzl, N., and Lo Monaco, C.: OISO - OCÉAN INDIEN SERVICE D'OBSERVATION,  
2011 <https://doi.org/10.18142/228>, 1998.  
2012  
2013 Metzl, N., Pierre, C., and Vangriesheim, A.: Hydrographic and Chemical measurements during the R/V  
2014 L'Atalante BIOZAIRE III Cruise in the Atlantic Ocean (14 December, 2003 - 7 January 2004).  
2015 <http://cdiac.esd.ornl.gov/ftp/oceans/BIOZAIRE3>. Carbon Dioxide Information Analysis Center, Oak Ridge  
2016 National Laboratory, US Department of Energy, Oak Ridge, Tennessee. doi:  
2017 10.3334/CDIAC/OTG.BIOZAIRE3, 2016.  
2018  
2019 Metzl, N., Ferron, B. Lherminier, P. Sarthou, G. Thierry, V.: Discrete profile measurements of dissolved  
2020 inorganic carbon (DIC), total alkalinity (TALK), temperature and salinity during the multiple ships Observatoire  
2021 de la variabilité interannuelle et décennale en Atlantique Nord (OVIDE) project, OVIDE-2006, OVIDE-2008,  
2022 OVIDE-2010, OVIDE-2012, OVIDE-2014 cruises in the North Atlantic Ocean from 2006-05-23 to 2014-06-30  
2023 (NCEI Accession 0177219). Version 1.1. NOAA National Centers for Environmental Information. Dataset.  
2024 doi:10.25921/v0qt-ms48 [access date], 2018.  
2025  
2026 Metzl, N., Fin, J., Lo Monaco, C., et al.: ~~SNAPO-CO2 data set~~-A synthesis of total alkalinity and ~~total~~-dissolved  
2027 inorganic carbon ~~observationsmeasurements~~ in the global ocean (1993-2022)-) SNAPO-CO2-V1 dataset.  
2028 SEANOE. <https://doi.org/10.17882/95414>, 2023.

2029 Mignot, A., Claustre, H., Cossarini, G., D'Ortenzio, F., Gutknecht, E., Lamouroux, J., Lazzari, P., Perruche, C.,  
2030 Salon, S., Sauzède, R., Taillandier, V., and Teruzzi, A.: Using machine learning and Biogeochemical-Argo  
2031 (BGC-Argo) floats to assess biogeochemical models and optimize observing system design, *Biogeosciences*, 20,  
2032 1405–1422, <https://doi.org/10.5194/bg-20-1405-2023>, 2023.  
2033  
2034 Millero, F. J., Lee, K. and Roche, M.: Distribution of alkalinity in the surface waters of the major oceans. *Mar.*  
2035 *Chem.* **60**, 111–130. [https://doi.org/10.1016/S0304-4203\(97\)00084-4](https://doi.org/10.1016/S0304-4203(97)00084-4). 1998.  
2036  
2037 Mongwe, N. P., Vichi, M., and Monteiro, P. M. S: The seasonal cycle of *p*CO<sub>2</sub> and CO<sub>2</sub> fluxes in the Southern  
2038 Ocean: Diagnosing anomalies in CMIP5 earth system models. *Biogeosciences*, 15(9), 2851–2872.  
2039 <https://doi.org/10.5194/bg-15-2851-2018>, 2018.  
2040  
2041 Mortier, L., Ait Ameer, N., and Taillandier, V.: SOMBA-GE-2014 cruise, RV Téthys II,  
2042 <https://doi.org/10.17600/14007500>, 2014.  
2043  
2044 Moutin, T., and Bonnet, S.: OUTPACE cruise, RV L'Atalante, <https://doi.org/10.17600/15000900>, 2015.  
2045  
2046 Moutin, T., Wagener, T., Caffin, M., Fumenia, A., Gimenez, A., Baklouti, M., Bouruet-Aubertot, P., Pujo-Pay,  
2047 M., Leblanc, K., Lefevre, D., Helias Nunige, S., Leblond, N., Grosso, O., and de Verneil, A.: Nutrient  
2048 availability and the ultimate control of the biological carbon pump in the western tropical South Pacific Ocean,  
2049 *Biogeosciences*, 15, 2961-2989, <https://doi.org/10.5194/bg-15-2961-2018>, 2018.  
2050  
2051 Newton, J.A., Feely, R. A., Jewett, E. B., Williamson, P. and Mathis, J.: Global Ocean Acidification Observing  
2052 Network: Requirements and Governance Plan. Second Edition, GOA-ON, [http://www.goa-on.org/docs/GOA-](http://www.goa-on.org/docs/GOA-ON-plan-print.pdf)  
2053 ~~ON-plan-print.pdf~~, <https://www.iaea.org/sites/default/files/18/06/goa-on-second-edition-2015.pdf>, 2015.  
2054  
2055 Nykjaer, L.: Mediterranean Sea surface warming 1985-2006. *Clim. Res.* 39, 11–17. doi: 10.3354/cr00794, 2009.  
2056  
2057 Obernosterer, I.: MOBYDICK-THEMISTO cruise, RV Marion-Dufresne, <https://doi.org/10.17600/18000403>,  
2058 2018.

2059  
2060 OCADS: Coastal Carbon Data, [https://www.ncei.noaa.gov/access/ocean-carbon-acidification-data-](https://www.ncei.noaa.gov/access/ocean-carbon-acidification-data-system/oceans/coastal_carbon_data.html)  
2061 [system/oceans/coastal\\_carbon\\_data.html](https://www.ncei.noaa.gov/access/ocean-carbon-acidification-data-system/oceans/coastal_carbon_data.html), 2023  
2062  
2063 Olafsson, J., Olafsdottir, S.R., Benoit-Cattin, A., Danielsen, M., Arnarson, T.S., and Takahashi, T.: Rate of  
2064 Iceland Sea acidification from time series measurements. *Biogeosciences* 6, 2661–2668.  
2065 <https://doi.org/10.5194/bg-6-2661-2009>, 2009.  
2066  
2067 Olivier, L., Boutin, J., Reverdin, G., Lefèvre, N., Landschützer, P., Speich, S., Karstensen, J., Labaste, M.,  
2068 Noisel, C., Ritschel, M., Steinhoff, T., and Wanninkhof, R.: Wintertime process study of the North Brazil  
2069 Current rings reveals the region as a larger sink for CO<sub>2</sub> than expected, *Biogeosciences*, 19, 2969–2988,  
2070 <https://doi.org/10.5194/bg-19-2969-2022>, 2022.  
2071  
2072 Olsen, A., Key, R. M., van Heuven, S., Lauvset, S. K., Velo, A., Lin, X., Schirnick, C., Kozyr, A., Tanhua, T.,  
2073 Hoppema, M., Jutterström, S., Steinfeldt, R., Jeansson, E., Ishii, M., Pérez, F. F., and Suzuki, T.: The Global  
2074 Ocean Data Analysis Project version 2 (GLODAPv2) – an internally consistent data product for the world ocean,  
2075 *Earth Syst. Sci. Data*, 8, 297–323, <https://doi.org/10.5194/essd-8-297-2016>, 2016.  
2076  
2077 Olsen, A., Lange, N., Key, R. M., Tanhua, T., Álvarez, M., Becker, S., Bittig, H. C., Carter, B. R., Cotrim da  
2078 Cunha, L., Feely, R. A., van Heuven, S., Hoppema, M., Ishii, M., Jeansson, E., Jones, S. D., Jutterström, S.,  
2079 Karlsen, M. K., Kozyr, A., Lauvset, S. K., Lo Monaco, C., Murata, A., Pérez, F. F., Pfeil, B., Schirnick, C.,  
2080 Steinfeldt, R., Suzuki, T., Telszewski, M., Tilbrook, B., Velo, A., and Wanninkhof, R.: GLODAPv2.2019 – an  
2081 update of GLODAPv2, *Earth Syst. Sci. Data*, 11, 1437–1461, <https://doi.org/10.5194/essd-11-1437-2019>, 2019.  
2082  
2083 Olsen, A., Lange, N., Key, R. M., Tanhua, T., Bittig, H. C., Kozyr, A., Álvarez, M., Azetsu-Scott, K., Becker, S.,  
2084 Brown, P. J., Carter, B. R., Cotrim da Cunha, L., Feely, R. A., van Heuven, S., Hoppema, M., Ishii, M.,  
2085 Jeansson, E., Jutterström, S., Landa, C. S., Lauvset, S. K., Michaelis, P., Murata, A., Pérez, F. F., Pfeil, B.,  
2086 Schirnick, C., Steinfeldt, R., Suzuki, T., Tilbrook, B., Velo, A., Wanninkhof, R., and Woosley, R. J.: An updated  
2087 version of the global interior ocean biogeochemical data product, GLODAPv2.2020, *Earth Syst. Sci. Data*, 12,  
2088 3653–3678, <https://doi.org/10.5194/essd-12-3653-2020>, 2020.  
2089  
2090 Orr, J. C., Epitalon, J.-M., and Gattuso, J.-P.: Comparison of ten packages that compute ocean carbonate  
2091 chemistry, *Biogeosciences*, 12(5), 1483–1510, doi:10.5194/bg-12-1483-2015, 2015.  
2092  
2093 [Orr, J. C., Epitalon, J.-M., Dickson, A. G., and Gattuso, J.-P.: Routine uncertainty propagation for the marine](#)  
2094 [carbon dioxide system, \*Marine Chemistry\*, Vol. 207, 84-107, doi:10.1016/j.marchem.2018.10.006., 2018.](#)  
2095  
2096 Parard, G., Lefèvre, N., and Boutin, J.: Sea water fugacity of CO<sub>2</sub> at the PIRATA mooring at 6°S, 10°W. *Tellus-*  
2097 *B*, DOI: 10.1111/j.1600-0889.2010.00503.x. 2010.  
2098  
2099 Pérez F. F., Vázquez-Rodríguez, M., Mercier, H., Velo, A., Lherminier, P. and Ríos, A. F.: Trends of  
2100 anthropogenic CO<sub>2</sub> storage in North Atlantic water masses. *Biogeosciences*, 7, 1789-1807, [doi:10.5194/bg-7-](https://doi.org/10.5194/bg-7-1789-2010)  
2101 [1789-2010](https://doi.org/10.5194/bg-7-1789-2010), 2010. Code de champ modifié  
2102  
2103 Pérez, F. F., Mercier, H., Vazquez-Rodriguez, M., Lherminier, P., Velo, A., Pardo, P., Roson, G., and Rios, A.:  
2104 Reconciling air-sea CO<sub>2</sub> fluxes and anthropogenic CO<sub>2</sub> budgets in a changing North Atlantic. *Nature*  
2105 *Geosciences*, 6, 146-152, [doi:10.1038/ngeo1680](https://doi.org/10.1038/ngeo1680), 2013. Code de champ modifié  
2106  
2107 Pérez, F., Fontela, M., García-Ibáñez, M. et al. : Meridional overturning circulation conveys fast acidification to  
2108 the deep Atlantic Ocean. *Nature* 554, 515–518. Doi: 10.1038/nature25493, 2018.  
2109  
2110 Pesant, S., Not, F., Picheral, M., Kandels-Lewis, S., Le Bescot, N., Gorsky, G., Iudicone, D., Karsenti, E.,  
2111 Speich, S., Troublé, R., Dimier, C., Searson, S., and Tara Oceans Consortium Coordinators: Open science

2112 resources for the discovery and analysis of Tara Oceans data. *Scientific Data* 2:150023. doi:  
2113 10.1038/sdata.2015.23, 2015.

2114

2115 Petrenko, A.: LATEX10 cruise, RV *Téthys II*, <https://doi.org/10.17600/10450150>, 2010.

2116

2117 Petrenko, A.A., Doglioli, A.M., Nencioli, F., Kersalé, M., Hu, Z., and d'Ovidio, F.: A review of the LATEX  
2118 project: mesoscale to submesoscale processes in a coastal environment. *Ocean Dynam.*, doi: 10.1007/s10236-  
2119 017-1040-9, 2017.

2120

2121 Petton, S., Pouvreau, S., and Fleury, E. : ECOSCOPA network : high frequency environmental database.  
2122 SEANOE. <https://doi.org/10.17882/86131>, 2023.

2123

2124 Pfeil, B., Olsen, A., Bakker, D. C. E., Hankin, S., Koyuk, H., Kozyr, A., Malczyk, J., Manke, A., Metzl, N.,  
2125 Sabine, C. L., Akl, J., Alin, S. R., Bates, N., Bellerby, R. G. J., Borges, A., Boutin, J., Brown, P. J., Cai, W.-J.,  
2126 Chavez, F. P., Chen, A., Cosca, C., Fassbender, A. J., Feely, R. A., González-Dávila, M., Goyet, C., Hales,  
2127 B., Hardman-Mountford, N., Heinze, C., Hood, M., Hoppema, M., Hunt, C. W., Hydes, D., Ishii, M.,  
2128 Johannessen, T., Jones, S. D., Key, R. M., Körtzinger, A., Landschützer, P., Lauvset, S. K., Lefèvre, N.,  
2129 Lenton, A., Lourantou, A., Merlivat, L., Midorikawa, T., Mintrop, L., Miyazaki, C., Murata, A., Nakadate, A.,  
2130 Nakano, Y., Nakaoka, S., Nojiri, Y., Omar, A. M., Padin, X. A., Park, G.-H., Paterson, K., Perez, F. F., Pierrot,  
2131 D., Poisson, A., Ríos, A. F., Santana-Casiano, J. M., Salisbury, J., Sarma, V. V. S. S., Schlitzer, R.,  
2132 Schneider, B., Schuster, U., Sieger, R., Skjelvan, I., Steinhoff, T., Suzuki, T., Takahashi, T., Tedesco, K.,  
2133 Telszewski, M., Thomas, H., Tilbrook, B., Tjiputra, J., Vandemark, D., Veness, T., Wanninkhof, R., Watson,  
2134 A. J., Weiss, R., Wong, C. S., and Yoshikawa-Inoue, H.: A uniform, quality controlled Surface Ocean CO2  
2135 Atlas (SOCAT), *Earth Syst. Sci. Data*, 5, 125-143, doi:10.5194/essd-5-125-2013, 2013.

2136

2137 Picheral, M., Searson, S., Taillandier, V., Bricaud, A., Boss, E., Ras, J., Claustre, H., Ouhssain, M., Morin, P.,  
2138 Coppola, L., Gattuso, J.-P., Metzl, N., Thuillier, D., Gorsky, G., Tara Oceans Consortium, Coordinators; Tara  
2139 Oceans Expedition, Participants: Vertical profiles of environmental parameters measured on discrete water  
2140 samples collected with Niskin bottles during the Tara Oceans expedition 2009-2013.  
2141 doi:10.1594/PANGAEA.836319, 2014.

2142

2143 Pilcher, D. J., Brody, S. R., Johnson, L., and Bronselaer, B.: Assessing the abilities of CMIP5 models to  
2144 represent the seasonal cycle of surface ocean pCO<sub>2</sub>, *J. Geophys. Res. Oceans*, 120, 4625–4637,  
2145 doi:10.1002/2015JC010759, 2015.

2146

2147 Poisson, A., Culkin, F., and Ridout, P.: Intercomparison of CO<sub>2</sub> measurements. *Deep Sea Research Part A.*  
2148 *Oceanographic Research Papers*, 37, 10, 1647-1650, [https://doi.org/10.1016/0198-0149\(90\)90067-6](https://doi.org/10.1016/0198-0149(90)90067-6), 1990.

2149

2150 Pujo-Pay, M., Durrieu de Madron, X., and Conan, P.: PERLE3 cruise, RV *Pourquoi pas ?*,  
2151 <https://doi.org/10.17600/18001342>, 2020.

2152

2153 Pujo-Pay, M., Durrieu de Madron, X., and Conan, P.: PERLE4 cruise, RV *L'Atalante*,  
2154 <https://doi.org/10.17600/18001980>, 2021.

2155

2156 Rabouille C.: AMOR-BFLUX cruise, RV *Téthys II*, <https://doi.org/10.17600/15008700>, 2015.

2157

2158 Racapé, V., Metzl, N., Pierre, C., Reverdin, G., Quay, P.D., and Olafsdottir, S. R.: The seasonal cycle of the  
2159 d13C<sub>DIC</sub> in the North Atlantic Subpolar Gyre. *Biogeosciences*, 11, 6, 1683-1692, doi:10.5194/bg-11-1683-2014,  
2160 2014.

2161

2162 Revelle, R., and Suess, H. E.: Carbon dioxide exchange between atmosphere and ocean and the question of an  
2163 increase of atmospheric CO<sub>2</sub> during the past decades. *Tellus* 9, 18–27. doi:10.1111/j.2153-  
2164 3490.1957.tb01849.x., 1957.

2165

Code de champ modifié

2166 Reverdin, G.: STRASSE cruise, RV Thalassa, <https://doi.org/10.17600/12040060>, 2012.

2167

2168 Reverdin, G., Metzl, N., Olafsdottir, S., Racapé, V., Takahashi, T., Benetti, M., Valdimarsson, H., Benoit-Cattin,  
2169 A., Danielsen, M., Fin, J., Naamar, A., Pierrot, D., Sullivan, K., Bringas, F., and Goni, G.: SURATLANT: a  
2170 1993–2017 surface sampling in the central part of the North Atlantic subpolar gyre, *Earth Syst. Sci. Data*, 10,  
2171 1901-1924, <https://doi.org/10.5194/essd-10-1901-2018>, 2018.

2172

2173 Reverdin, G., Metzl, N., Olafsdottir, S., Racapé, V., Takahashi, T., Benetti, M., Valdimarsson, H., Quay, P. D.,  
2174 Benoit-Cattin, A., Danielsen, M., Fin, J., Naamar, A., Pierrot, D., Sullivan, K., Bringas, F., and Goni, G.:  
2175 SURATLANT: a surface dataset in the central part of the North Atlantic subpolar gyre. SEANOE.  
2176 <https://doi.org/10.17882/54517>, 2022.

2177

2178 Ridame, C., Dekaezemacker, J., Guieu, C., Bonnet, S., L'Helguen, S., and Malien, F.: Contrasted Saharan dust  
2179 events in LNLC environments: impact on nutrient dynamics and primary production, *Biogeosciences*, 11, 4783–  
2180 4800, <https://doi.org/10.5194/bg-11-4783-2014>, 2014.

2181

2182 Robertson, J. E., Robinson, C., Turner, D. R., Holligan, P., Watson, A. J., Boyd, P., Fernandez, E., and Finch,  
2183 M.: The impact of a coccolithophore bloom on oceanic carbon uptake in the northeast Atlantic during summer  
2184 1991, *Deep Sea Res., Part I*, 41(2), 297–314, 1994.

2185

2186 Rödenbeck, C., Keeling, R. F., Bakker, D. C. E., Metzl, N., Olsen, A., Sabine, C., and Heimann, M.: Global  
2187 surface-ocean pCO<sub>2</sub> and sea-air CO<sub>2</sub> flux variability from an observation-driven ocean mixed-layer scheme,  
2188 *Ocean Sci.*, 9, 193–216, <https://doi.org/10.5194/os-9-193-2013>, 2013.

2189

2190 Rödenbeck, C., Bakker, D. C. E., Gruber, N., Iida, Y., Jacobson, A.R., Jones, S., Landschützer, P., Metzl, N.,  
2191 Nakaoka, S., Olsen, A., Park, G.-H., Peylin, P., Rodgers, K. B., Sasse, T. P., Schuster, U., Shutler, J. D., Valsala,  
2192 V., Wanninkhof, R., Zeng, J. Data-based estimates of the ocean carbon sink variability – First results of the  
2193 Surface Ocean pCO<sub>2</sub> Mapping intercomparison (SOCOM). *Biogeosciences* 12: 7251-7278. doi:10.5194/bg-12-  
2194 7251-2015, 2015.

2195

2196 Sabine, C. L., Feely, R. A., Gruber, N., Key, R. M., Lee, K., Bullister, J. L., Wanninkhof, R., Wong, C. S.,  
2197 Wallace, D. W. R., Tilbrook, B., Millero, F. J., Peng, T.-H., Kozyr, A., Ono, T., and Rios, A. F.: The Oceanic  
2198 Sink for Anthropogenic CO<sub>2</sub>, *Science*, 305, 367-371, <https://doi.org/10.1126/science.1097403>, 2004.

2199

2200 Sabine, C. L., Hankin, S., Koyuk, H., Bakker, D. C. E., Pfeil, B., Olsen, A., Metzl, N., Kozyr, A., Fassbender,  
2201 A., Manke, A., Malczyk, J., Akl, J., Alin, S. R., Bellerby, R. G. J., Borges, A., Boutin, J., Brown, P. J., Cai, W.-  
2202 J., Chavez, F. P., Chen, A., Cosca, C., Feely, R.A., González-Dávila, M., Goyet, C., Hardman-Mountford, N.,  
2203 Heinze, C., Hoppema, M., Hunt, C. W., Hydes, D., Ishii, M., Johannessen, T., Key, R. M., Körtzinger, A.,  
2204 Landschützer, P., Lauvset, S. K., Lefèvre, N., Lenton, A., Lourantou, A., Merlivat, L., Midorikawa, T.,  
2205 Mintrop, L., Miyazaki, C., Murata, A., Nakadate, A., Nakano, Y., Nakaoka, S., Nojiri, Y., Omar, A. M., Padin,  
2206 X. A., Park, G.-H., Paterson, K., Perez, F. F., Pierrot, D., Poisson, A., Ríos, A. F., Salisbury, J., Santana-  
2207 Casiano, J. M., Sarma, V. V. S. S., Schlitzer, R., Schneider, B., Schuster, U., Sieger, R., Skjelvan, I., Steinhoff,  
2208 T., Suzuki, T., Takahashi, T., Tedesco, K., Telszewski, M., Thomas, H., Tilbrook, B., Vandemark, D., Veness,  
2209 T., Watson, A. J., Weiss, R., Wong, C. S., and Yoshikawa-Inoue, H.: Surface Ocean CO<sub>2</sub> Atlas (SOCAT)  
2210 gridded data products, *Earth Syst. Sci. Data*, 5, 145-153, doi:10.5194/essd-5-145-2013, 2013.

2211

2212 Salt, L. A., Beaumont, L., Blain, S., Bucciarelli, E., Grosstefan, E., Guillot, A., L'Helguen, S., Merlivat, L.,  
2213 Répécaud, M., Quémener, L., Rimmelin-Maury, P., Tréguer, P., and Bozec, Y.: The annual and seasonal  
2214 variability of the carbonate system in the Bay of Brest (Northwest Atlantic Shelf, 2008–2014). *Marine*  
2215 *Chemistry*, doi:10.1016/j.marchem.2016.09.003. 2016.

2216

2217 Sasse, T. P., McNeil, B. I., and Abramowitz, G.: A novel method for diagnosing seasonal to inter-annual surface  
2218 ocean carbon dynamics from bottle data using neural networks, *Biogeosciences*, 10, 4319–4340,  
2219 <https://doi.org/10.5194/bg-10-4319-2013>, 2013.



2220  
2221 Sauzède, R., Claustre, H., Pasqueron de Fommervault, O., Bittig, H., Gattuso, J.-P., Legendre, L. and Johnson,  
2222 K. S.: Estimates of water-column nutrients and carbonate system parameters in the global ocean: A novel  
2223 approach based on neural networks. *Front. Mar. Sci.* 4:128. doi:10.3389/fmars.2017.00128, 2017.  
2224  
2225 Seelmann, K., Steinhoff, T., Aßmann, S., and Körtzinger, A.: Enhance Ocean Carbon Observations: Successful  
2226 Implementation of a Novel Autonomous Total Alkalinity Analyzer on a Ship of Opportunity. *Front. Mar. Sci.*  
2227 7:571301. doi: 10.3389/fmars.2020.571301, 2020.  
2228  
2229 Schlitzer, R.: Ocean Data View, Ocean Data View, <http://odv.awi.de> (last access: 13 March 2019), 2018.  
2230  
2231 Schneider, A., Wallace, D. W. R., and Körtzinger, A.: Alkalinity of the Mediterranean Sea, *Geophys. Res. Lett.*,  
2232 34, L15608, doi:10.1029/2006GL028842, 2007.  
2233  
2234 Schuster, U., Watson, A.J., Bates, N., Corbière, A., Gonzalez-Davila, M., Metzl, N., Pierrot, D. and Santana-  
2235 Casiano, M.: Trends in North Atlantic sea surface pCO<sub>2</sub> from 1990 to 2006. *Deep-Sea Res II*,  
2236 doi:10.1016/j.dsr2.2008.12.011, 2009.  
2237  
2238 Schuster, U., McKinley, G. A., Bates, N., Chevallier, F., Doney, S. C., Fay, A. R., González-Dávila, M., Gruber,  
2239 N., Jones, S., Krijnen, J., Landschützer, P., Lefèvre, N., Manizza, M., Mathis, J., Metzl, N., Olsen, A., Rios, A.  
2240 F., Rödenbeck, C., Santana-Casiano, J. M., Takahashi, T., Wanninkhof, R., and Watson, A. J.: An assessment of  
2241 the Atlantic and Arctic sea-air CO<sub>2</sub> fluxes, 1990–2009, *Biogeosciences*, 10, 607–627,  
2242 <https://doi.org/10.5194/bg-10-607-2013>, 2013.  
2243  
2244 Sims, R. P., Holding, T. M., Land, P. E., Piolle, J.-F., Green, H. L., and Shutler, J. D.: OceanSODA-UNEXE: a  
2245 multi-year gridded Amazon and Congo River outflow surface ocean carbonate system dataset, *Earth Syst. Sci.*  
2246 *Data*, 15, 2499–2516, <https://doi.org/10.5194/essd-15-2499-2023>, 2023.  
2247  
2248 Skjelvan, I., Lauvset, S.K., Johannessen, T., et al.: Decadal trends in Ocean Acidification from the Ocean  
2249 Weather Station M in the Norwegian Sea, *Journal of Marine Systems*,  
2250 <https://doi.org/10.1016/j.jmarsys.2022.103775>, 2022.  
2251  
2252 Speich, S., and The Embarked Science Team: EUREC4A-OA. Cruise Report. 19 January – 19 February 2020.  
2253 Vessel: L'ATALANTE. <https://doi.org/10.13155/80129>, 2021  
2254  
2255 Takahashi, T., Sutherland, S. C., Sweeney, C., Poisson, A., Metzl, N., Tilbrook, B., Bates, N., Wanninkhof, R.,  
2256 Feely, R. A., Sabine, C., Olafsson, J., and Nojiri, Y.: Global Sea-Air CO<sub>2</sub> Flux Based on Climatological Surface  
2257 Ocean pCO<sub>2</sub>, and Seasonal Biological and Temperature Effect. *Deep-Sea Res. II*, 49, 9-10, 1601-1622,  
2258 [https://doi.org/10.1016/S0967-0645\(02\)00003-6](https://doi.org/10.1016/S0967-0645(02)00003-6). 2002  
2259  
2260 Takahashi, T., Sutherland, S. C., Wanninkhof, R., Sweeney, C., Feely, R. A., Chipman, D. W., Hales, B.,  
2261 Friederich, G., Chavez, F., Sabine, C., Watson, A. J., Bakker, D. C., Schuster, U., Metzl, N., Yoshikawa-Inoue,  
2262 H., Ishii, M., Midorikawa, T., Nojiri, Y., Körtzinger, A., Steinhoff, T., Hoppema, M., Olafsson, J., Arnarson, T.  
2263 S., Tilbrook, B., Johannessen, T., Olsen, A., Bellerby, R., Wong, C., Delille, B., Bates, N., and de Baar, H. J.:  
2264 Climatological mean and decadal change in surface ocean pCO<sub>2</sub>, and net sea air CO<sub>2</sub> flux over the global  
2265 oceans. *Deep-Sea Res. II*, 56 (8-10), 554–577, <http://dx.doi.org/10.1016/j.dsr2.2008.12.009>. 2009.  
2266  
2267 Takahashi, T., Sutherland, S. C., Chipman, D. W., Goddard, J. G., Ho, C., Newberger, T., Sweeney, C. and  
2268 Munro, D. R.: Climatological distributions of pH, pCO<sub>2</sub>, total CO<sub>2</sub>, alkalinity, and CaCO<sub>3</sub> saturation in the  
2269 global surface ocean, and temporal changes at selected locations. *Marine Chemistry*, 164, 95–125,  
2270 doi:10.1016/j.marchem.2014.06.004. 2014.  
2271  
2272 Tanhua, T., Pouliquen, S., Hausman, J., O'Brien, K., Bricher, P., de Bruin, T., Buck, J. J. H., Burger, E. F.,  
2273 Carval, T., Casey, K. S., Diggs, S., Giorgetti, A., Glaves, H., Harscoat, V., Kinkade, D., Muelbert, J. H.,

2274 Novellino, A., Pfeil, B., Pulsifer, P. L., Van de Putte, A., Robinson, E., Schaap, D., Smirnov, A., Smith, N.,  
2275 Snowden, D., Spears, T., Stall, S., Tacoma, M., Thijsse, P., Tronstad, S., Vandenberghe, T., Wengren, M.,  
2276 Wyborn, L. and Zhao, Z.: Ocean FAIR Data Services. *Front. Mar. Sci.* 6:440. doi: 10.3389/fmars.2019.00440,  
2277 2019.

2278  
2279 Tanhua, T., Lauvset, S.K., Lange, N. et al.: A vision for FAIR ocean data products. *Commun Earth Environ* 2,  
2280 136. <https://doi.org/10.1038/s43247-021-00209-4>, 2021

2281  
2282 Testor, P., Bosse, A., and Coppola, L.: MOOSE-GE, <https://doi.org/10.18142/235>, 2010.

2283  
2284 Testor, P.: DEWEX-MERMEX 2013 LEG1 cruise, RV Le Suroît, <https://doi.org/10.17600/13020010>, 2013.

2285  
2286 Tilbrook, B., Jewett, E. B., DeGrandpre, M. D., Hernandez-Ayon, J. M., Feely, R. A., Gledhill, D. K., Hansson,  
2287 L., Isensee, K., Kurz, M. L., Newton, J. A., Siedlecki, S. A., Chai, F., Dupont, S., Graco, M., Calvo, E., Greeley,  
2288 D., Kapsenberg, L., Lebec, M., Pelejero, C., Schoo, K. L., and Telszewski, M.: An Enhanced Ocean  
2289 Acidification Observing Network: From People to Technology to Data Synthesis and Information Exchange.  
2290 *Frontiers in Marine Science*, 6, 337, DOI:10.3389/fmars.2019.00337, 2019.

2291  
2292 Touratier, F., Azouzi, L. and Goyet, C.: CFC-11,  $\Delta 14C$  and 3H tracers as a means to assess anthropogenic CO<sub>2</sub>  
2293 concentrations in the ocean. *Tellus B*, 59(2), 318–325, doi:10.1111/j.1600-0889.2006.00247.x, 2007.

2294  
2295 Touratier, F., and Goyet, C.: Decadal evolution of anthropogenic CO<sub>2</sub> in the north western Mediterranean Sea  
2296 from the mid-1990's to the mid-2000's. *Deep Sea Research Part I*.doi:10.1016/j.dsr.2009.05.015, 2009.

2297  
2298 Touratier, F., Goyet, C., Houpert, L., Durrieu de Madron, X., Lefèvre, D., Stabholz, M., and Guglielmi, V.: Role  
2299 of deep convection on anthropogenic CO<sub>2</sub> sequestration in the Gulf of Lions (northwestern Mediterranean Sea).  
2300 *Deep-Sea Research Part I*. doi.org/10.1016/j.dsr.2016.04.003, 2016.

2301  
2302 Turk, D., Dowd, M., Lauvset, S. K., Koelling, J., Alonso-Pérez, F. and Pérez, F. F.: Can Empirical Algorithms  
2303 Successfully Estimate Aragonite Saturation State in the Subpolar North Atlantic? *Front. Mar. Sci.* 4:385. doi:  
2304 10.3389/fmars.2017.00385, 2017.

2305  
2306 Ulses, C., Estournel, C., Marsaleix, P., Soetaert, K., Fourier, M., Coppola, L., Lefèvre, D., Touratier, F., Goyet,  
2307 C., Guglielmi, V., Kessouri, F., Testor, P., and Durrieu de Madron, X.: Seasonal dynamics and annual budget of  
2308 dissolved inorganic carbon in the northwestern Mediterranean deep convection region, *Biogeosciences Discuss.*  
2309 [preprint], <https://doi.org/10.5194/bg-2022-219>, in review, **2022accepted, 2023**.

2310  
2311 UNESCO: Intercomparison of total alkalinity and total inorganic carbon determinations in seawater. UNESCO  
2312 Tech. Pap. Mar. Sci. 59., 1990

2313  
2314 UNESCO: Reference materials for oceanic carbon dioxide measurements. UNESCO Tech. Pap. Mar. Sci. 60.,  
2315 1991

2316  
2317 United Nations. The Sustainable Development Goals 2020, 68pp. <https://unstats.un.org/sdgs/report/2020/>, 2020

2318  
2319 Vangriesheim A., Pierre, C., Aminot, A., Metzl, N., Baurand, F., and Caprais, J.-C.: The influence of Congo  
2320 river discharges in the surface and deep layers of the Gulf of Guinea. *Deep-Sea Res. II*, doi:  
2321 10.1016/j.dsr2.2009.04.002, 2009.

2322  
2323 Vazquez-Rodriguez, M., Perez, F., Velo, A., Rios, A., and Mercier, H.: Observed acidification trends in the  
2324 North Atlantic water masses. *Biogeosciences*, 9, 5217-5230, doi:10.5194/bg-9-5217-2012, 2012.

2325  
2326 Velo, A., Perez, F. F., Brown, P., Tanhua, T., Schuster, U., and Key, R. M.: CARINA alkalinity data in the  
2327 Atlantic Ocean, *Earth Syst. Sci. Data*, 1, 45–61, <https://doi.org/10.5194/essd-1-45-2009>, 2009.

Code de champ modifié

2328  
2329 von Schuckmann, K., Cheng, L., Palmer, M. D., Hansen, J., Tassone, C., Aich, V., Adusumilli, S., Beltrami, H.,  
2330 Boyer, T., Cuesta-Valero, F. J., Desbruyères, D., Domingues, C., García-García, A., Gentine, P., Gilson, J.,  
2331 Gorfer, M., Haimberger, L., Ishii, M., Johnson, G. C., Killick, R., King, B. A., Kirchengast, G., Kolodziejczyk,  
2332 N., Lyman, J., Marzeion, B., Mayer, M., Monier, M., Monselesan, D. P., Purkey, S., Roemmich, D., Schweiger,  
2333 A., Seneviratne, S. I., Shepherd, A., Slater, D. A., Steiner, A. K., Straneo, F., Timmermans, M.-L., and Wijffels,  
2334 S. E.: Heat stored in the Earth system: where does the energy go?, *Earth Syst. Sci. Data*, 12, 2013–2041,  
2335 <https://doi.org/10.5194/essd-12-2013-2020>, 2020.

2336  
2337 von Schuckmann, K., Minière, A., Gues, F., Cuesta-Valero, F. J., Kirchengast, G., Adusumilli, S., Straneo, F.,  
2338 Ablain, M., Allan, R. P., Barker, P. M., Beltrami, H., Blazquez, A., Boyer, T., Cheng, L., Church, J.,  
2339 Desbruyeres, D., Dolman, H., Domingues, C. M., García-García, A., Giglio, D., Gilson, J. E., Gorfer, M.,  
2340 Haimberger, L., Hakuba, M. Z., Hendricks, S., Hosoda, S., Johnson, G. C., Killick, R., King, B., Kolodziejczyk,  
2341 N., Korosov, A., Krinner, G., Kuusela, M., Landerer, F. W., Langer, M., Lavergne, T., Lawrence, I., Li, Y.,  
2342 Lyman, J., Marti, F., Marzeion, B., Mayer, M., MacDougall, A. H., McDougall, T., Monselesan, D. P., Nitzbon,  
2343 J., Otosaka, I., Peng, J., Purkey, S., Roemmich, D., Sato, K., Sato, K., Savita, A., Schweiger, A., Shepherd, A.,  
2344 Seneviratne, S. I., Simons, L., Slater, D. A., Slater, T., Steiner, A. K., Suga, T., Szekely, T., Thiery, W.,  
2345 Timmermans, M.-L., Vanderkelen, I., Wijffels, S. E., Wu, T., and Zemp, M.: Heat stored in the Earth system  
2346 1960–2020: where does the energy go?, *Earth Syst. Sci. Data*, 15, 1675–1709, [https://doi.org/10.5194/essd-15-](https://doi.org/10.5194/essd-15-1675-2023)  
2347 [1675-2023](https://doi.org/10.5194/essd-15-1675-2023), 2023.

2348  
2349 Wagener, T., Metzl, N., Caffin, M., Fin, J., Helias Nunige, S., Lefevre, D., Lo Monaco, C., Rougier, G., and  
2350 Moutin, T.: Carbonate system distribution, anthropogenic carbon and acidification in the western tropical South  
2351 Pacific (OUTPACE 2015 transect), *Biogeosciences*, 15, 5221–5236, <https://doi.org/10.5194/bg-15-5221-2018>,  
2352 2018a.

2353  
2354 Wagener, T., Metzl, N., Caffin, M., Fin, J., Helias Nunige, S., Lefevre, D., Lo Monaco, C., Rougier, G., and  
2355 Moutin, T.: Discrete profile measurements of dissolved inorganic carbon (DIC), total alkalinity (TALK),  
2356 temperature, salinity and other parameters during the R/V L'Atalante "Oligotrophy from Ultra-oligoTrophy  
2357 PACific Experiment" (OUTPACE) cruise (EXPCODE 35A320150218) in the South Pacific Ocean from 2015-  
2358 02-18 to 2015-04-03 (NCEI Accession 0177706). Version 1.1. NOAA National Centers for Environmental  
2359 Information. Dataset. doi:10.25921/wbkb-0q19 [access date], 2018b.

2360  
2361 Walton, D. W. H., and Thomas, J.: Cruise Report - Antarctic Circumnavigation Expedition (ACE) 20th  
2362 December 2016 - 19th March 2017 (1.0). Zenodo. <https://doi.org/10.5281/zenodo.1443511>, 2018.

2363  
2364 Wanninkhof, R., Park, G.-H., Takahashi, T., Sweeney, C., Feely, R., Nojiri, Y., Gruber, N., Doney, S. C.,  
2365 McKinley, G. A., Lenton, A., Le Quéré, C., Heinze, C., Schwinger, J., Graven, H., and Khatiwala, S.: Global  
2366 ocean carbon uptake: magnitude, variability and trends, *Biogeosciences*, 10, 1983–2000, doi:10.5194/bg-10-  
2367 1983-2013, 2013.

2368  
2369 Watson, A. J., Schuster, U., Bakker, D. C. E., Bates, N., Corbiere, A., Gonzalez-Davila, M., Freidrich, T.,  
2370 Hauck, J., Heinze, C., Johannessen, T., Koertzing, A., Metzl, N., Olafsson, J., Olsen, A., Oschlies, A., Padin,  
2371 X., Pfeil, B., Rios, A., Santana-Casiano, M., Steinhoff, T., Telszewski, M., Wallace, D. W. R., and Wanninkhof,  
2372 R.: Tracking the variable North Atlantic sink for atmospheric CO<sub>2</sub>, *Science*, 326, 1391,  
2373 doi:10.1126/science.1177394. 2009.

2374  
2375 Watson, A. J., Schuster, U., Shutler, J.D. et al.: Revised estimates of ocean-atmosphere CO<sub>2</sub> flux are consistent  
2376 with ocean carbon inventory. *Nat Commun* 11, 4422, <https://doi.org/10.1038/s41467-020-18203-3>, 2020.

2377  
2378 Williams, N. L., Juranek, L. W., Johnson, K. S., Feely, R. A., Riser, S. C., Talley, L. D., et al.: Empirical  
2379 algorithms to estimate water column pH in the Southern Ocean. *Geophysical Research Letters*, 43, 3415–3422.  
2380 <https://doi.org/10.1002/2016GL068539>, 2016.

2381

2382 Williams, N. L., Juranek, L. W., Feely, R. A., Johnson, K. S., Sarmiento, J. L., Talley, L. D., Dickson,  
2383 A. G., Gray, A. R., Wanninkhof, R., Russell, J. L., Riser, S. C., and Takeshita, Y.: Calculating surface  
2384 ocean pCO<sub>2</sub> from biogeochemical Argo floats equipped with pH: An uncertainty analysis, *Global Biogeochem.*  
2385 *Cycles*, 31, 591–604, doi:10.1002/2016GB005541., 2017.  
2386

2387 Williams, N. L., Juranek, L. W., Feely, R. A., Russell, J. L., Johnson, K. S., and Hales, B.: Assessment of the  
2388 carbonate chemistry seasonal cycles in the Southern Ocean from persistent observational platforms. *Journal of*  
2389 *Geophysical Research: Oceans*, 123. <https://doi.org/10.1029/2017JC012917>, 2018.  
2390

2391 Wimart-Rousseau, C., Lajaunie-Salla, K., Marrec, P., Wagener, T., Raimbault, P., Lagadec, V., Lafont, M.,  
2392 Garcia, N., Diaz, F., Pinazo, C., Yohia, C., Garcia, F., Xueref-Remy, I., Blanc, P.-E., Armengaud, A., and  
2393 Lefèvre, D.: Temporal variability of the carbonate system and air-sea CO<sub>2</sub> exchanges in a Mediterranean human-  
2394 impacted coastal site. *Estuarine, Coastal and Shelf Science*. <https://doi.org/10.1016/j.ecss.2020.106641>, 2020a.  
2395

2396 Wimart-Rousseau, C., Wagener, T., Raimbault, P., Lagadec, V., Lafont, M., Garcia, N., and Lefèvre, D.:  
2397 Oceanic carbonate chemistry measurements from discrete samples collected at the SOLEMIO station (Bay of  
2398 Marseille - North western Mediterranean Sea) between 2016 and 2019. *SEANOE*.  
2399 <https://doi.org/10.17882/72356>, 2020b.  
2400

2401 Wimart-Rousseau, C., Wagener, T., Álvarez, M., Moutin, T., Fourier, M., Coppola, L., Niclas-Chirurgien, L.,  
2402 Raimbault, P., D'Ortenzio, F., Durrieu de Madron, X., Taillandier, V., Dumas, F., Conan, P., Pujo-Pay, M. and  
2403 Lefèvre, D.: Seasonal and Interannual Variability of the CO<sub>2</sub> System in the Eastern Mediterranean Sea: A Case  
2404 Study in the North Western Levantine Basin. *Front. Mar. Sci.* 8:649246. doi: 10.3389/fmars.2021.649246, 2021  
2405

2406 WMO/GCOS, 2018: <https://gcos.wmo.int/en/global-climate-indicators>, 2018  
2407

2408 Wu, Y., Hain, M. P., Humphreys, M. P., Hartman, S., and Tyrrell, T.: What drives the latitudinal gradient in  
2409 open-ocean surface dissolved inorganic carbon concentration?, *Biogeosciences*, 16, 2661-2681,  
2410 <https://doi.org/10.5194/bg-16-2661-2019>, 2019.  
2411

2412